January 2010

The Staggered Chiral Perturbation Theory In The Two-Flavor Case And Su(2) Chiral Analysis Of The Milc Data

Xining Du
Washington University in St. Louis

WASHINGTON UNIVERSITY

Department of Physics

Dissertation Examination Committee:
Claude Bernard, Chair
Mark Alford
James H. Buckley
Michael C. Ogilvie
Richard Rochberg
Stanley Sawyer

THE STAGGERED CHIRAL PERTURBATION THEORY IN THE TWO-FLAVOR CASE AND SU(2) CHIRAL ANALYSIS OF THE MILC DATA

by

Xining Du

A dissertation presented to the
Graduate School of Arts and Sciences
of Washington University in
partial fulfillment of the
requirements for the degree
of Doctor of Philosophy

August 2010

Saint Louis, Missouri

Abstract

rt of the Standard Model (SM), Quantum Chromodynamics (QCD) is a widely accepted theory to describe the physics of quarks and gluons. Formulating QCD on finite discrete lattices in Euclidean space-time not only enables one to study the theory non-perturbatively, but also provides a framework analogous to statistical systems, in which numerical methods can be applied. In this work, we concentrate on one specific fermion formalism, staggered fermions. To interpret the data obtained from numerical simulations with staggered fermions, a particular version of chiral perturbation theory (χPT), rooted staggered χPT (rSχPT), is needed to incorporate the discretization effects, mainly taste-violations, and the fourth root procedure used for the staggered fermion formalism.

In the light pseudoscalar sector, I study rSχPT in the two-flavor case. The pion mass and decay constant are calculated through NLO for a partially-quenched theory. In the limit where the strange quark mass is large compared to the light quark masses and the taste splittings, I show that the SU(2) staggered chiral theory emerges from the SU(3) staggered chiral theory, as expected. Explicit relations between SU(2) and SU(3) low energy constants and taste-violating parameters are given. The results are useful for SU(2) chiral fits to asqtad data and allow one to incorporate effects from

varying strange quark masses.

By using these formulae and continuum NNLO chiral logarithms, I then perform a systematic chiral analysis to the MILC lattice data in the light pseudoscalar sector. Superfine ($a \approx 0.06$ fm) and ultrafine ($a \approx 0.045$ fm) ensembles are used, where light sea quark masses and taste splittings are small compared to the simulated strange quark mass. Correlated fits with Bayesian analysis are done for both the pion mass and the pion decay constant. Physical quantities are obtained by extrapolating the results to the continuum and full QCD case where the light quarks masses are physical. I give results for the pion decay constant, SU(2) low-energy constants and the chiral condensate in the two-flavor chiral limit.

Acknowledgments

First, I would like to thank my advisor, Prof. Claude Bernard, for the valuable advice and assistance at almost every stage of my research, for his enormous patience in explaining all kinds of physics concepts in great detail, as well as helping me to correct many mistakes and polishing the English for my writing. This whole work would not be possible if it is not for his inspiration, advice and continuous support. I am grateful for him spending time to talk with me about life and career decisions, from which I have really benefited a lot.

I would also like to thank Prof. Mark Alford and Prof. Michael C. Ogilvie, for their discussions and suggestions during the committee meeting, which encouraged me to think about how to express complicated physics ideas in a relatively simple way. Meanwhile, I would like to thank my previous advisor, Prof. Chuan Liu, who guided me to the world of lattice field theory and inspired my interests in this research area.

I am indebted to many of my colleagues and friends here, especially Tianyu Zhao, Jian Wu, Yun Wang and Wei Zhang. It is their kind assistance that helped me go through the tough times, and it is the fun time sharing together with them that made my stay in St.Louis more delightful.

A special thanks goes to my beloved one, Wei, for her understanding and support

in these past years. She always trusted me and encouraged me to look on the bright side when I met difficulties in life and research. Many thanks to her for spending much time in preparing dinner every day and calming me down during the time of writing the thesis.

Finally, I own my deepest gratitude to my parents and my two sisters. I would not be able to go this far if it were not for their unconditional love and support throughout my studies. This thesis is dedicated to them.

Contents

Abstract ii

Acknowledgments iv

List of Figures ix

List of Tables x

1 Introduction to Lattice QCD 1
- 1.1 Quantum Chromodynamics . . . 1
- 1.2 Quantum field theory on the lattice . . . 3
- 1.3 Gauge theory on the lattice . . . 5
- 1.4 Fermions on the lattice . . . 7
- 1.5 Path integral on the lattice . . . 9
- 1.6 Measuring physical quantities on the lattice . . . 10
  - 1.6.1 Extrapolations . . . 12

2 Staggered Fermions 15
- 2.1 Wilson Fermions . . . 15
- 2.2 Staggered Fermions . . . 18
  - 2.2.1 Symmetries of the staggered action . . . 21
  - 2.2.2 Fourth-root procedure . . . 24
- 2.3 The "asqtad" staggered action . . . 24
  - 2.3.1 Tadpole improvement . . . 24
  - 2.3.2 Asqtad improved staggered fermions . . . 26

3 Staggered Chiral Perturbation Theory 30
- 3.1 Chiral Perturbation Theory . . . 31
- 3.2 Staggered Chiral Perturbation Theory . . . 39
  - 3.2.1 SET for staggered fermions . . . 40
  - 3.2.2 SχPT Lagrangian at LO . . . 42
- 3.3 Rooted Staggered Chiral Perturbation Theory . . . 50
- 3.4 Partially-Quenched Chiral Perturbation Theory . . . 52
- 3.5 Pion mass and decay constant in partially-quenched SU(3) rSχPT . . . 57

4 SU(2) Staggered Chiral Perturbation Theory 62
4.1 Motivation for SU(2) χPT . . . 62
4.2 SU(2) chiral perturbation theory in the continuum . . . 63
4.3 Cayley-Hamilton relations . . . 67
4.4 Staggered computations . . . 71
4.4.1 Brief review of SχPT . . . 71
4.4.2 Two-flavor PQ-SχPT at LO . . . 74
4.4.3 Two-flavor PQ-rSχPT at NLO . . . 78
4.4.4 Rooting and partial quenching . . . 79
4.4.5 PION MASS AND DECAY CONSTANT . . . 79
4.5 Relation of SU(2) and SU(3) staggered chiral perturbation theories . 88
4.6 Remarks and conclusion . . . 93

5 SU(2) Chiral Fitting to MILC Data 96
5.1 Light pseudoscalar meson mass and decay constant . . . 97
5.2 Measuring taste splittings . . . 98
5.3 Determining lattice spacings . . . 100
5.4 NNLO SU(2) chiral analysis . . . 102
5.4.1 Motivation for SU(2) chiral analysis . . . 102
5.5 Fitting in detail . . . 103
5.5.1 Fit formulae for pion mass and decay constant . . . 103
5.5.2 Datasets used for SU(2) analysis . . . 107
5.5.3 Fitting strategies . . . 108
5.5.4 Finite volume corrections . . . 114
5.6 Central value fit . . . 115
5.6.1 List of parameters . . . 115
5.6.2 Quark masses and condensates . . . 118
5.6.3 Summary of results . . . 119
5.7 Discussion and Outlook . . . 119

Appendix I γ Matrices and Euclidean Field Theory 122

Appendix II Detailed Descriptions of Computer Codes 124
INTRODUCTION TO THE FITTING CODE . . . 124
STEPS TO PERFORM A COMPLETE SU(2) CHIRAL ANALYSIS FROM A CERTAIN DATA FILE . . . 125
DETAILED DESCRIPTIONS OF ALL FILES . . . 130
/DAT . . . 130
dat_files_thin_F031009_SF0072_UF0056_ml0101502ms.csh . . . 130
/EXEC . . . 132
linalg.c . . . 132
whichspacing.c . . . 133
schpt2.c . . . 133
cofit_np.c . . . 141
minp.c . . . 144

r1_ALLTON-variation.c 144
r1_ALLTON_main.c 147
makefile 147
/PLOT 151
makeplot_2loop.csh 151
finite_vol_correct_all_pts_2loop.csh 153
extract_pts_all_2loop_mloverms0101502.csh 155
make_fit_lines_some_2loop_from0.csh 156
fit_line_all_2loop.csh 157
sbq_all_2loop.csh 160
solve_all_2loop.csh 162
/SUMMARY 166
dof.csh 166
dofphys.csh 166
doubaru.csh 167
dompi.csh 167
dol3.csh 167
dol4.csh 167

List of Figures

1.1 Schematic diagram of a $N \times N$ lattice with lattice spacing a in 2-D spacetime. 5
1.2 A plaquette on the lattice around the square near point x in $\mu - \nu$ plane 7

2.1 A 2-D schematic diagram showing the values of $\eta_\mu(x)$ on the lattice. . 19
2.2 A tadpole diagram for the fermion self energy in the lattice perturbation theory. 25
2.3 Four-fermion taste violation diagrams. Two incoming fermions change their tastes by exchanging a gluon with momentum π/a as shown in figure (a), or exchanging two or more gluons with total momentum π/a as shown in figure (b). 28
2.4 Multi-link staples used in the "asq" action 29

3.1 The hairpin disconnected vertex from the $\mathcal{U}'$ term. (a) diagram in the chiral theory. (b) the corresponding quark flow diagram. 48
3.2 (a) The complete flavor-neutral, taste-vector propagator between U_V and D_V. It is obtained by summing over all diagrams in (b), where different numbers of taste-vector hairpin vertices are inserted. 48
3.3 Sample pion self energy diagrams and possible quark flow diagrams. (a) and (b) are two diagrams contributing to the pion self energy. (c) and (d) are the corresponding two possible quark flow diagrams. The diagram in figure (c) gets a factor 1/4 while the diagram in figure (d) does not. 51
3.4 A sample tadpole diagram which contributes to the pion self energy. Here the meson P_5^+ is the Goldstone pion composed of x and y valence quarks. The propagator in the loop is between two flavor-neutral, taste-vector mesons X_V and Y_V, and the corresponding quark flow diagram is a disconnected diagram. 59

5.1 Squared masses of pions for various tastes on the lattices with $a \approx 0.12$fm are shown as functions of quark masses. The splittings appear to be independent of quark masses. All quantities are in units of r_1. (The scale r_1 is defined below in section (5.3).) Plot is from Ref. [1]. . 99
5.2 SU(2) chiral fits to f_π(left) and $m_\pi^2/(m_x+m_y)$(right). Only points with the valence quark masses equal ($m_x = m_y$) are shown on the plots . . 117
5.3 Test of convergence of SU(3) χPT fits in the continuum, with the strange quark mass fixed at $0.6m_s^{phys}$. Plots are from Ref. [2]. 120

List of Tables

5.1 Ensembles used in this analysis. Here, (F), (SF) and (UF) stand for fine, superfine and ultrafine lattices respectively. The quantities am_l and am_s are the light and strange sea quark masses in lattice units; $m_\pi L$ is the (sea) Goldstone pion mass times the linear spatial size. The fine ensembles are not used in our central value fit, but only in estimating systematic errors. 109

5.2 Kaon masses and lightest (sea) pion masses on some sample ensembles. Here three different pion masses are shown: Goldstone, RMS and singlet. $r_1 = 0.3117\,\mathrm{fm}$ is used. 110

Chapter 1

Introduction to Lattice QCD

1.1 Quantum Chromodynamics

It is now widely accepted that the physics of fundamental particles can be described by the theory called the Standard Model (SM). In this theory, the electro-magnetic (EM) and weak interactions are unified under the framework of $SU(2)_L \times U(1)$ group symmetry, and the strong interactions are described by the second part of the SM, quantum chromodynamics (QCD), which is formulated on a $SU(3)$ gauge group. Overall, the $SU(3) \times SU(2) \times U(1)$ Standard Model successfully explains almost all the experimental results regarding fundamental interactions (with the exception of gravity), hence it remains a basis of modern particle physics.

The QCD part of the Standard Model studies the interactions between quarks and gluons. In this framework, there are six flavors of quarks: u, d, s, t, c, b and each flavor has three different colors: red, green, blue. The strong force between quarks is mediated by eight (color) species of gluons, in a similar way as EM force

is mediated by photons. However, unlike photons, which do not carry EM charges and do no interact with each other, gluons carry color charges and they interact with other gluons. This is a fundamental difference between a non-Abelian gauge theory, like QCD, and an Abelian gauge theory, like quantum electrodynamics (QED). As a result, QCD exhibits many features distinct from that of QED, and the physics in QCD is much richer.

There are two well-known properties of QCD:

- Asymptotic Freedom: The strong coupling constant, $\alpha_S = g^2/(4\pi)$, decreases as the energy scale is increased. When the energy gets higher (smaller separations), α_S becomes smaller, and eventually it goes to zero in the infinite energy limit. In this region (roughly, energy $\Lambda \sim 2$GeV or larger), one can apply the perturbation theory to calculate physical quantities since the expansion parameter α_S is significantly less than 1, and the truncation errors are generally under control.

- Confinement: Although quarks and gluons carry color charges, all physical particles must be color singlets. That is to say, free quarks can not exist in nature; they are always confined in hadrons: quark or gluon bound states that are color singlets. In terms of quark interactions, this phenomenon can be effectively described by a linear potential term between two quarks at long distance r:

$$V(r) = \sigma r + c + \mathcal{O}(\frac{1}{r}), \tag{1.1}$$

  where σ is called the "string tension" because when r gets large, $V(r)$ rises linearly $\sim \sigma r$, as it would for a "string" between the quarks of constant energy

per unit length.

These two properties are closely related to the beta function, which governs the behavior of the coupling constant α_S under scale change. For QCD with N_c colors and N_f fermion flavors, the one-loop beta function is:

$$\beta(g) \equiv \mu \frac{\partial g}{\partial \mu} = -\frac{g^3}{16\pi^2}\left[\frac{11}{3}N_c - \frac{2}{3}N_f\right]. \tag{1.2}$$

where μ is the energy scale. In reality, there are three colors and six flavors, and the beta function is negative. As a consequence, the strong coupling constant will increase as one decreases the energy scale μ. In the low energy region ($\Lambda \lesssim 1\text{GeV}$), the coupling constant will be too large for the perturbation theory to be applicable. One therefore needs to use some non-perturbative treatment. Among all of the non-perturbative approaches, the theory built on the lattice is the only one that comes directly from the first principles of QCD.

1.2 Quantum field theory on the lattice

Most quantum field theories, such as QCD and QED, suffer from ultraviolet divergences when one calculates physical quantities beyond the lowest order. In the language of Feynman diagrams, these divergences come from loop integrals with internal virtual particles. In principle these particles can carry infinitely large momentum, hence the integral is divergent. The divergence comes from $\int d^4p$ at large momentum p, or equivalently, the infinite number of degrees of freedom at short distance in the continuum theory. To deal with this problem systematically, regularization and

renormalization are used to remove the divergences and obtain finite physical results in the end. The first step, regularization, is needed to cut off the integrals and make number of degrees of freedom finite (as on lattice) or effectively finite (other regularizations). Then renormalization expresses all physical results in terms of physically measurable quantities, after which the cutoff can be taken away.

There are many regularization methods available, and which one is being used depends on the actual circumstances and usually the symmetries of the underlying theory. One method of doing regularization is to use the discrete version of space-time instead of the continuous one. Suppose space-time is only defined on discrete points separated by a and the dimension of whole lattice is $(Na)^4$ where N is the number of lattice sites in each of the spatial and temporal directions. Quantum fields are defined on lattice sites or on the links between nearest neighbor lattice sites. By doing this, we actually put an ultraviolet energy cutoff $\Lambda = \frac{\pi}{a}$, as well as an infra-red energy cutoff $\frac{\pi}{Na}$ in the theory. The divergences in loop integrals are thus removed, and we obtain a well-defined quantum field theory. More importantly, by putting the quantum fields on a lattice with finite volume and finite lattice spacing, the infinite degrees of freedom in continuous space-time now become finite. As we will see in section (1.5), the infinite dimensional integrals in the path integral formulation become multi-dimensional integrals. In Euclidean space-time, the quantum field theory on a lattice is very similar to a statistical system, and we can apply many numerical methods that are commonly used in the latter to study the former. This is the key point that makes it possible to calculate physical oberservables from a quantum field theory defined on the lattice.

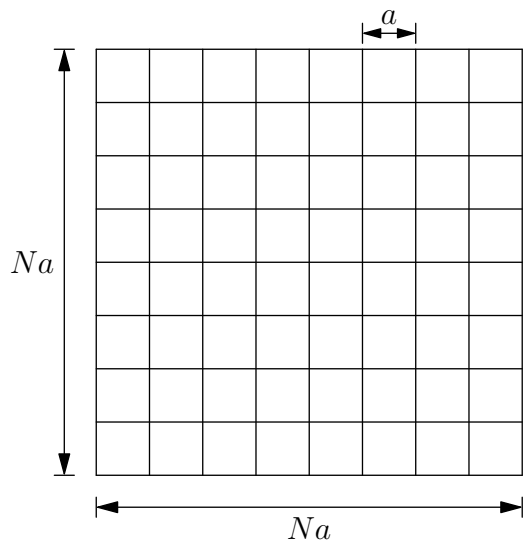

Figure 1.1: Schematic diagram of a $N \times N$ lattice with lattice spacing a in 2-D spacetime.

Here, we begin by introducing the discrete version of actions of two kinds of building blocks of QCD: gauge bosons and fermions.

1.3 Gauge theory on the lattice

Because of its fundamental role in modern physics, gauge field theory is one of the most important quantum field theories that need to be studied on the lattice. The first successful attempt to formulate quantum gauge theory on a lattice was done by Wilson in 1974 [3], where he proposed this to study confinement and other non-perturbative effects in QCD.

The continuum Lagrangian density for SU(3) gauge theory is (in Euclidean space):

$$\mathcal{L} = \frac{1}{4} F_{\mu\nu} F^{\mu\nu}, \tag{1.3}$$

where the field strength is $F_{\mu\nu} = F^a_{\mu\nu}\lambda_a/2$ with λ_a as the eight generators of the

SU(3) gauge group. The field strength component $F^a_{\mu\nu}$ is related to the gauge vector potential $A_\mu = A^a_\mu \lambda_a/2$ by

$$F^a_{\mu\nu} = \partial_\mu A^a_\nu - \partial_\nu A^a_\mu + g f^{abc} A^b_\mu A^c_\nu, \tag{1.4}$$

where g is the coupling constant, and f^{abc} is the group structure constant defined by commutations of SU(3) generators

$$\left[T^a, T^b\right] = i f^{abc} T^c. \tag{1.5}$$

In Wilson's approach, gauge fields are associated with links on the lattice between adjacent lattice sites. For a link between site x and $x + a\hat{\mu}$, one defines the gauge field as a matrix element $U_\mu(x)$ in the gauge group:

$$U(x, x + a\hat{\mu}) = U_\mu(x) = e^{iagA_\mu(x)}; \quad U^\dagger_\mu(x) = U_{-\mu}(x + a\hat{\mu}). \tag{1.6}$$

Under a local gauge transformation $V(x)$, an element $\psi(x)$ in the color space at point x transforms as $\psi(x) \to V(x)\psi(x)$, while the gauge link $U_\mu(x)$ transforms as $U_\mu(x) \to V(x)U_\mu(x)V^\dagger(x + a\hat{\mu})$. One can construct quantities that are invariant under local gauge transformations. The simplest one for pure gauge field is the 1×1 plaquette $W_{\mu\nu}(x)$, *i.e.*, the product of gauge links $U_\mu(x)$ around an elementary square of lattice, as shown in figure (1.2). Writing in terms of gauge links, the plaquette is

$$W_{\mu\nu}(x) = U_\mu(x)U_\nu(x + a\hat{\mu})U^\dagger_\mu(x + a\hat{\nu})U^\dagger_\nu(x). \tag{1.7}$$

The gauge action is the sum over all the plaquettes on the lattice:

$$S_g = \frac{6}{g^2} \sum_x \sum_{\mu<\nu} \mathrm{ReTr} \frac{1}{3}(1 - \mathrm{W}_{\mu\nu}). \tag{1.8}$$

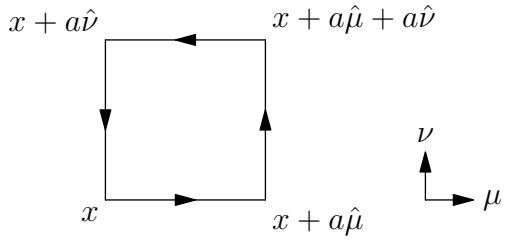

Figure 1.2: A plaquette on the lattice around the square near point x in $\mu - \nu$ plane

If we expand the $U_\mu(x)$ matrices in the continuum limit, $a \to 0$, this reduces to the action in the continuum form:

$$S_g \to \int d^4x (\frac{1}{4} F_{\mu\nu} F^{\mu\nu}) + \mathcal{O}(a^2) \tag{1.9}$$

The lattice artifacts appear at order $\mathcal{O}(a^2)$. The Wilson action can be improved by choosing an appropriate linear combinations of 1×1 and 1×2 Wilson loops to remove the $\mathcal{O}(a^2)$ effects.

1.4 Fermions on the lattice

The continuum free fermion action in Euclidean space-time is [4]:

$$S_f = \int d^4x (\bar{\psi}(x) \gamma_\mu \partial_\mu \psi(x) + m \bar{\psi}(x) \psi(x)). \tag{1.10}$$

In contrast to the gauge fields on the links, fermion fields are defined on each lattice site x. The continuum derivative is replaced by the difference operator on the lattice:

$$\partial_\mu \psi(x) \to \Delta_\mu \psi(x) \equiv \frac{1}{2a} \left(\psi(x + a\hat{\mu}) - \psi(x - a\hat{\mu}) \right). \tag{1.11}$$

The free fermion action thus takes the following form on the lattice:

$$S_f^{lat} = \sum_{x,\mu} \bar{\psi}(x) \gamma_\mu \Delta_\mu \psi(x) + m \sum_x \bar{\psi}(x) \psi(x). \tag{1.12}$$

In the presence of gauge fields, the ordinary derivative in the fermion action should be replaced by the covariant derivative to make the action invariant under local gauge transformations. Correspondingly, we introduce the gauge links to connect fermion fields on adjacent lattice sites to make the action invariant:

$$S_f^{lat} \to \frac{1}{2a}\sum_{x,\mu}\big(\bar{\psi}(x)\gamma_\mu U_\mu(x)\psi(x+a\hat{\mu}) - \bar{\psi}(x)\gamma_\mu U_\mu(x-a\hat{\mu})\psi(x-a\hat{\mu})\big) + m\sum_x \bar{\psi}(x)\psi(x). \tag{1.13}$$

This first attempt at a fermion action is the "naive action". It has the so called "doubling problem". Consider the free fermion propagator in momentum space:

$$S(p) = \frac{1}{m + \frac{i}{a}\gamma_\mu \sin(p_\mu a)}, \tag{1.14}$$

where the momentum ranges from $\frac{-\pi}{a}$ to $\frac{\pi}{a}$. In the chiral limit $m \to 0$, besides the usual pole at $p = (0,0,0,0)$, there are another 15 poles in the propagator located at the corners of Brillouin zone

$$p = \{(\frac{\pi}{a},0,0,0), \cdots, (\frac{\pi}{a},\frac{\pi}{a},\frac{\pi}{a},\frac{\pi}{a}).\} \tag{1.15}$$

These doublers can appear in loops and contribute to physical processes. However, they do not correspond to any real particles and need to be eliminated from the original theory. Several fermion action formalisms are proposed to address this issue. Commonly used ones are the Wilson fermions, staggered fermions, overlap fermions and the domain wall fermions. We will discuss Wilson fermions and staggered fermions in the next chapter. For other fermion formalisms, more details can be found in many textbooks and review articles [4, 5, 6, 7, 8].

1.5 Path integral on the lattice

A classical field can be quantized by using the Feynman path integral formulation. In the case of QCD, one can write down the partition functional on the lattice

$$\mathcal{Z} = \int [dU][d\bar{\psi}][d\psi] e^{-S_G - \bar{\psi} M(U) \psi}, \tag{1.16}$$

where $M = D + m$ and $S_G(U)$ is the gauge action written in terms of gauge links. We use the symbol "[ ]" in integrands $[dU], [d\bar{\psi}]$ and $[\psi]$ to denote the integration over all field configurations. For each configuration, one specifies values of all the fields on all lattice sites and links. For example, $[dU]$ is actually $\prod_{i,x} dU_i(x)$ in which indices x and i run over all lattice points and four directions in 4-D space-time, and $dU_i(x)$ is the Haar measure on the group. The expectation value of a physical quantity $\mathcal{O}$ can be calculated from the ratio

$$\langle \mathcal{O} \rangle = \frac{\int [dU][d\bar{\psi}][d\psi] \mathcal{O} e^{-S_G(U) - \bar{\psi} M(U) \psi}}{\mathcal{Z}}. \tag{1.17}$$

One can integrate the fermion part in the partition function $\mathcal{Z}$ and obtain

$$\mathcal{Z} = \int [dU] e^{-S_G(U)} \det[M(U)], \tag{1.18}$$

and the expectation value of $\mathcal{O}$ becomes

$$\langle \mathcal{O} \rangle = \frac{\int [dU] \mathcal{O} e^{-S_G(U)} \det[M(U)]}{\mathcal{Z}}. \tag{1.19}$$

To perform the multi-dimensional integral, one has to rely on numerical methods like Monte Carlo or molecular dynamics. It turns out that it is more efficient to use the method of importance sampling: One generates a set of gauge field configurations

$\mathcal{U}_1, \mathcal{U}_2, \cdots, \mathcal{U}_N$ with the probability of each configuration $\propto e^{-S_G(U)} \det[M(U)]$. Then the average value $\bar{\mathcal{O}}$ will be a good approximation to $\langle \mathcal{O} \rangle$ if N is large:

$$\bar{\mathcal{O}} = \frac{1}{N} \sum_{i=1}^{N} \mathcal{O}(\mathcal{U}_i) \simeq \langle \mathcal{O} \rangle, \tag{1.20}$$

where $\mathcal{O}(\mathcal{U}_i)$ is the physical oberservable $\mathcal{O}$ measured on the i-th gauge field configuration. The configuration average $\bar{\mathcal{O}}$ will approach the true expectation value $\langle \mathcal{O} \rangle$ in the limit $N \to \infty$.

Since the fermion determinant $\det[M(U)]$ is not a local function of the gauge field U, it is expensive to calculate its change under a change in the gauge field. As a result, people used to ignore its effect by replacing it just by 1, which is the so-called "quenched" approximation. Under this approximation, the equation (1.19) takes the quenched version

$$\langle \mathcal{O} \rangle_{quenched} = \frac{\int [dU] \mathcal{O} e^{-S_G(U)}}{\int [dU] e^{-S_G(U)}}. \tag{1.21}$$

In the language of Feynman diagrams, using the quenched approximation is equivalent to ignoring all internal quark loops. The underlying theory is not really QCD, and it is not easy to estimate the systematic errors of results from quenched calculations. Nowadays, with much more powerful supercomputers and large scale clusters, dynamical (unquenched) simulations have become the norm, and the results are now much more reliable than the quenched ones.

1.6 Measuring physical quantities on the lattice

Various physical quantities can be constructed from the gauge field links $U_i(x)$ and/or fermion fields $\bar{\psi}(x), \psi(x)$. A very important kind of physical observable is particle

spectroscopy, *i.e.*, masses of mesons, baryons and glueballs. Since the main topic of this work is about light mesons, here we illustrate the method of measuring their masses on the lattice.

Suppose we already have gauge field ensemble including many gauge configurations. For an operator $\mathcal{O}(x,t)$, which annihilates a particle at space-time (x,t), we can calculate the correlation function $\langle\mathcal{O}(x,t)\mathcal{O}^\dagger(0,0)\rangle$ by inserting a complete set of energy eigenstates $1=\sum_{n=1}^{\infty}|n\rangle\langle n|$

$$\begin{aligned} C_{\mathcal{O}^\dagger\mathcal{O}}(t) &= \langle\mathcal{O}(x,t)\mathcal{O}^\dagger(0,0)\rangle, \\ &= \sum_n \langle 0|\mathcal{O}(x,t)|n\rangle\langle n|\mathcal{O}^\dagger(0,0)|0\rangle, \\ &= \sum_n \langle 0|\mathcal{O}(x)|n\rangle\langle n|\mathcal{O}^\dagger|0\rangle e^{-E_n t}, \end{aligned} \tag{1.22}$$

where E_n is the energy of the state $|n\rangle$. In the last step in Eq. (1.22) we have used the equation (5.43) in appendix. If we are only interested in states with momentum p, we can calculate the correlation function of the operator $\sum_x e^{ipx}\mathcal{O}(x,t)$. For zero-momentum states, the operator is simply $\sum_x \mathcal{O}(x,t)$ and now $E_n \to M_n$, the mass of the n-th state, and the correlation function is

$$\begin{aligned} C_{\mathcal{O}^\dagger\mathcal{O}}(t) &= \langle\sum_x \mathcal{O}(x,t)\mathcal{O}^\dagger(0,0)\rangle \\ &= \sum_n \langle 0|\mathcal{O}|n\rangle\langle n|\mathcal{O}^\dagger|0\rangle e^{-M_n t}. \end{aligned} \tag{1.23}$$

Note that only those states $|n\rangle$ with the same quantum numbers as the desired state $\mathcal{O}^\dagger|0\rangle$ can contribute. Here we assume that the index n only takes values for these states, where $|1\rangle$ is the one with the lowest energy (or mass in zero-momentum case). If the time separation t is large enough, the contribution from the state $|1\rangle$ will

dominate the summation and the correlation function is

$$C_{\mathcal{O}^\dagger\mathcal{O}}(t) \simeq |\langle 0|\mathcal{O}|1\rangle|^2 e^{-M_1 t}. \tag{1.24}$$

For any t, we define effective mass of the propagator by

$$m(t) = \log\left(\frac{C(t)}{C(t+1)}\right). \tag{1.25}$$

The asymptotic value of $m(t)$ will be M_1. In practice, the mass M_1 can be found from the "plateau" on the plot of $m(t)$ as a function of time distance t.

In practice, this process is in some sense inverted. We want to know the mass of a particle like a pion. Our task is then to find the interpolating operator $\mathcal{O}$ which has the same quantum numbers as a pion. In general, there can be many choices of an operator with the desired quantum numbers. A good choice can make the overlap with the desired state large (or the overlap with other states small) so that one can achieve a better signal to noise ratio.

1.6.1 Extrapolations

Results obtained on the lattice are "physical" quantities at finite lattice spacing, finite volume and usually with unphysical light quark masses. The real physical regime is in the continuum limit, infinite volume and with physical light quark masses. Several extrapolations are needed to obtain results in this region from results obtained on the lattice. These are continuum extrapolations, infinite volume extrapolations and light quark mass extrapolations.

We use the lattice as a cutoff method. However, this is artificial since the real world is still continuous, at least to the energy scale which can be probed today.

Therefore, an extrapolation to the point $a = 0$ is needed. This can be done by doing lattice calculations with several different lattice spacings and extrapolating the quantity according to some function of a. The form of this function usually depends on the action used in the simulations.

Similarly, the lattice simulations are done within a finite volume, while the real case is infinite volume (relative to the scale of strong interactions). One performs calculations with several choices of volumes, and then extrapolates the results to the limit where $L \to \infty$.

At present, most lattice QCD simulations are done with unphysical light sea quark masses. The masses of up and down sea quarks in the simulations are heavier than their physical values. This is due to two reasons:

- Simulations with small quark masses need more computing power. When the quark mass gets smaller, the condition number κ of the Dirac matrix $(\not{D} + m)$ becomes large.[1] The complex conjugate (CG) algorithm, which is used to invert Dirac matrices, slows down.

- The finite volume corrections from a particle of mass m are $\sim e^{-mL}$. Since the lightest pseudoscalar, the pion, couples to all physical states, we should have $m_\pi L \gg 1$ so that finite volume corrections are negligible. In practice, this condition is often set to be $m_\pi L \geq 4$. When light quark masses are smaller, a bigger lattice with larger $L = Na$ is needed, and this requires more computing resources.

[1] The condition number of a positive hermitian matrix A is $\kappa = \lambda_{max}/\lambda_{min}$, where λ_{max} and λ_{min} are maximal and minimal eigenvalues of A.

The physical quantities calculated with unphysical light quark masses are thus not the quantities corresponding to the real world. One needs to perform the calculations at several different quark masses and extrapolate the results to the point with physical light quark mass.

It turns out that all of these three extrapolations can be done with the help of chiral perturbation theory (χPT), which we will talk about in Chapter [3]. After all these extrapolations, one finally obtains the physical quantity which can be used to compare with experiments or serve as input to other models/theories.

Chapter 2

Staggered Fermions

We know that the naive fermion action on the lattice has the issue of doubling. People have been using several different fermion actions to deal with this problem. In this chapter, we will focus on the Kogut-Susskind fermion formalism, also called the staggered fermions. As a comparison, I will first give a brief discussion about the Wilson fermion formalism, which is more straightforward but also sacrifices more symmetries.

2.1 Wilson Fermions

One way to deal with the fermion doubling problem was proposed by Wilson [9]. In the naive fermion action, he added a second-derivative-like operator

$$S^W = -\frac{r}{2a}\sum_{x,\mu}\bar{\psi}(x)(\psi(x+a\hat{\mu}) - 2\psi(x) + \psi(x-a\hat{\mu})) \simeq -\frac{ar}{2}\bar{\psi}D^2\psi. \tag{2.1}$$

This is an dimension-five operator with an explicit factor of lattice spacing a. In the language of the renormalization group, this term is "irrelevant" in the continuum

limit $a \to 0$. In tree processes, its effects explicitly vanish in this limit, and in divergent loop diagrams, it only serves to renormalize lower-dimension operators. Therefore, one can always add this term to the naive action without changing the desired continuum action.

Adding S^W to the naive fermion action S^{naive}, we obtain the Wilson action

$$\begin{aligned} S^{naive+W} &= m_q \sum_x \bar{\psi}(x)\psi(x) + \frac{1}{2a}\sum_{x,\mu} \bar{\psi}(x)\gamma_\mu(\psi(x+a\hat{\mu}) - \psi(x-a\hat{\mu})) \\ &\quad - \frac{r}{2a}\sum_{x,\mu} \bar{\psi}(x)[\psi(x+a\hat{\mu}) - 2\psi(x) + \psi(x-a\hat{\mu})] \\ &= \sum_{x,\mu} \bar{\Psi}_x M_{xy} \Psi(x), \end{aligned} \tag{2.2}$$

where the Dirac matrix M_{xy} is

$$M_{xy}a = \delta_{xy} - \kappa \sum_\mu [(r-\gamma_\mu)\delta_{x,y-a\hat{\mu}} - (r+\gamma_\mu)\delta_{x,y+a\hat{\mu}}], \tag{2.3}$$

with the rescaled field $\Psi = \psi/\sqrt{2\kappa}$ and hopping parameter $\kappa = 1/(2m_q a + 8r)$. We can see that the free fermion propagator (in absence of gauge fields) in momentum space is:

$$\begin{aligned} S(p) = M^{-1}(p) &= \frac{a}{1 - 2\kappa \sum_\mu (r\cos(p_\mu a) - i\gamma_\mu \sin(p_\mu a))} \\ &= \frac{(m_q a + 4r)}{\frac{1}{a}\left[\sum_\mu (i\gamma_\mu \sin(p_\mu a)) + m_q a + \sum_\mu r(1-\cos(p_\mu a))\right]}, \end{aligned} \tag{2.4}$$

where we have used the definition of the hopping parameter κ in the last step. The term $\sum_\mu r(1-\cos(p_\mu a))$ in Eq. (2.4) acts just like a mass term, which gives all the doublers, except the one at $p = (0,0,0,0)$, an effective mass at the order of $\frac{2r}{a}$. For example, the doubler near $p = (\frac{\pi}{a}, 0, 0, 0)$ in the Brillouin zone obtains an additional mass $\cong r(1 - 2\cos(\pi))/a = 2r/a$. In the continuum limit, these fiveteen doublers

become heavy ($\sim \frac{1}{a}$) and thus decouple from the theory. The only physical pole in the propagator is the state located at $p = (0, 0, 0, 0)$ in the Brillouin zone. Thus the Wilson fermion action is free of doublers.

By using the following property of the the naive Dirac matrix

$$\gamma_5 D^{naive} \gamma_5 = -D^{naive}, \tag{2.5}$$

one can see that in the massless limit, the naive fermion action is invariant under the global chiral transformation $\psi \to e^{i\epsilon\gamma_5}\psi, \bar{\psi} \to \bar{\psi}e^{i\epsilon\gamma_5}$. Indeed,

$$\begin{aligned} S^{naive} = \bar{\psi} D_{naive} \psi &\to \bar{\psi} e^{i\epsilon\gamma_5} D_{naive} e^{i\epsilon\gamma_5} \psi \\ &= \bar{\psi} e^{i\epsilon\gamma_5} e^{-i\epsilon\gamma_5} D_{naive} \psi \\ &= \bar{\psi} D_{naive} \psi \\ &= S^{naive}. \end{aligned} \tag{2.6}$$

The naive fermion action thus keeps the chiral symmetry although it suffers from the problem of doublers. On the contrary, the Wilson action, while free from doublers, breaks the chiral symmetry at $\mathcal{O}(a)$ since the Wilson term acts like a mass term and it is not invariant under the global chiral transformation. This is the main drawback of the Wilson fermion formalism. Due to the lack of chiral symmetry, the quarks can obtain masses even if the bare quark masses are zero, and this makes the data analysis more complicated. Furthermore, without the protection of chiral symmetry, in simulations with Wilson quarks at small masses, one may encounter "exceptional" configurations where the results become divergent and thus ruin the calculations [4].

While the discretization errors of the naive fermion action is at $\mathcal{O}(a^2)$, The Wilson fermion action has discretization errors at $\mathcal{O}(a)$. One can remove the $\mathcal{O}(a)$ lattice

artifacts by adding another irrelevant dimension-five operator and choosing appropriate coefficients. This new operator is called the Sheikholeslami-Wohlert (SW) term, or the clover term.

$$S_{SW} = \frac{iaq}{4} c_{SW} \sum_x \bar{\phi}(x) \sigma_{\mu\nu} \mathcal{F}_{\mu\nu}(x) \phi(x), \tag{2.7}$$

where $\mathcal{F}_{\mu\nu}$ is the field strength and $\sigma_{\mu\nu} = \frac{i}{2}[\gamma_\mu, \gamma_\nu]$. Nowadays, the clover action is more widely used than the original Wilson action.

2.2 Staggered Fermions

Another way to reduce the number of doublers is to use the staggered fermions [10]. The idea is to diagonalize the Dirac matrices γ_μ by making a local change of variables $\bar{\psi}(x)$ and $\psi(x)$ in the naive fermion action:

$$\bar{\psi}(x) = \bar{\chi}(x)\Omega_x^\dagger, \quad \psi(x) = \Omega_x \chi(x), \tag{2.8}$$

where Ω_x is a 4×4 unitary matrix.

There are many solutions for Ω_x, one choice is

$$A_x = \Gamma_x = \gamma_1^{x_1/a} \gamma_2^{x_2/a} \gamma_3^{x_3/a} \gamma_4^{x_4/a}. \tag{2.9}$$

Making substitutions in Eq. (2.8) and using the identity

$$\Gamma_x^\dagger \gamma_\mu \Gamma_{x+\mu} = (-1)^{\sum_{\nu<\mu} x_\nu} \; I, \tag{2.10}$$

one can write the free fermion action as

$$S^{KS} = m_q \sum_x \bar{\chi}(x)\chi(x) + \frac{1}{2a} \sum_{x,\mu} \bar{\chi}(x)\eta_\mu(x) \; I[\chi(x + a\hat{\mu}) - \chi(x - a\hat{\mu})]. \tag{2.11}$$

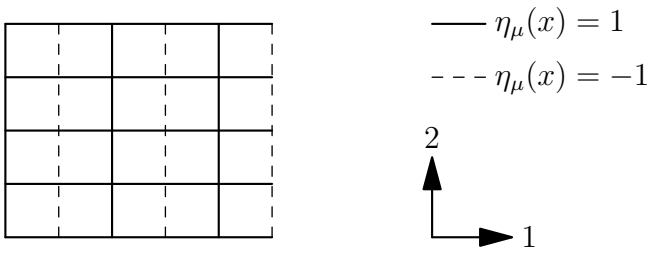

Figure 2.1: A 2-D schematic diagram showing the values of $\eta_\mu(x)$ on the lattice.

Here, I is the 4×4 identity matrix with Dirac indices and the phase factor $\eta_\mu(x)$ is

$$\eta_\mu(x) = (-1)^{\sum_{\nu<\mu} x_\nu/a}, \quad \eta_1(x) = 1. \tag{2.12}$$

$\eta_\mu(x)$ is an alternating number defined on the links between the nearest neighbor lattice sites with period $2a$, as shown in figure 2.1 in two-dimensional spacetime.

In Eq. (2.11), four Dirac components of the field $\chi(x)$ are decoupled and they are all completely equivalent. One can choose to keep only one Dirac component on each lattice site x, hence reduce the degrees of freedom by a factor of four. This will, in turn, reduce the number of doublers from sixteen to four. The presence of these four doublers can be seen more clearly in the spin-taste basis discussed below.

Based on the fact that Γ_x and $\eta_\mu(x)$ are periodic functions of x with period $2a$, it is natural to treat the 2^4 hyper-cubic lattice as the new unit cell. The sixteen components of the one-component field $\chi(x)$ in a hypercube can be collected into a new field $q(y)_{\alpha i}$ [11, 12]

$$q(y)_{\alpha i} = \frac{1}{8}\sum_A (\Gamma_A)_{\alpha i}\chi(2y + aA), \tag{2.13}$$

$$\bar{q}(y)_{i\alpha} = \frac{1}{8}\sum_A \bar{\chi}(2y + aA)(\Gamma_A)^\dagger_{i\alpha}, \tag{2.14}$$

where A is any one of the 16 vectors with components $A_\mu = 0$ or 1, and matrices

$\Gamma_A = \gamma_1^{A_1}\gamma_2^{A_2}\gamma_3^{A_3}\gamma_4^{A_4}$ are the same as defined above, and $2y + aA$ is where the original one-component field χ is defined. In Eqs. (2.13) and (2.14), indices α and i both run from 1 to 4. It turns out that the index α can be interpreted as the Dirac index and the index i represents the duplicity of four doublers. We call these doublers four "tastes" to be distinguished from "flavors". Correspondingly, the basis formed by the new field $q(y)_{\alpha i}$ is the so-called spin-taste basis.

The staggered action in Eq. (2.11) can be written in spin-taste basis as [13, 12]:

$$S^{KS} = 16 \sum_y \bar{q}(y) \left\{ m(I \otimes I) + \sum_\mu [(\gamma_\mu \otimes I) \bigtriangledown_\mu + a(\gamma_5 \otimes \xi_\mu \xi_5) \bigtriangleup_\mu] \right\} q(y), \quad (2.15)$$

where the taste matrices $\xi_\mu = \gamma_\mu^*$. The first and second-derivative operators $\bigtriangledown_\mu$ and $\bigtriangleup_\mu$ are defined as

$$\bigtriangledown_\mu f(y) = \frac{1}{4a}[f(y + 2a\hat{\mu}) - f(y - 2a\hat{\mu})], \quad (2.16)$$

$$\bigtriangleup_\mu f(y) = \frac{1}{4a^2}[f(y + 2a\hat{\mu}) - 2f(y) + f(y - 2a\hat{\mu})]. \quad (2.17)$$

For each flavor of fermions, the four doublers are shown explicitly, and there are no more doublers for the new field $q(y)$ which is defined on the "coarser" lattices.

All the above discussions are for free staggered fermions, *i.e.*, no gauge fields are involved. However, it is the interacting theory that we are interested since our goal is to simulate QCD where both fermions and gluons are present. From the free staggered action Eq. (2.11), the interacting action can be obtained by inserting appropriate gauge links $U_\mu(x)$ between nearest-neighbor lattice sites.

$$S_{int}^{KS} = m_q \sum_x \bar{\chi}(x)\chi(x) + \frac{1}{2a} \sum_{x,\mu} \bar{\chi}(x)\eta_\mu(x)\ I[U_\mu(x)\chi(x + a\hat{\mu}) - U_\mu^\dagger(x - a\hat{\mu})\chi(x - a\hat{\mu})]. \quad (2.18)$$

When we go to spin-taste basis, the definitions of $q(y)_{\alpha i}$ and $\bar{q}(y)_{i\alpha}$ in Eq. (2.14) are changed to

$$q(y)_{\alpha i} = \frac{1}{8}\sum_A U_A(y)(\Gamma_A)_{\alpha i}\chi(2y + aA), \tag{2.19}$$

$$\bar{q}(y)_{i\alpha} = \frac{1}{8}\sum_A \bar{\chi}(2y + aA)U_A^\dagger(y)(\Gamma_A)^\dagger_{i\alpha}, \tag{2.20}$$

where $U_A(y)$ is the product of gauge links along some path from $x = 2y$ to $x = 2y + aA$. Consequently, the interacting action in spin-taste basis now takes a much more complicated form

$$S_{int}^{KS} = 16\sum_y \bar{q}(y)\left\{m(I\otimes I) + \sum_\mu[(\gamma_\mu\otimes I)\bigtriangledown_\mu + aS_5 + a^2S_6 + \cdots]\right\}q(y), \tag{2.21}$$

where S_5 contains several dimension-five operators which break taste symmetries. The key point is that in the continuum limit $a \to 0$, these taste symmetry breaking effects are suppressed and one obtain a continuum theory with four degenerate tastes.

2.2.1 Symmetries of the staggered action

For simplicity, we consider the single-flavor staggered action with interaction to gauge fields. The action can be written in one-component basis as Eq. (2.18) or in spin-taste basis as Eq. (2.21).

In Eq. (2.21), the tastes can be treated in the same way as flavors, the symmetries and breaking patterns look very similar to those of ordinary χPT. In the continuum and massless limits, *i.e.*, $a \to 0, m \to 0$, only the kinetic term in Eq. (2.21) is left. The action has a $SU(4)_L \times SU(4)_R \times U(1)_V$ chiral symmetry where the axial symmetry $U(1)_A$ is violated due to the anomaly. The $U(1)_V$ part represents the fermion number

conservation and thus is trivial. The $SU(4)_L \times SU(4)_R$ symmetry is spontaneously broken to the diagonal $SU(4)_V$ vector symmetry, giving rise to fifteen massless Goldstone bosons. The mass term, $\sum_y \bar{q}(y) m (I \otimes I) q(y)$, breaks the $SU(4)_L \times SU(4)_R$ symmetry explicitly to $SU(4)_V$ and gives the Goldstone bosons masses $m_G^2 \propto m_q$.

A key point here is that even if the mass term is zero, the irrelevant terms in Eq. (2.21), *e.g.*, aS_5 and $a^2 S_6$, break the chiral symmetry explicitly at finite lattice spacing a because of the explicit taste structures in those terms. In the simpler case of free staggered fermion, this can be seen from the taste matrices $\sum_\mu \xi_\mu \xi_5$ in the last term in Eq. (2.15).[1] If the lattice spacing a is small enough so that the taste-violations can be treated as perturbations, these taste-violating terms then give Goldstone bosons finite masses, just as small quark mass terms do.

It turns out that, at finite lattice spacing but zero mass, symmetries of the one-flavor staggered fermion can be seen more clearly in the one-component basis. If we set $m = 0$ in Eq. (2.18), the action has a $U(1)_e \times U(1)_o$ even-odd symmetry [12]

$$\chi(x) \to e^{i\alpha_e} \chi(x), \qquad \bar{\chi}(x) \to \bar{\chi}(x) e^{-i\alpha_o}, \quad \text{if x = even}, \tag{2.22}$$

$$\chi(x) \to e^{i\alpha_o} \chi(x), \qquad \bar{\chi}(x) \to \bar{\chi}(x) e^{-i\alpha_e}, \quad \text{if x = odd}, \tag{2.23}$$

where a site is called oven or odd if $\sum_\mu (x_\mu/a)$ is even or odd. This even-odd symmetry is broken to the diagonal $U(1)_V$ symmetry ($\alpha_e = \alpha_o \equiv \alpha_V$) if we turn on the mass term.

Here, the even-odd symmetry looks very similar to a chiral symmetry. However, it turns out that there is a fundamental difference in the axial part. The axial even-odd

[1] Actually, the presence of Dirac matrix γ_5 in this term also breaks the chiral symmetry to a vector symmetry.

symmetry, where $\alpha_e = -\alpha_o \equiv \alpha_\epsilon$, takes the form in spin-taste basis

$$q(y) \to e^{i\alpha_\epsilon(\gamma_5 \otimes \xi_5)} q(y), \quad \bar{q}(y) \to \bar{q}(y) e^{i\alpha_\epsilon(\gamma_5 \otimes \xi_5)}. \tag{2.24}$$

This symmetry, called the $U(1)_\epsilon$ symmetry, is a taste non-singlet and thus free from the anomaly. It is kept as a symmetry on the quantum level when the mass term is zero, in contrast to the axial chiral symmetry which is violated due to the anomaly. An important consequence is that this $U(1)_\epsilon$ symmetry, together with other staggered symmetries, guarantees that there will not be any mass-term contributions from loop calculations if the bare quark mass is zero [14], *i.e.*, there is no additive mass renormalization for staggered fermions, contrary to the case of Wilson fermions.

To summarize, in the continuum limit with zero mass, the one-flavor staggered fermion action is invariant under a $SU(4)_L \times SU(4)_R \times U(1)_V$ symmetry which is then spontaneously broken to $SU(4)_V \times U(1)_V$. This gives fifteen massless Goldstone bosons. The mass term and the third term in Eq. (2.15) both break the $SU(4)_L \times SU(4)_R$ symmetry explicitly and give Goldstone bosons masses. The symmetry is finally broken to $U(1)_V$, the vector subgroup of $U(1)_e \times U(1)_o$, at finite lattice spacing with nonzero mass.

Untill now we have only talked about continuous symmetries. The staggered action also has many discrete symmetries including the shift symmetry, axis inversions, charge conjugate, *etc.* For a more complete discussion of the staggered symmetry group, see Ref. [12] and references therein.

2.2.2 Fourth-root procedure

As one can see from the spin-taste basis, there are four taste species for each flavor of quarks, and these four species are completely degenerate. The fermion action is block diagonal in taste space in the continuum limit, so each one contributes equally to the fermion determinant in the path integral formalism. One can get rid of the extra degrees of freedom by taking the fourth root of the fermion determinant and using it in generating gauge configurations. The partition function is then

$$\mathcal{Z} = \int [dU] e^{-S_G(U)} \det{}^{\frac{1}{4}}[M(U)]. \tag{2.25}$$

Although this is naively correct in the continuum limit, it may cause some concerns because of the behavior at finite lattice spacings. It has been shown that the fourth-root procedure produces, non-perturbatively, violations of locality at non-zero lattice spacing [15]. However, work over the last few years indicates that locality and universality are restored in the continuum limit of the lattice theory [16, 17, 18, 19]. Throughout this work, we will assume that the usage of the fourth-root procedure is legitimate.

2.3 The "asqtad" staggered action

2.3.1 Tadpole improvement

In this section, we will talk about an important improvement in the gauge field sector, the so-called "tadpole" improvement. Below, I will follow the discussions in Ref. [8] closely.

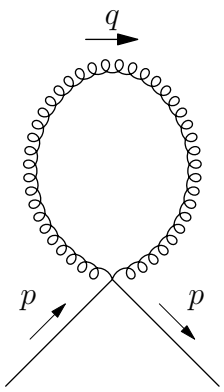

Figure 2.2: A tadpole diagram for the fermion self energy in the lattice perturbation theory.

Gauge fields are formulated on the lattice as gauge links $U_\mu(x) = e^{iagA_\mu(x)}$ connecting adjacent lattice sites. Expanding $U_\mu(x)$ in lattice spacing a,

$$U_\mu(x) = e^{iagA_\mu(x)} = 1 + iagA_\mu(x) - \frac{a^2g^2}{2}A_\mu^2(x) + \cdots \tag{2.26}$$

one finds that the third term generates a vertex where two quarks are connected to two gluons, while this vertex is absent in continuum QCD. These lattice artifacts should go away when one approaches the continuum limit $a \to 0$. However, it was shown that the artifacts, instead of being suppressed by powers of a, are only suppressed by powers of g^2 due to the effects of so-called tadpole diagrams [20]. In these diagrams, the ultraviolet divergences generated by the gluon loops would introduce a factor of $1/a^2$ which cancels the explicit a dependence of the vertex, hence only a factor of g^2 is left. A mean-field approach is proposed to remove these lattice artifacts. Notice that the divergence comes from the high momentum part of the gauge field, and one can split the gauge field into a high momentum (UV) part and a low momentum (IR)

part. By integrating out the UV part, one can write down the effective gauge link,

$$U_\mu(x) = e^{iag(A_\mu^{UV}(x)+A_\mu^{IR}(x))} = u_0 e^{iagA_\mu^{IR}(x)} = u_0\tilde{U}_\mu(x), \tag{2.27}$$

where u_0 is the tadpole factor. One then replaces all the gauge links $U_\mu(x)$ in the lattice action by $u_0\tilde{U}_\mu(x)$, and absorbs the tadpole factor u_0 in the coupling constant g to get the tadpole improved action. For example, the Wilson gauge action becomes

$$S_g = \sum \frac{1}{g^2}(\mathrm{Tr}U_p + h.c.) = \sum \frac{u_0^4}{g^2}(\mathrm{Tr}\tilde{U}_p + h.c.) = \frac{1}{\hat{g}^2}(\mathrm{Tr}\tilde{U}_p + h.c.), \tag{2.28}$$

where the rescaled coupling constant $\hat{g}^2 = g^2/u_0^4$. The perturbation theory in $\hat{g}^2$ then has no tadpoles and the convergence is improved [4].

There are two common choices for the tadpole factor u_0: one is the expectation value of the gauge links in Landau gauge, another is the fourth root of the expectation value of the plaquette,

$$u_0 = (\overline{\mathrm{Tr}U_p})^{1/4}. \tag{2.29}$$

These values are usually determined non-perturbatively.

2.3.2 Asqtad improved staggered fermions

From previous discussion, we know that at finite lattice spacing, the mass term and taste-violating term in the staggered action in Eq. (2.15) both break the taste symmetry explicitly and give Goldstone bosons masses. In typical numerical simulations, the contributions to Goldstone boson masses from taste-violations could be larger than those from finite quark masses. This makes it difficult to take the continuum limit, since lattice artifacts dominate over the physical effect from the mass. The

situation can be improved if one uses some modified versions of the staggered actions on the lattice that can reduce the taste-violations.

An important version of the improved staggered action is the so-called "asqtad" action. In the following discussions about the implementation of this action, I will follow closely to Ref. [12].

Recall that for every flavor of staggered fermion, the four taste species live on adjacent sites within the 2^4 hyper-cubic lattice. In momentum space, a fermion can change its taste by emitting or absorbing a gluon with momentum π/a. It is exchanging of these high momentum gluons that gives rise to the taste-violating effects, as shown in figure (2.3). Thus taste violations can be reduced by suppressing the coupling to these UV gluons in the staggered action [12]. Since the quarks on the lattice are connected by gauge links $U_\mu(x)$, the coupling between fermions and gluons can be altered by changing $U_\mu(x)$ in the interacting staggered fermion action. Instead of the original "thin links", one uses the "fat links" where products of link variables over different paths from site x to site $x + a\mu$ are added to the gauge links.

For example, one can make the substitution

$$U_\mu(x) \to U_\mu(x) + \omega a^2 \sum_{\nu \neq \mu} \Delta^l_\nu U_\mu(x), \tag{2.30}$$

where the lattice Laplacian Δ^l_ν is defined as

$$\Delta^l_\nu U_\mu(x) = \frac{1}{a^2}[U_\nu(x)U_\mu(x+a\hat{\nu})U_\nu\dagger(x+a\hat{\mu})+U^\dagger_\nu(x-a\hat{\nu})U_\mu(x-a\hat{\nu})U_\nu(x-a\hat{\nu}+a\hat{\mu})-2U_\mu(x)]. \tag{2.31}$$

After coupling to fermions, the second term in Eq. (2.30) produces a new term in the fermion action. Because of the explicit factor of a^2, this term vanishes as $a \to 0$,

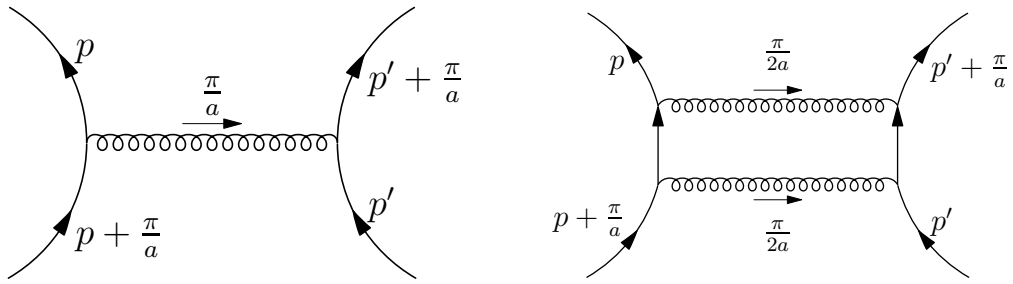

(a) (b)

Figure 2.3: Four-fermion taste violation diagrams. Two incoming fermions change their tastes by exchanging a gluon with momentum π/a as shown in figure (a), or exchanging two or more gluons with total momentum π/a as shown in figure (b). hence it does not change the desired continuum action.

In momentum space, one can expand $U_\mu(x)$ to first order in g and get the following substitution rule [12]:

$$A_\mu(p) \to A_\mu(p) + \omega \sum_{\nu \neq \mu} [2A_\mu(p)(\cos(ap_\nu) - 1) + 4\sin(\frac{ap_\mu}{2})\sin(\frac{ap_\nu}{2})A_\nu(p)]. \quad (2.32)$$

The second term in Eq. (2.30) is actually a 3-link staple shown in figure 2.4(a). If one sets the coefficient $\omega = 1/4$, one can eliminate the coupling to gluons $A_\mu(p)$ with one single transverse momentum $p_\nu(\nu \neq \mu) = \frac{\pi}{a}$. Coupling to longitudinal gluons with $\nu = \mu$ is automatically cancelled between the forward and backward parts of the lattice fermion derivatives [21]. Similarly, 5-link and 7-link staples can be added to eliminate the coupling to gluons with more components of momentum equal to π/a [12]

$$U_\mu(x) \to U_\mu^{f7}(x) = U_\mu(x) + \frac{a^2}{4}\sum_{\nu \neq \mu} \Delta_\nu^l U_\mu(x) + \frac{a^4}{32}\sum_{\rho \neq \nu \neq \mu} \Delta_\rho^l \Delta_\nu^l U_\mu(x)$$
$$+ \frac{a^6}{384}\sum_{\sigma \neq \rho \neq \nu \neq \mu} \Delta_\sigma^l \Delta_\rho^l \Delta_\nu^l U_\mu(x). \quad (2.33)$$

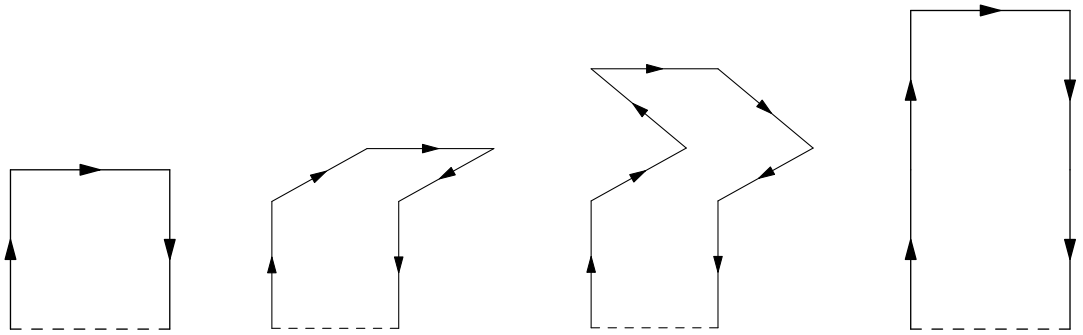

(a) 3-link staple (b) 5-link staple (c) 7-link staple (d) straight 5-link staple

Figure 2.4: Multi-link staples used in the "asq" action

Furthermore, one can add the "straight 5-link staples" [22] in the gauge link $U_\mu(x)$ and the Naik term [23] in fermion derivative to get the complete $\mathcal{O}(a^2)$ improved staggered action - so-called "asq" action.

$$U_\mu(x) \to U_\mu^{f7L}(x) = U_\mu^{f7} - \frac{a^2}{4}\sum_{\nu\neq\mu}\Delta_\nu^{2l}U_\mu(x), \tag{2.34}$$

$$\nabla_\mu\chi(x) \to \nabla_\mu\chi(x) - \frac{a^2}{6}(\Delta_\mu)^3\chi(x). \tag{2.35}$$

Finally, one can replace the coefficients in this action by the tadpole improved ones, obtaining the final version of "asqtad" improved fermion action, which is the action used extensively by the MILC collaboration. The asqtad action reduces the taste violations and has better scaling properties than the ordinary staggered action.

Although the fat links eliminate coupling to a single gluon with transverse momentum components as π/a, taste-violations can still occur by exchanging two or more gluons with total momentum π/a, as shown in figure (2.3(b)). The taste-violations for asqtad fermions are at $\mathcal{O}(\alpha_s^2 a^2)$, while the generic discretization errors are at $\mathcal{O}(\alpha_s a^2)$.

Chapter 3

Staggered Chiral Perturbation Theory

Although lattice QCD is the most powerful non-perturbative method from first principles, it is very difficult to simulate continuum QCD with physical light quark masses ($m_u, m_d \sim m_l$). The reason is that the computing resources needed in simulations grow like, roughly speaking, four to six powers of $1/m_l$, depending on the algorithms. Simulations with physical light quark masses and reasonable size of lattices are extremely difficult and time consuming to implement on modern supercomputers. In practice, one usually performs simulations at several different light quark masses which are higher than the physical values, and then extrapolates the results, *i.e.*, hadron masses, decay constant, *etc.*, to the point with physical light quark masses. A systematic way to do the extrapolation is to use the chiral perturbation theory (χPT). In χPT, the functional dependences of physical quantities on the light quark masses are given explicitly, thus can be used as the fit functions to guide us to the

chiral limit.

3.1 Chiral Perturbation Theory

It is a fact that masses of three light quarks up, down and strange are much smaller than other three quarks charm, bottom and top [24]:

$$\left(\begin{array}{l} m_u = 0.005\text{GeV} \\ m_d = 0.009\text{GeV} \\ m_s = 0.175\text{GeV} \end{array}\right) \ll 1\text{GeV} \leq \left(\begin{array}{l} m_c = (1.15 - 1.35)\text{GeV} \\ m_b = (4.0 - 4.4)\text{GeV} \\ m_t = 174\text{GeV} \end{array}\right), \tag{3.1}$$

where the scale 1GeV is approximately the mass of a typical hadron composed of light quarks, *e.g.*, $m_\rho = 770$MeV. If we are only interested in the physics of those light hadrons, we can, to an excellent approximation, ignore the three heavy quarks aside from their perturbative effects and consider the QCD sector of light quarks only. The QCD Lagrangian for light quarks is:

$$\mathcal{L} = \bar{\psi}^f(x)(\not{D} + M)\psi^f(x), \tag{3.2}$$

where $f = u, d, s$ are flavor indices and automatically summed over, and M is the quark mass matrix in flavor basis:

$$M = \text{Diag}(m_u, m_d, m_s). \tag{3.3}$$

If we define the left hand field ψ_L and right hand field ψ_R

$$\psi_L = \frac{1}{2}(1 - \gamma_5)\psi, \qquad \psi_R = \frac{1}{2}(1 + \gamma_5)\psi, \tag{3.4}$$

$$\bar{\psi}_L = \bar{\psi}\frac{1}{2}(1 + \gamma_5), \qquad \bar{\psi}_R = \bar{\psi}\frac{1}{2}(1 - \gamma_5), \tag{3.5}$$

we can write Eq. (3.2) in the following form:

$$\mathcal{L} = \bar{\psi}_L^f(x) \not{D} \psi_L^f(x) + \bar{\psi}_R^f(x) \not{D} \psi_R^f(x) + \bar{\psi}_L^f(x) M \psi_R^f(x) + \bar{\psi}_R^f(x) M^\dagger \psi_L^f(x). \tag{3.6}$$

In the zero quark mass limit, *i.e.*, $m_u = m_d = m_s = 0$, this action is invariant under a global $U(3)_L \times U(3)_R$ transformation on the flavor basis:

$$\psi_L \to U_L \psi_L, \qquad \psi_R \to U_R \psi_R, \tag{3.7}$$

$$\bar{\psi}_L \to \bar{\psi}_L U_L^\dagger, \qquad \bar{\psi}_R \to \bar{\psi}_R U_R^\dagger, \tag{3.8}$$

with $U_{LR} \in U(3)$. We say that the action in Eq. (3.2) has the $U(3)_L \times U(3)_R$ chiral symmetry. It turns out that the axial $U(1)$ symmetry, with $U_L = U_R^\dagger = \exp(i\theta) I$, is violated due to chiral anomaly on the quantum level, hence the original chiral symmetry group is reduced to $SU(3)_L \times SU(3)_R \times U(1)_V$, with $U(1)_V$ corresponding to the quark number conversation. In the following, we will only concentrate on the $SU(3)_L \times SU(3)_R$ part.

Empirical facts about the hadron spectrum suggest that the chiral symmetry in QCD is spontaneously broken from $SU(3)_L \times SU(3)_R$ to its subgroup $SU(3)_V$ in which $U_L = U_R = U$. This will result in eight Nambu-Goldstone bosons with zero masses if the three light quarks are massless. Further analysis show that these bosons must be pseudoscalars. In reality, there are indeed eight light mesons with masses much smaller than other hadrons:

$$m_{\pi^+,\pi^-,\pi^0} \sim 140\text{MeV}, \tag{3.9}$$

$$m_{K^+,K^-,K^0,\bar{K}^0} \sim 500\text{MeV}, \tag{3.10}$$

$$m_\eta \sim 545\text{MeV}. \tag{3.11}$$

This can be explained if the three light quarks have nonzero but small masses compared to $\Lambda_{QCD} \sim 1\text{GeV}$, so that the massless pseudoscalar bosons obtain finite masses by treating the quark masses as small perturbations.

A systematic way to study the physics near the chiral limit in QCD is Chiral Perturbation Theory (χPT) [25, 26, 27]. The essential point of χPT that in the low energy region of QCD ($\Lambda \ll 1\text{GeV}$), the physics can be described by the effective field theory where the degrees of freedom are the light physical states, pseudoscalar mesons, instead of quarks and gluons. Possible terms of the effective theory are constrained by the underlying symmetries of QCD.

For χPT in the light meson sector, one can collect eight pseudo-Goldstone bosons into a field ϕ:

$$\phi = \begin{pmatrix} \frac{\pi^0}{\sqrt{2}} + \frac{\eta}{\sqrt{6}} & \pi^+ & K^+ \\ \pi^- & -\frac{\pi^0}{\sqrt{2}} + \frac{\eta}{\sqrt{6}} & K^0 \\ K^- & \bar{K}^0 & -\frac{2\eta}{\sqrt{6}} \end{pmatrix} \sim \begin{pmatrix} u\bar{u} & u\bar{d} & u\bar{s} \\ d\bar{u} & d\bar{d} & d\bar{s} \\ s\bar{u} & s\bar{d} & s\bar{s} \end{pmatrix}, \tag{3.12}$$

and define an $SU(3)$ matrix Σ in terms of ϕ as

$$\Sigma = \exp \frac{2i\phi}{f}. \tag{3.13}$$

Under a $SU(3)_L \times SU(3)_R$ chiral transformation, Σ and $\Sigma^\dagger$ transform as

$$\Sigma \to U_L \Sigma U_R^\dagger, \qquad \Sigma^\dagger \to U_R \Sigma^\dagger U_L^\dagger. \tag{3.14}$$

In the low energy region, physics is dominated by the would-be-Goldstone mesons (π, K, η, *etc.*) since their masses are significantly smaller than other hadrons. If we are only interested in this energy region, it is possible to construct an effective Lagrangian

in terms of matrices Σ and $\Sigma^\dagger$ since they actually describes the Goldstone bosons. The Lagrangian should be local, Lorentz invariant, and most importantly, invariant under $SU(3)_L \times SU(3)_R$ transformation. It turns out that the simplest term one can write down is $\mathrm{Tr}(\partial_\mu \Sigma \partial_\mu \Sigma^\dagger)$. Terms that only involve Σ and $\Sigma^\dagger$ without derivatives are trivial, which can be seen by using $\Sigma\Sigma^\dagger = 1$.

In the QCD Lagrangian, Eq. (3.6), the quark mass term breaks chiral symmetry explicitly. Contribution to the effective Lagrangian from quark masses can be obtained by using the "spurion" analysis. One images that under the $SU(3)_L \times SU(3)_R$ chiral transformation, the quark mass matrix M transforms as

$$M \to U_L M U_R^\dagger, \qquad M^\dagger \to U_R M^\dagger U_L^\dagger, \tag{3.15}$$

so that the last two terms in Eq. (3.6) are invariant under the chiral transformation. Now, with $\Sigma, \Sigma^\dagger$ and $M, M^\dagger$, one can construct a term $\mathrm{Tr}(M\Sigma^\dagger + M^\dagger\Sigma)$ in the effective Lagrangian. Note that the real quark mass matrix M is a constant matrix and does not transform, so the matrix M here is a "spurion". This analysis is useful to keep track of the chiral symmetry breaking patterns, and serves as a powerful tool in constructing chiral Lagrangians.

Now, one can write down the chiral Lagrangian (in Euclidean space):

$$\mathcal{L} = \frac{f^2}{8}\mathrm{Tr}(\partial_\mu \Sigma \partial_\mu \Sigma^\dagger) - \frac{\mu f^2}{4}\mathrm{Tr}(M\Sigma^\dagger + M^\dagger\Sigma), \tag{3.16}$$

where f and μ are two low energy constants (LEC). We will see later that f can be related to the pion decay constant, while μ is related to the quark condensate in the chiral limit.

Expanding Eq. (3.16) to second order, one finds the masses of these pseudo-Goldstone bosons:

$$M_{\pi^+}^2 = \mu(m_u + m_d), \tag{3.17}$$

$$M_{K^+}^2 = \mu(m_u + m_s), \tag{3.18}$$

$$M_{\pi^0}^2 = \mu(m_u + m_d + \mathcal{O}\left(\frac{(m_u - m_d)^2}{m_s}\right)), \tag{3.19}$$

$$M_{\eta}^2 = \frac{1}{3}\mu(m_u + m_d + 4m_s + \mathcal{O}\left(\frac{(m_u - m_d)^2}{m_s}\right)). \tag{3.20}$$

If one drops the terms proportional to $(m_u - m_d)^2/m_s$, which is $\sim 1/30$ of m_u or m_d, one finds the Gell-Mann-Okubo relation:

$$M_{\eta}^2 = \frac{1}{3}(2M_{K^+}^2 + 2M_{K^0}^2 - M_{\pi^+}^2), \tag{3.21}$$

which agrees with experimental data within a few percent. This is one piece of evidence that supports the validity of using this effective Lagrangian.

One can see from the formulae of meson masses that the quark mass m_q always appears together with μ as a scale-independent combination $\chi = 2\mu m_q$. It is then reasonable to treat the squared momentum of a physical (onshell) meson as the same order as the quark mass. That is, $p^2 \sim M_{meson}^2 \sim \mu m_q$, which is usually written as $p^2 \sim m_q$. According to this power counting rule, the two terms in the chiral Lagrangian given in Eq. (3.16) are the two lowest order terms. The Next-to-Leading (NLO) order will be $\mathcal{O}(p^4, p^2 m_q, m_q^2)$. The power counting is essential in χPT calculation, and it also plays an important role in the renormalization of χPT.

In general, one can introduce external currents in the QCD action and map them to the chiral Lagrangian. The rationale behind this external field approach is that,

in the absence of anomalies, the Ward Identities obeyed by the Green functions are equivalent to an invariance of the generating functional under a local transformation of the external fields [28]. In practice, four currents are added: left and right hand currents l_μ and r_μ, scalar and pseudoscalar quark densities s and p. They are all color-neutral, 3×3 hermitian matrices. The QCD action is

$$\begin{aligned}\mathcal{L}_{QCD} = \mathcal{L} =& \bar{\psi}_L^f(x)(\not{D} - i\gamma_\mu l_\mu)\psi_L^f(x) + \bar{\psi}_R^f(x)(\not{D} - i\gamma_\mu r_\mu)\psi_R^f(x) \\ &+ \bar{\psi}_L^f(x)(s+ip)\psi_R^f(x) + \bar{\psi}_R^f(x)(s-ip)\psi_L^f(x). \end{aligned} \tag{3.22}$$

Now, instead of global chiral transformations, we enforce a local chiral transformation. To make the QCD action invariant under this transformation, these external currents transform as

$$l_\mu \to U_L l_\mu U_L^\dagger - i\partial_\mu U_L U_L^\dagger, \tag{3.23}$$

$$r_\mu \to U_R r_\mu U_R^\dagger - i\partial_\mu U_R U_R^\dagger ., \tag{3.24}$$

$$(s+ip) \to U_L(s+ip)U_R^\dagger, \tag{3.25}$$

$$(s-ip) \to U_R(s-ip)U_L^\dagger. \tag{3.26}$$

Correspondingly, the partial derivative in the chiral Lagrangian is replaced by the covariant derivative D_μ to make the chiral Lagrangian invariant under local chiral transformations.

$$\partial_\mu \Sigma \to D_\mu \Sigma = \partial_\mu \Sigma - i l_\mu \Sigma + i \Sigma r_\mu. \tag{3.27}$$

One can see that in the presence of external currents, $D_\mu\Sigma$ transforms as $D_\mu\Sigma \to U_L D_\mu \Sigma U_R^\dagger$ under a chiral transformation. With these new building blocks, we can

write down the lowest order Lagrangian

$$\mathcal{L} = \frac{f^2}{8}\mathrm{Tr}(D_\mu \Sigma D_\mu \Sigma^\dagger) - \frac{f^2}{8}\mathrm{Tr}(\chi\Sigma^\dagger + \chi^\dagger\Sigma), \tag{3.28}$$

where $\chi = 2\mu(s + ip)$ is acting like the original mass term. One can always recover the ordinary SU(3) chiral Lagrangian by setting $l_\mu = r_\mu = 0$ and $p = 0, s = M = \mathrm{Diag}(m_u, m_d, m_s)$.

In Eq. (3.28), we can write the field ϕ as $\phi = \phi_a T_a$ with T_a the generators of SU(3) group

$$\mathrm{Tr}(T_a T_b) = \delta_{ab}, \quad [T_a, T_b] = \sqrt{2} i f_{abc} T_c. \tag{3.29}$$

One can calculate the conserved left and right handed currents by taking the derivative of the chiral Lagrangian with respect to the external fields l_μ and r_μ [29]. To the lowest order, we have

$$J^L_\mu = \frac{\partial_\mu \mathcal{L}}{\partial_\mu l_\mu} = \frac{i}{4} f^2 \partial_\mu \Sigma \Sigma^\dagger \cong -\frac{1}{2} f \partial_\mu \phi, \tag{3.30}$$

$$J^R_\mu = \frac{\partial_\mu \mathcal{L}}{\partial_\mu r_\mu} = -\frac{i}{4} f^2 \Sigma^\dagger \partial_\mu \Sigma \cong \frac{1}{2} f \partial_\mu \phi. \tag{3.31}$$

Writing $J^{L,R}_\mu$ in T_a basis, $J^{L,R}_\mu = {J^{L,R}_\mu}_a T_a$, we get the equation

$$\langle 0 | {J^R_\mu}_a(x) - {J^L_\mu}_a(x) | \phi_a(p) \rangle = -ip_\mu f \delta_{ab} e^{-ipx}, \tag{3.32}$$

or

$$\langle 0 | \bar{d}\gamma_\mu\gamma_5 u | \pi^+(p) \rangle = \langle 0 | A^{12}_\mu(x) | \pi^+(p) \rangle = \langle 0 | (J^R_\mu - J^L_\mu)^{12}(x) | \pi^+(p) \rangle = -ip_\mu f e^{-ipx}. \tag{3.33}$$

where the superscript "12" represents the (1,2) element of the 3×3 matrix. By comparing it with the definition of pion decay constant $F_\pi \cong 93$MeV

$$\langle \bar{d}\gamma_\mu\gamma_5 u | \pi^+(p) \rangle = -i\sqrt{2} F_\pi p_\mu, \tag{3.34}$$

we conclude that, at LO, the parameter f equals the pion decay constant $f_\pi = \sqrt{2}F_\pi \cong 130.4\text{GeV}$. Actually, all the meson decay constants are equal at this order, *i.e.*, $f = f_\pi = f_K = f_\eta$.

If one takes the derivative with respect to the scalar current s and sets all other currents to zero, one gets

$$\langle \bar{u}u \rangle = \langle \bar{d}d \rangle = \langle \bar{s}s \rangle = \frac{\delta Z}{\delta s} = \frac{\mu f^2}{4} \langle \text{Tr}(\Sigma + \Sigma^\dagger) \rangle \cong \frac{\mu f^2}{2}. \tag{3.35}$$

This relates the chiral condensate in the chiral limit to the LO LEC μ.

At Next-to-Leading (NLO) order, *i.e.*, $\mathcal{O}(p^4, p^2 m_q, m_q^2)$, the SU(3) χPT Lagrangian is (in Euclidean space):

$$\begin{aligned}
\mathcal{L}^{(6)} = & - L_1 \text{Tr}(D_\mu \Sigma^\dagger D_\mu \Sigma)^2 - L_2 \text{Tr}(D_\mu \Sigma^\dagger D_\nu \Sigma^\dagger) \text{Tr}(D_\mu \Sigma^\dagger D_\nu \Sigma^\dagger) \\
& - L_3 \text{Tr}(D_\mu \Sigma^\dagger D_\mu \Sigma D_\nu \Sigma^\dagger D_\nu \Sigma) + L_4 \text{Tr}(D_\mu \Sigma^\dagger D_\mu \Sigma) \text{Tr}(\Sigma^\dagger \chi + \Sigma \chi^\dagger) \\
& + L_5 \text{Tr}(D_\mu \Sigma^\dagger D_\mu \Sigma (\Sigma^\dagger \chi + \Sigma \chi^\dagger)) \\
& - L_6 \text{Tr}(\Sigma^\dagger \chi + \Sigma \chi^\dagger)^2 - L_7 \text{Tr}(\Sigma^\dagger \chi - \Sigma \chi^\dagger)^2 - L_8 \text{Tr}(\Sigma^\dagger \chi \Sigma^\dagger \chi + \Sigma \chi^\dagger \Sigma \chi^\dagger) \\
& + i L_9 \text{Tr}(F_{L\mu\nu} D_\mu \Sigma^\dagger D_\nu \Sigma + F_{R\mu\nu} D_\mu \Sigma D_\nu \Sigma^\dagger) + L_{10} \text{Tr}(\Sigma F_{L\mu\nu} \Sigma^\dagger F_{R\mu\nu}) \\
& + \text{contact terms},
\end{aligned} \tag{3.36}$$

where $L_1 - -L_{10}$ are ten NLO SU(3) LECs. Here, we do not show contact terms which involve only external fields. These terms do not contribute to physical results like scattering amplitudes or the meson spectrum because they do not contain the dynamical field Σ. As a result, we will not consider these terms in this work.

3.2 Staggered Chiral Perturbation Theory

In lattice QCD simulations, various formulations of fermions are used. They should all approach to the same continuum form as the lattice spacing goes to zero, *i.e.*, we expect that they are all in the same universality class. However, at finite lattice spacing, there will be extra effects from lattice artifacts associated with each fermion formalism. These terms could break the chiral symmetry explicitly even when the light quark masses are zero. One then needs to generalize χPT to the cases of fermions on the lattice and incorporate the effects of chiral symmetry breaking at finite lattice spacing under the same framework. It turns out that this can be done using similar analysis as is done in ordinary χPT. Since we use staggered fermions in this work, here we concentrate on the formulation of χPT for staggered fermions.

In the spin-taste basis, there are four tastes for each single flavor of staggered fermions. In the continuum limit, the Dirac operator is expected to be proportional to the identity in taste space. Therefore, the continuum staggered action has a $SU(4)$ taste symmetry. At finite lattice spacing, the taste symmetry is broken and the effects need to be included in the formalism of χPT. This was done in the one-flavor case by Lee and Sharpe [30] and then generalized to multi-flavor case by Aubin and Bernard [31, 32]. The resulting chiral theory for staggered fermions is called "staggered chiral perturbation theory" (SχPT). Correspondingly, the SχPT which takes into account the fourth root procedure is called "rooted staggered chiral perturbation theory" (rSχPT).

To obtain the form of SχPT, two steps are needed. First, one writes down the

Symanzik Effective Theory (SET) for staggered fermions, and then one can construct the chiral Lagrangian using spurion analysis, which is the same technique used to incorporate quark mass terms in ordinary χPT.

3.2.1 SET for staggered fermions

The idea of the SET is that one can parameterize the lattice artifacts of an action S by writing down an effective continuum action S_{SET} as an expansion in powers of the lattice spacing a [33]

$$\mathcal{L}_{SET} = \mathcal{L}_{cont} + \sum_{n=1}^{\infty} a^n \mathcal{L}^{n+4} \tag{3.37}$$

where $\mathcal{L}^{n+4}$ is the term with dimension $n+4$. Note that the SET is defined in the continuum, and it is supposed to describe physics with momentum far below the lattice cutoff, *i.e.*, $p \ll 1/a$. The possible form of operators in the SET are constrained by the underlying symmetries. For staggered fermions, there are no dimension five operators that respect all the symmetries [29, 34].[1] The first scaling violation terms appear at order a^2, which can be seen from figure (2.3(a)), in which two quarks interact by exchanging a gluon with one or more momentum components equal to π/a. Because different taste species in momentum space are located on the corners of Brillouin zone, this high momentum gluon will change the taste of each quark and keep both quarks still on shell, instead of driving them off shell. Effectively, such

[1] Apparently, there is a dimension-five operator in the staggered action written in spin-taste basis, shown in Eq. (2.15). However, it turns out that this operator will be pushed to dimension-six if we redefine the fermion fields [35, 12]. We know this is possible because with momentum space definitions of tastes, there are no taste violations in the free theory.

diagrams produce $\mathcal{O}(a^2)$ four quark operators in the SET. The operators have the form

$$\mathcal{O}_{ss'tt'} = \bar{q}_i(\gamma_s \otimes \xi_t)q_i\bar{q}_j(\gamma_{s'} \otimes \xi_{t'})q_j, \tag{3.38}$$

where i, j are flavor indices, s, s' are spin indices and t, t' are taste indices. Color indices are not shown here explicitly. In principle, they should be there and contracted in such a way that the operators are color singlets. Operators that are in the form of Eq. (3.38) but with different color structures are actually distinct operators in the SET. However, they are mapped to the same term in the chiral Lagrangian since they violate chiral symmetry in the same way. We are only interested in finding all possible terms in the chiral Lagrangian. The coefficients of these terms are arbitrary anyway. Therefore, we can always omit color indices for our purposes here.

Careful analysis show that the spin and taste matrices must satisfy the following properties [12]:

$$U(1)_\epsilon \text{ symmetry} \rightarrow \{\gamma_5 \otimes \xi_5, \gamma_s \otimes \xi_t\} = 0, \tag{3.39}$$

$$\text{shift symmetry} \rightarrow \xi_t = \xi_{t'} \tag{3.40}$$

$$\text{rotational and parity symmetries} \rightarrow \gamma_s = \gamma_{s'} \tag{3.41}$$

All of the operators satisfying these conditions are gathered into two groups, "type A" and "type B", depending on whether there are mixings between the spin indices and taste indices. Operators with the spin and taste indices summed over separately are

called "type A" operators. There are twelve of them, listed by Lee and Sharpe [30]:

$$\mathcal{L}_6^{FF(A)} \sim [S \times A] + [S \times V] + [A \times S] + [V \times S] + [P \times A] + [P \times V] \\ + [A \times P] + [V \times P] + [T \times A] + [T \times V] + [A \times T] + [V \times T], \quad (3.42)$$

where S, P, T, A, V (scalar, pseudoscalar, tensor, axial vector, vector) represent the spin or taste matrices. For example, $[A \times T]$ represents the four-quark operator

$$[A \times T] \equiv \sum_{\mu} \sum_{\nu<\rho} \bar{q}(\gamma_{\mu 5} \otimes \xi_{\nu\rho}) q \bar{q}(\gamma_{5\mu} \otimes \xi_{\rho\nu}) q. \quad (3.43)$$

Operators which have common indices in the spin and taste matrices are called "type B" operators. There are four of them:

$$\mathcal{L}_6^{FF(B)} \sim [T_\mu \times A_\mu] + [T_\mu \times V_\mu] + [A_\mu \times T_\mu] + [V_\mu \times T_\mu], \quad (3.44)$$

where, for example, $[V_\mu \times T_\mu]$ represents the operator [36]

$$[V_\mu \times T_\mu] \equiv \sum_{\mu} \sum_{\nu \neq \mu} \{\bar{q}_i(\gamma_\mu \otimes \xi_{\mu\nu}) q_i \bar{q}_j(\gamma_\mu \otimes \xi_{\nu\mu}) q_j - \bar{q}_i(\gamma_\mu \otimes \xi_{\mu\nu 5}) q_i \bar{q}_j(\gamma_\mu \otimes \xi_{5\nu\mu}) q_j\}. \quad (3.45)$$

Now we have all the possible operators which break the $SU(4)$ taste symmetry on quark level. The second step is to find the corresponding terms in the chiral Lagrangian that break the taste symmetry in the same manner. This can be done by using the spurion analysis, which is shown in the next section.

3.2.2 SχPT Lagrangian at LO

To construct the chiral theory for staggered fermions, it is convenient if we do not distinguish flavor and taste in the beginning and integrate the symmetries into a larger group. For N_f flavors of unrooted staggered fermions, in the continuum case,

the theory is invariant under a $SU(4N_f)_L \otimes SU(4N_f)_R$ chiral symmetry, which is then spontaneously broken to the subgroup $SU(4N_f)_V$, resulting in $16(N_f)^2 - 1$ massless Goldstone bosons. The taste symmetry $U(4)_L \times U(4)_R$ is explicitly broken at finite lattice spacing by taste-violating terms, and the flavor symmetry $SU(N_f)_L \times SU(N_f)_R$ is explicitly broken by non-zero quark masses. If we treat these explicit symmetry breaking terms as perturbations, we will find that these would-be-Goldstone bosons acquire finite masses at non-zero quark mass or non-zero lattice spacings.

Without taste-violating terms, the leading order ($\mathcal{O}(p^2, m_q)$) chiral Lagrangian is [12]

$$\mathcal{L} = \frac{f^2}{8}\mathrm{Tr}(\partial_\mu \Sigma \partial_\mu \Sigma^\dagger) - \frac{f^2}{8}\mathrm{Tr}(\chi\Sigma + \chi\Sigma^\dagger) + \frac{m_0^2}{24}[\mathrm{Tr}(\Phi)]^2, \tag{3.46}$$

with $\Sigma = \exp(i\Phi/f)$. The field Φ is given by

$$\Phi = \begin{pmatrix} U & \pi^+ & K^+ & \cdots \\ \pi^- & D & K^0 & \cdots \\ K^- & \bar{K^0} & S\cdots & \\ \cdots & \cdots & \cdots & \ddots \end{pmatrix}, \tag{3.47}$$

where each entry is a 4×4 matrix in the taste space, $\pi^+ = \sum_B \pi_B^+ T_B$. The taste group generators T_B are defined as $T_B = \{\xi_5, i\xi_{\mu 5}, i\xi_{\mu\nu}(\mu > \nu), \xi_\mu, I\}$. The mass matrix is $\chi = 2\mu(m_u I, m_d I, m_s I, \cdots)$ in which I is the 4×4 unit matrix in taste space. In Eq. (3.46), m_0 is the anomaly contribution to the flavor and taste singlet $\eta_I' \propto \mathrm{Tr}(\Phi)$. Integrating out this singlet is equivalent to keeping the singlet explicitly in the Lagrangian, and taking $m_0 \to \infty$ at the end of the calculation [37].

Now we need to incorporate taste-violating terms in the chiral Lagrangian. As mentioned before, the lowest order taste-violations are at $\mathcal{O}(a^2)$. Before we proceed, a

power counting scheme must be specified because the chiral Lagrangian is essentially a perturbative expansion in powers of momentum and quark masses. One thus needs to compare the relative size of a typical taste-violating term $a^2\delta$ and $p^2 \sim m_\pi^2 \sim \mu m_q$. For lattice simulations with asqtad staggered quarks, one finds that the contributions to pion mass from taste-violations are comparable to the contributions from quark masses [1], *i.e.*, $a^2\delta \sim \mu m_q$, where $a^2\delta$ is a typical taste-violating contribution to the pion mass (taste splittings). As a result, we use the following rule

$$p^2 \sim m_\pi^2 \sim \mu m_q \sim a^2\delta, \tag{3.48}$$

when we construct the chiral Lagrangian including taste-violations.

At leading order, we should have terms at $\mathcal{O}(a^2)$ as well as terms at $\mathcal{O}(p^2)$ and $\mathcal{O}(m_q)$. The latter two are the usual LO terms in the ordinary $SU(4N_f)$ chiral Lagrangian, Eq. (3.46). The $\mathcal{O}(a^2)$ terms can be constructed from $\mathcal{O}(a^2)$ taste-violating operators in the SET using a spurion analysis.

Here we show an example of finding terms in chiral Lagrangian corresponding to the "type-A" operator $\mathcal{O}_{[T\times V]} = a^2\bar{q}_i(\gamma_{\mu\nu}\otimes\xi_\rho)q_i\bar{q}_j(\gamma_{\nu\mu}\otimes\xi_\rho)q_j$. Using $q_i = q_i^R + q_i^L$, this operator can be written as

$$\mathcal{O}_{[T\times V]} = a^2[\bar{q}_i^L(\gamma_{\mu\nu}\otimes\xi_\rho)q_i^R + \bar{q}_i^R(\gamma_{\mu\nu}\otimes\xi_\rho)q_i^L]^2 = a^2[\bar{q}_i^L(\gamma_{\mu\nu}\otimes F_1)q_i^R + \bar{q}_i^R(\gamma_{\mu\nu}\otimes F_2)q_i^L]^2, \tag{3.49}$$

where we introduce two spurions F_1 and F_2. Eventually they will take the values

$$F_1 = a\xi_\rho^{(N_f)} \equiv a\xi_\rho \otimes I_{flavor}, \quad F_2 = a\xi_\rho^{(N_f)} \equiv a\xi_\rho \otimes I_{flavor}, \tag{3.50}$$

where N_f is the number of flavors and I_{flavor} is the identity matrix in flavor space.

Under an $SU(4N_f)_L \times SU(4N_f)_R$ chiral transformation, q and $\bar{q}$ transform as

$$q_L \to Lq_L, \quad q_R \to Rq_R, \quad \bar{q}_L \to \bar{q}_L L^\dagger, \quad \bar{q}_R \to \bar{q}_R R^\dagger. \tag{3.51}$$

If F_1 and F_2 transform as $F_1 \to LF_1R^\dagger, F_2 \to RF_2L^\dagger$, the operator $\mathcal{O}_{[T\times V]}$ will be "invariant" under chiral transformations.

The building blocks for the chiral Lagrangian include $\Sigma, \Sigma^\dagger$ and $\chi, \chi^\dagger$ from ordinary χPT, and the two new objects F_R and F_L. Focusing on the $\mathcal{O}(a^2)$ terms, the mass matrices χ and $\chi^\dagger$ can not appear since otherwise the operators will be at higher order $\mathcal{O}(a^2 m_q)$. Similarly, we can not use derivatives since otherwise the operator will be at $\mathcal{O}(a^2 p^2)$. It can be found that there are three possible combinations of these blocks, *i.e.*, three operators in the chiral Lagrangian:

$$\begin{gathered}
\mathrm{Tr}(F_1\Sigma^\dagger)\mathrm{Tr}(F_2\Sigma) \to \mathrm{Tr}(\xi_\rho^{(N_f)}\Sigma^\dagger)\mathrm{Tr}(\xi_\rho^{(N_f)}\Sigma), \\
\mathrm{Tr}(F_1\Sigma^\dagger)\mathrm{Tr}(F_1\Sigma^\dagger) + \mathrm{Tr}(F_2\Sigma)\mathrm{Tr}(F_2\Sigma) \to \mathrm{Tr}(\xi_\rho^{(N_f)}\Sigma^\dagger)\mathrm{Tr}(\xi_\rho^{(N_f)}\Sigma^\dagger) + \mathrm{Tr}(\xi_\rho^{(N_f)}\Sigma)\mathrm{Tr}(\xi_\rho^{(N_f)}\Sigma), \\
\mathrm{Tr}(F_1\Sigma^\dagger F_1\Sigma^\dagger) + \mathrm{Tr}(F_2\Sigma F_2\Sigma) \to \mathrm{Tr}(\xi_\rho^{(N_f)}\Sigma^\dagger\xi_\rho^{(N_f)}\Sigma^\dagger) + \mathrm{Tr}(\xi_\rho^{(N_f)}\Sigma\xi_\rho^{(N_f)}\Sigma).
\end{gathered} \tag{3.52}$$

One can perform the same analysis for other eleven type-A operators and find in total eight linearly independent operators.

The "type-B" operators only have the joint 90° space-time and taste rotational symmetry. Derivatives in chiral operators are needed to carry the space-time indices and break the $SO(4)$ rotational symmetry, hence the chiral operators are higher order *e.g.*, $\mathcal{O}(a^2p^2)$. As a result, the "type-B" operators do not contribute to the staggered chiral Lagrangian at $\mathcal{O}(a^2)$ [30].

Finally, one can write down the staggered chiral Lagrangian to LO, *i.e.*, $\mathcal{O}(q^2, m_q, a^2)$:

$$\mathcal{L} = \frac{f^2}{8}\mathrm{Tr}(\partial_\mu \Sigma \partial_\mu \Sigma^\dagger) - \frac{f^2}{8}\mathrm{Tr}(\chi\Sigma^\dagger + \chi\Sigma) + \frac{m_0^2}{24}(\mathrm{Tr}(\Phi))^2 + a^2\mathcal{V}. \tag{3.53}$$

The taste-breaking potential $\mathcal{V} = \mathcal{U} + \mathcal{U}'$ is given by:

$$\begin{aligned}
-\mathcal{U} \equiv \sum_k C_k \mathcal{O}_k =& C_1 \mathrm{Tr}(\xi_5^{(N_f)} \Sigma \xi_5^{(N_f)} \Sigma^\dagger) \\
&+ C_3 \frac{1}{2} \sum_\nu [\mathrm{Tr}(\xi_\nu^{(N_f)} \Sigma \xi_\nu^{(N_f)} \Sigma) + h.c.] \\
&+ C_4 \frac{1}{4} \sum_\nu [\mathrm{Tr}(\xi_{\nu 5}^{(N_f)} \Sigma \xi_{5\nu}^{(N_f)} \Sigma) + h.c.] \\
&+ C_6 \sum_{\mu<\nu} \mathrm{Tr}(\xi_{\mu\nu}^{(N_f)} \Sigma \xi_{\nu\mu}^{(N_f)} \Sigma^\dagger),
\end{aligned} \tag{3.54}$$

$$\begin{aligned}
-\mathcal{U}' \equiv \sum_{k'} C_{k'} \mathcal{O}_{k'} =& C_{2V} \frac{1}{4} \sum_\nu [\mathrm{Tr}(\xi_\nu^{(N_f)} \Sigma) \mathrm{Tr}(\xi_\nu^{(N_f)} \Sigma) + h.c.] \\
&+ C_{2A} \frac{1}{4} \sum_\nu [\mathrm{Tr}(\xi_{\nu 5}^{(N_f)} \Sigma) \mathrm{Tr}(\xi_{5\nu}^{(N_f)} \Sigma) + h.c.] \\
&+ C_{5V} \frac{1}{2} \sum_\nu [\mathrm{Tr}(\xi_\nu^{(N_f)} \Sigma) \mathrm{Tr}(\xi_\nu^{(N_f)} \Sigma^\dagger)] \\
&+ C_{5A} \frac{1}{2} \sum_\nu [\mathrm{Tr}(\xi_{\nu 5}^{(N_f)} \Sigma) \mathrm{Tr}(\xi_{5\nu}^{(N_f)} \Sigma^\dagger)],
\end{aligned} \tag{3.55}$$

where *h.c.* indicates Hermitian conjugate.

Note that $\mathcal{U}$ consists of terms with single trace while $\mathcal{U}'$ consists of terms with double traces. Expanding $\mathcal{U}$ and $\mathcal{U}'$ to the second order in chiral fields, we find all terms which are in the same form as ordinary ($\mathcal{O}(m_q)$) mass terms. These terms are at $\mathcal{O}(a^2)$, so they give extra contribution to meson mass at LO. While terms in $\mathcal{U}$ contribute to all meson mass, terms in $\mathcal{U}'$ only contributes to masses of flavor-neutral mesons, *i.e.*, U, D, S, *etc.*. In practice, we treat the quadratic terms in $\mathcal{U}'$ as vertices and sum to all orders to get the propagators of flavor-neutral mesons. This will be

illustrated below. First let us focus on the mass terms from $\mathcal{U}$.

Combining the ordinary mass ($\propto m_q$) and extra contributions from the taste-breaking potential $\mathcal{U}$, the pseudoscalar meson mass takes the form

$$m_{P_B}^2 = \mu(m_x + m_y) + a^2\Delta_B, \tag{3.56}$$

where x and y are the valence quarks composing meson P, and B is the taste structure. Because $\mathcal{U}$ keeps the $SO(4)$ taste symmetry, which can be seen from the contracting of taste indices in the Lorenz-invariant form, the contribution from the taste-breaking part $a^2\Delta_B$ also has this symmetry. In another words, the degeneracy of sixteen mesons P_B in continuum case is lifted according to the irreducible representations of $SO(4)$ group at finite lattice spacing a. The value of Δ_B thus falls into five groups (P, V, T, A, I)[2] corresponding to the taste structure $(\xi_5, i\xi_{\mu 5}, i\xi_{\mu\nu}, \xi_\mu, I)$ respectively. One can calculate Δ_B by expanding terms in $\mathcal{U}$ to second order

$$\Delta_P = 0, \tag{3.57}$$

$$\Delta_A = \frac{16}{f^2}(C_1 + 3C_3 + C_4 + 3C_6), \tag{3.58}$$

$$\Delta_T = \frac{16}{f^2}(2C_3 + 2C_4 + 4C_6), \tag{3.59}$$

$$\Delta_V = \frac{16}{f^2}(C_1 + C_3 + 3C_4 + 3C_6), \tag{3.60}$$

$$\Delta_I = \frac{16}{f^2}(4C_3 + 4C_4). \tag{3.61}$$

These taste splittings are flavor independent. Each meson, whether flavor-neutral or flavor-charged, obtains the same contribution as long as the taste structure is the same.

[2]The identity I is sometimes called "S" for scalar, as in Eq. (3.42).

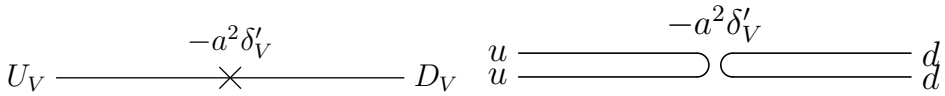

(a) (b)

Figure 3.1: The hairpin disconnected vertex from the $\mathcal{U}'$ term. (a) diagram in the chiral theory. (b) the corresponding quark flow diagram.

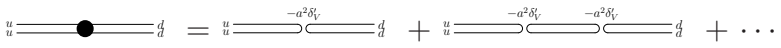

(a) (b) (c)

Figure 3.2: (a) The complete flavor-neutral, taste-vector propagator between U_V and D_V. It is obtained by summing over all diagrams in (b), where different numbers of taste-vector hairpin vertices are inserted.

As explained before, we treat the quadratic terms in $\mathcal{U}'$ as vertices. For example, one such term is

$$\frac{a^2\delta'_V}{2}(U_\mu + D_\mu + S_\mu + \cdots)^2, \tag{3.62}$$

with $a^2\delta'_V \equiv a^2\frac{16}{f^2}(C_{2V} - C_{5V})$. This is a two point vertex mixing flavor-neutral, taste-vector mesons. If we draw the underlying quark flow diagram, say, for the vertex between U_V and D_V, it will look like figure (3.1). This diagram is called the disconnected "hairpin" diagram. It is disconnected in the sense that the valence quark lines are not connected, although they are still connected by gluons in QCD. In order to get the flavor-neutral meson propagator, one needs to sum over all intermediate disconnected vertices, as shown in figure (3.2). Using the resummation method in Refs. [38, 31], one obtain the following propagator between flavor-neutral mesons M

and N in the taste-vector channel

$$D^V_{MN} = -a^2\delta'_V \frac{\prod_L (q^2 + m^2_{L_V})}{(q^2 + m^2_{M_V})(q^2 + m^2_{N_V}) \prod_F (q^2 + m^2_{F_V})}, \tag{3.63}$$

where L labels the unmixed flavor-neutral mesons in the "UDS" basis and F labels the eigenvalues of the full mass matrix (include the effects of $\mathcal{U}'$ in the taste-vector channel). For $n = 3$, the eigenstates of the full mass matrix are π^0_V, η_V and η'_V and their masses are listed in Ref. [31]

$$\begin{aligned}
m^2_{\pi^0_V} &= m^2_{U_V} = m^2_{D_V} = 2\mu\hat{m} + a^2\Delta_V, \\
m^2_{\eta_V} &= \frac{1}{2}\left(m^2_{U_V} + m^2_{S_V} + \frac{3}{4}a^2\delta'_V - Z \right) , \\
m^2_{\eta'_V} &= \frac{1}{2}\left(m^2_{U_V} + m^2_{S_V} + \frac{3}{4}a^2\delta'_V + Z \right) ; \\
Z &\equiv \sqrt{\left(m^2_{S_V} - m^2_{U_V}\right)^2 - \frac{a^2\delta'_V}{2}\left(m^2_{S_V} - m^2_{U_V}\right) + \frac{9(a^2\delta'_V)^2}{16}} ,
\end{aligned} \tag{3.64}$$

where the up and down quark masses are set equal: $m_u = m_d = \hat{m}$.

Similarly, one can find the propagators of flavor-neutral, taste-axial mesons by following the same procedure.

$$D^A_{MN} = -a^2\delta'_A \frac{\prod_L (q^2 + m^2_{L_A})}{(q^2 + m^2_{M_A})(q^2 + m^2_{N_A}) \prod_F (q^2 + m^2_{F_A})}, \tag{3.65}$$

where the eigenstates of the full mass matrix are π^0_A, η_A and η'_A, whose masses can be obtained by substituting V by A in Eq. (3.64).

Finally, the m^2_0 term in Eq. (3.46) produces a vertex mixing flavor-neutral, taste-singlet mesons ($U_I, D_I, S_I, etc.$)

$$\frac{-2m^2_0}{3}(U_I + D_I + S_I + \cdots)^2. \tag{3.66}$$

It has the same form as the flavor-neutral, taste-vector vertex in Eq. (3.62), thus can be treated on the same footing. One then finds the propagator in the flavor-neutral, taste-singlet channel

$$D^I_{MN} = -\frac{4m_0^2}{3}\frac{\prod_L(q^2+m^2_{L_I})}{(q^2+m^2_{M_I})(q^2+m^2_{N_I})\prod_F(q^2+m^2_{F_I})}. \tag{3.67}$$

Since we will take m_0^2 to infinity in the end, we only need the masses of eigenstates of the full mass matrix in the flavor-neutral, taste-singlet sector in that limit. They are [31]

$$m^2_{\pi^0_I} = m^2_{U_I} = m^2_{D_I}, \tag{3.68}$$

$$m^2_{\eta_I} = \frac{m^2_{U_I}}{3} + \frac{2m^2_{S_I}}{3}, \tag{3.69}$$

$$m^2_{\eta'_I} = m_0^2. \tag{3.70}$$

3.3 Rooted Staggered Chiral Perturbation Theory

The chiral theory we build so far is actually for unrooted staggered fermions. In SχPT this can be seen from the fact that for each pseudo-Goldstone boson with certain flavor structure, there are sixteen copies with different taste structures. These unphysical particles can appear in loops and give extra contributions. In order to get the physical results, one needs to take into account the fourth-root procedure, which is used for staggered quarks, in the framework of staggered chiral perturbation theory. In the language of Feynman diagrams, taking the fourth-root is equivalent to dividing the contribution of each sea quark loop by four. Correspondingly, one can draw the underlying quark flow diagrams for each Feynman diagram in terms of

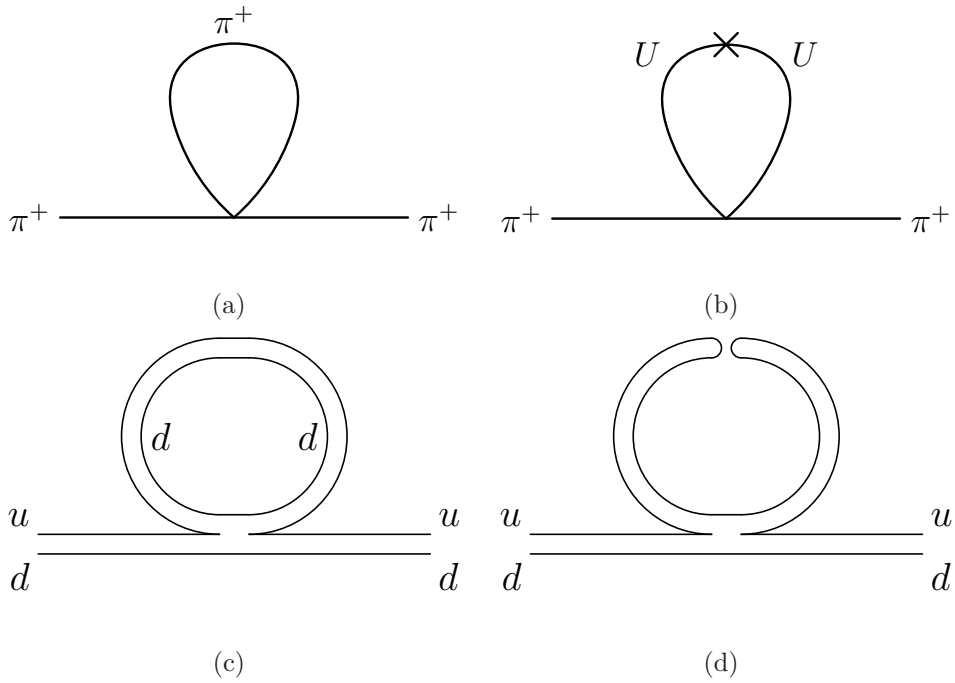

Figure 3.3: Sample pion self energy diagrams and possible quark flow diagrams. (a) and (b) are two diagrams contributing to the pion self energy. (c) and (d) are the corresponding two possible quark flow diagrams. The diagram in figure (c) gets a factor 1/4 while the diagram in figure (d) does not.

Goldstone mesons. There can be many possibilities of quark flow diagrams for one single diagram represented by mesons. In figure (3.3) we show the pion self-energy tadpole diagrams, which are typical in χPT calculations, and two possible quark flow diagrams. We associate a factor of 1/4 for each internal sea quark loop appearing in the quark flow diagrams. For example, the contribution from diagram in figure 3.3(c) is multiplied by 1/4 while the contribution from diagram in figure 3.3(d) is not. By studying the quark flow diagrams carefully, one can find the appropriate factor for each channel and obtain final results by summing over contributions from all diagrams.

It turns out that the fourth-rooting can be incorporated more systematically by using the replica method [39, 16, 35]. We will illustrate this method later in the calculations of the pion mass and decay constant.

Again, there are concerns about the usage of fourth-root procedure in staggered chiral perturbation theory. Recent work shows that rSχPT is the correct chiral effective theory for rooted staggered quarks [16, 35], thereby reproducing the continuum χPT in the $a \to 0$ limit. For a recent review of the fourth-root procedure see Ref. [12] and references therein.

3.4 Partially-Quenched Chiral Perturbation Theory

In QCD, the correlation function of a charged pion is

$$\begin{aligned}
\langle \pi^+(x)\pi^-(0)\rangle &= \langle \bar{u}(x)\gamma_5 d(x)\bar{d}(0)\gamma_5 u(0)\rangle \\
&= \frac{1}{Z}\int DU \prod_{i=1}^{f} D\bar{q}_i Dq_i e^{-S_{gauge}-S_{fermion}}\bar{u}(x)\gamma_5 d(x)\bar{d}(0)\gamma_5 u(0) \\
&= \frac{1}{Z}\int DU e^{-S_{gauge}} \int \prod_{i=1}^{f} D\bar{q}_i Dq_i e^{-\int \bar{q}(\not{D}+M)q}\bar{u}(x)\gamma_5 d(x)\bar{d}(0)\gamma_5 u(0) \\
&= -\frac{1}{Z}\int DU e^{-S_{gauge}} \mathrm{Det}(\not{D}+M)\mathrm{Tr}\left[\gamma_5(\not{D}+m_u)^{-1}_{0x}\gamma_5(\not{D}+m_d)^{-1}_{x0}\right]. \\
&= -\langle \gamma_5(\not{D}+m_u)^{-1}_{0x}\gamma_5(\not{D}+m_d)^{-1}_{x0}\rangle, \qquad (3.71)
\end{aligned}$$

where we have performed the integral of fermion fields explicitly. In the last step in Eq. (3.71), we assume that the probability distribution of gauge configurations is $\propto e^{-S_{gauge}}\mathrm{Det}(\not{D}+M)$. It can be seen that the sea quarks which contribute the

fermion determinant and the valence quarks which appear in the propagators are in some sense independent. One can choose their masses to be different, or even use different fermion actions for these two types of quarks. These choices result in some "altered" versions of QCD: the former is the so-called partially-quenched QCD (PQ-QCD) and the latter is the mixed action QCD. There are some diseases with these QCD versions. For example, they violate unitarity since external states and intermediate states are not the same. Nevertheless, we will find that they are useful in helping us to extract physical results. Below I will concentrate on the PQ-QCD, where valence quark masses are different from sea quark masses.

An important fact is that PQ-QCD has ordinary QCD as its subset [38]. From PQ-QCD, one can always go to the full QCD limit by taking valence quark masses equal to sea quark masses. People are interested in PQ-QCD simulations mainly for the following reasons:

1. The computation of quark propagators are relatively easy compared to the generations of dynamical gauge configurations. For each gauge ensemble generated with the same sea quark content, one can use several sets of valence quarks to compute quark propagators, correlation functions and "physical" quantities like masses of mesons composed of valence quarks. We use the quote marks here because these quantities do not correspond to real physical quantities in QCD.

2. From PQ-QCD, one can construct partially-quenched χPT (PQχPT), using the same method used above in constructing ordinary χPT. Except for some minor differences like the presence of double poles and extra operators in PQχPT, the

form of PQχPT is basically the same as χPT. LECs in PQχPT take the same values as LECs in χPT because, simply speaking, the LECs do not depend on quark masses. More importantly, PQχPT enables us to pin down LECs more easily from PQ-QCD simulation results. For example, the NLO analytic contribution to m_π^2 in SU(3) PQχPT is

$$\sim (2L_8 - L_5)(m_x + m_y) + 2(2L_6 - L_4)(2\hat{m} + m_s), \tag{3.72}$$

where m_x and m_y are the valence masses and $\hat{m}$ and m_s are the sea quark masses. (We have set light sea quark masses equal: $m_u = m_d = \hat{m}$.) In ordinary SU(3) χPT, the corresponding contribution is

$$\sim (2L_8 - L_5)2\hat{m} + 2(2L_6 - L_4)(2\hat{m} + m_s). \tag{3.73}$$

In order to find $(2L_8 - L_5)$, one only needs to change valence quark masses in PQ-QCD simulations, while one needs to change sea quark masses in ordinary QCD simulations. Clearly it is more economic to use the partially-quenched approach since changing valence quarks is easier in lattice simulations.

Because of these advantages, PQ-QCD is often used in modern lattice QCD simulations, and the data obtained, *e.g.*, meson masses, decay constants, can be analyzed by using formulae from PQχPT.

To implement partial-quenching in QCD, one can use the trick by Morel [40]. If there are N_v valence quarks and N_s sea quarks, one introduces N_v pseudo-fermions (bosonic fermions) with masses equal to those of the valence quarks, in order to cancel the contributions from N_v valence quarks to the functional determinant. In

another words, the valence quarks are quenched because, equivalently, there is no net contributions from them to the determinant. Indeed, the N_v pseudo-fermions behave like bosons but they are still four-spinor objects. In the path integral formalism, they give factors $\det(D+m)^{-1}$ in the functional determinant which exactly cancel the contributions from the N_v valence quarks. With N_v+N_s quarks and N_v pseudo-fermions, the Lagrangian is invariant under a graded chiral symmetry group $SU(N_v+N_s|N_v)_L \times SU(N_v+N_s|N_v)_R$. An element in the $SU(N_v+N_s|N_v)$ group takes the form

$$U = \begin{pmatrix} A & B \\ C & D \end{pmatrix}, \tag{3.74}$$

where A is an $(N_v+N_s)\times(N_v+N_s)$ matrix composed of commuting numbers, D is an $N_v \times N_v$ matrix composed of commuting numbers. C and B are matrices of anti-commuting numbers, with dimension $N_v \times (N_v+N_s)$ and $(N_v+N_s)\times N_v$ respectively.

If valence quark masses m_v^2 and sea quark masses m_s^2 are both small, and their differences $|m_s^2 - m_v^2|$ are also small [29], one can construct the corresponding PQχPT for PQ-QCD. Since the symmetry group is enlarged to $SU(N_v+N_s|N_v)$, the chiral field Φ becomes a $(2N_v+N_s)\times(2N_v+N_s)$ matrix

$$\Phi = \begin{pmatrix} \phi & \chi^\dagger \\ \chi & \tilde{\phi} \end{pmatrix}, \tag{3.75}$$

where ϕ is the $(N_v+N_s)\times(N_v+N_s)$ matrix for ordinary mesons, $\tilde{\phi}$ is a $N_v \times N_v$ matrix for mesons made of pseudo-fermions, χ and $\chi^\dagger$ are mesons made of one fermion and one pseudo-fermion. The LO chiral Lagrangian then takes the form [4]

$$\mathcal{L}_{PQ} = \frac{f^2}{4}\mathrm{Str}(\mathrm{D}_\mu \Sigma \mathrm{D}_\mu \Sigma^\dagger) - \frac{\mathrm{f}^2}{4}\mathrm{Str}(\chi\Sigma + \chi\Sigma^\dagger) + \frac{\mathrm{m}_0^2}{6}\Phi_0^2, \tag{3.76}$$

in which $\Sigma = \exp i\Phi/f$. Here, the super-trace Str is defined as $\mathrm{StrU} = \mathrm{TrA} - \mathrm{TrD}$ for a matrix U defined in Eq. (3.74).

At NLO, the chiral Lagrangian of SU(3) PQχPT takes the form

$$\begin{aligned}
\mathcal{L}^{(4)}_{PQ} = & - L_1 \mathrm{Str}(\mathrm{D}_\mu\Sigma^\dagger \mathrm{D}_\mu\Sigma)^2 - \mathrm{L}_2 \mathrm{Str}(\mathrm{D}_\mu\Sigma^\dagger \mathrm{D}_\nu\Sigma^\dagger)\mathrm{Str}(\mathrm{D}_\mu\Sigma^\dagger \mathrm{D}_\nu\Sigma^\dagger) \\
& - L_3 \mathrm{Str}(\mathrm{D}_\mu\Sigma^\dagger \mathrm{D}_\mu\Sigma \mathrm{D}_\nu\Sigma^\dagger \mathrm{D}_\nu\Sigma) + \mathrm{L}_4 \mathrm{Str}(\mathrm{D}_\mu\Sigma^\dagger \mathrm{D}_\mu\Sigma)\mathrm{Str}(\Sigma^\dagger\chi + \Sigma\chi^\dagger) \\
& + L_5 \mathrm{Str}(\mathrm{D}_\mu\Sigma^\dagger \mathrm{D}_\mu\Sigma(\Sigma^\dagger\chi + \Sigma\chi^\dagger)) \\
& - L_6 \mathrm{Str}(\Sigma^\dagger\chi + \Sigma\chi^\dagger)^2 - \mathrm{L}_7 \mathrm{Str}(\Sigma^\dagger\chi - \Sigma\chi^\dagger)^2 - \mathrm{L}_8 \mathrm{Str}(\Sigma^\dagger\chi\Sigma^\dagger\chi + \Sigma\chi^\dagger\Sigma\chi^\dagger) \\
& + iL_9 \mathrm{Str}(\mathrm{F}_{\mathrm{L}\mu\nu}\mathrm{D}_\mu\Sigma^\dagger \mathrm{D}_\nu\Sigma + \mathrm{F}_{\mathrm{R}\mu\nu}\mathrm{D}_\mu\Sigma \mathrm{D}_\nu\Sigma^\dagger) + \mathrm{L}_{10} \mathrm{Str}(\Sigma \mathrm{F}_{\mathrm{L}\mu\nu}\Sigma^\dagger \mathrm{F}_{\mathrm{R}\mu\nu}) \\
& + \text{contact terms} \\
& + L_{PQ}[\mathrm{Str}(\mathrm{D}_\mu\Sigma^\dagger \mathrm{D}_\nu\Sigma \mathrm{D}_\mu\Sigma^\dagger \mathrm{D}_\nu\Sigma) - \frac{1}{2}\mathrm{Str}(\mathrm{D}_\mu\Sigma^\dagger \mathrm{D}_\mu\Sigma)^2 \\
& - \mathrm{Str}(\mathrm{D}_\mu\Sigma^\dagger \mathrm{D}_\nu\Sigma^\dagger)\mathrm{Str}(\mathrm{D}_\mu\Sigma^\dagger \mathrm{D}_\nu\Sigma^\dagger) + 2\mathrm{Str}(\mathrm{D}_\mu\Sigma^\dagger \mathrm{D}_\mu\Sigma \mathrm{D}_\nu\Sigma^\dagger \mathrm{D}_\nu\Sigma)]. \qquad (3.77)
\end{aligned}$$

Basically, it has the same form as the NLO chiral Lagrangian of ordinary SU(3) χPT in Eq. (3.36), but with the trace Tr replaced by the super-trace Str. Another difference from ordinary χPT is that the last term in Eq. (3.77) is an extra operator that appears in NLO PQχPT. This is the so-called unphysical operator [41]. When we go to the full QCD case, this operator will vanish due to Cayley-Hamilton relations for dimension-three matrices. We will come back to this issue when we talk about the SU(2) χPT in the next chapter.

There is another way to formulate the partially-quenched chiral Lagrangian: the so called "replica" method. Furthermore, this method can be extended in the case of SχPT to take into account the fourth root procedure. We will illustrate this method in the next chapter.

Above is only a brief introduction to the PQ-QCD and PQχPT. For more detailed discussion and subtleties involved, we refer the reader to Ref. [42, 37, 38, 29] and references therein.

3.5 Pion mass and decay constant in partially-quenched SU(3) rSχPT

In partially-quenched SU(3) rSχPT, where the two valence quarks are x, y, one can calculate the mass of the flavor-nonsinglet meson $P^+ = x\bar{y}$ up to NLO, *i.e.*, $\mathcal{O}(p^4, p^2 m_q, m_q^2, p^2 a^2, m_q a^2, a^4)$. For simplicity, we concentrate on the true Goldstone particle P_5^+.

In the 2+1 generic case ($m_u = m_d \equiv \hat{m} \neq m_s$ and no degeneracies between valence

and sea quarks), the NLO expressions for $m_{P_5^+}$ and $f_{P_5^+}$ are [1]

$$\begin{aligned}
\frac{(m_{P_5^+}^{\rm NLO})^2}{(m_x+m_y)} &= \mu\Bigg\{1+\frac{1}{16\pi^2 f^2}\Bigg(\frac{2}{3}\sum_j R_j^{[3,2]}(\{\mathcal{M}_{XY_I}^{[3]}\})\,\ell(m_j^2) \\
&\quad -2a^2\delta_V'\sum_j R_j^{[4,2]}(\{\mathcal{M}_{XY_V}^{[4]}\})\,\ell(m_j^2) - 2a^2\delta_A'\sum_j R_j^{[4,2]}(\{\mathcal{M}_{XY_A}^{[4]}\})\,\ell(m_j^2) + a^2(L''+L')\Bigg) \\
&\quad +\frac{16\mu_{\rm tree}}{f^2}\,(2L_8-L_5)\,(m_x+m_y) + \frac{32\mu_{\rm tree}}{f^2}\,(2L_6-L_4)\,(2\hat{m}+m_s)\Bigg\} \qquad (3.78)
\end{aligned}$$

$$\begin{aligned}
f_{P_5^+}^{\rm NLO} &= f\Bigg\{1+\frac{1}{16\pi^2 f^2}\Bigg[-\frac{1}{32}\sum_{Q,B}\ell\left(m_{Q_B}^2\right)+\frac{1}{6}\Bigg(R_{X_I}^{[2,2]}(\{\mathcal{M}_{X_I}^{[2]}\})\tilde{\ell}(m_{X_I}^2) \\
&\quad +R_{Y_I}^{[2,2]}(\{\mathcal{M}_{Y_I}^{[2]}\})\tilde{\ell}(m_{Y_I}^2)+\sum_j D_{j,X_I}^{[2,2]}(\{\mathcal{M}_{X_I}^{[2]}\})\ell(m_j^2) \\
&\quad +\sum_j D_{j,Y_I}^{[2,2]}(\{\mathcal{M}_{Y_I}^{[2]}\})\ell(m_j^2)-2\sum_j R_j^{[3,2]}(\{\mathcal{M}_{XY_I}^{[3]}\})\ell(m_j^2)\Bigg) \\
&\quad +\frac{1}{2}a^2\delta_V'\Bigg(R_{X_V}^{[3,2]}(\{\mathcal{M}_{X_V}^{[3]}\})\tilde{\ell}(m_{X_V}^2)+R_{Y_V}^{[3,2]}(\{\mathcal{M}_{Y_V}^{[3]}\})\tilde{\ell}(m_{Y_V}^2) \\
&\quad +\sum_j D_{j,X_V}^{[3,2]}(\{\mathcal{M}_{X_V}^{[3]}\})\ell(m_j^2)+\sum_j D_{j,Y_V}^{[3,2]}(\{\mathcal{M}_{Y_V}^{[3]}\})\ell(m_j^2) \\
&\quad +2\sum_j R_j^{[4,2]}(\{\mathcal{M}_{XY_V}^{[4]}\})\ell(m_j^2)\Bigg)+\Big(V\to A\Big)+a^2(L''-L')\Bigg] \\
&\quad +\frac{8\mu_{\rm tree}}{f^2}L_5\,(m_x+m_y)+\frac{16\mu_{\rm tree}}{f^2}L_4\,(2\hat{m}+m_s)\Bigg\}. \qquad (3.79)
\end{aligned}$$

Here μ and f are LO LECs, and L_4, L_5, L_6, L_8 are NLO LECs. These are all LECs that also appear in the continuum SU(3) χPT. δ_V' and δ_A' are LO taste-violating parameters, and L', L'' are linear combinations of NLO ($\mathcal{O}(a^2p^2, a^2m_q, a^4)$) taste-violating parameters. The index Q runs over all mesons composed one valence quark (x, y) and one sea quark (u, d, s), and B represents all sixteen taste structures.

In Eqs. (3.78) and (3.79), functions $R_j^{[n,k]}$ and $D_{j,i}^{[n,k]}$ are residues that come from integrating the flavor-neutral meson propagators in tadpole diagrams, like the one shown in figure 3.4. Its contribution to the pion self-energy is

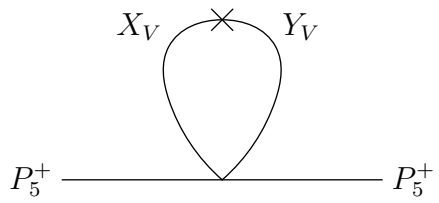

Figure 3.4: A sample tadpole diagram which contributes to the pion self energy. Here the meson P_5^+ is the Goldstone pion composed of x and y valence quarks. The propagator in the loop is between two flavor-neutral, taste-vector mesons X_V and Y_V, and the corresponding quark flow diagram is a disconnected diagram.

$$\begin{aligned}
\sim \int d^4p D^V_{XY} &= (-a^2\delta'_V)\int d^4p \frac{\prod_L (q^2+m^2_{L_V})}{(q^2+m^2_{X_V})(q^2+m^2_{Y_V})\prod_F (q^2+m^2_{F_V})} \\
&= (-a^2\delta'_V)\int d^4p \frac{(q^2+m^2_{U_V})(q^2+m^2_{D_V})(q^2+m^2_{S_V})}{(q^2+m^2_{X_V})(q^2+m^2_{Y_V})(q^2+m^2_{\pi^0_V})(q^2+m^2_{\eta_V})(q^2+m^2_{\eta'_V})} \\
&= (-a^2\delta'_V)\int d^4p \frac{(q^2+m^2_{U_V})(q^2+m^2_{S_V})}{(q^2+m^2_{X_V})(q^2+m^2_{Y_V})(q^2+m^2_{\eta_V})(q^2+m^2_{\eta'_V})}, \quad (3.80)
\end{aligned}$$

where we have used Eq. (3.63) and set $m_u = m_d = \hat{m}$ in the last step. The integrand is in the form

$$\mathcal{I}^{[n,k]}(\{\mathcal{M}\};\{\mu\}) \equiv \frac{\prod_{a=1}^{k}(q^2+\mu_a^2)}{\prod_{i=1}^{n}(q^2+m_i^2)}, \quad (3.81)$$

where $\{\mathcal{M}\}$ and $\{\mu\}$ are two sets of masses, and $m_i \in \{\mathcal{M}\}, \mu_a \in \{\mu\}$. If $n > k$ and there are no degeneracies in the denominator mass set $\{\mathcal{M}\}$, one can use "Lagrange's formula" to write $\mathcal{I}^{[n,k]}(\{\mathcal{M}\};\{\mu\})$ as [31]

$$\mathcal{I}^{[n,k]}(\{\mathcal{M}\};\{\mu\}) = \sum_{i=1}^{n} R_i^{[n,k]}(\{\mathcal{M}\};\{\mu\})\frac{1}{q^2+m_i^2}, \quad (3.82)$$

with the residue function R defined as

$$R_i^{[n,k]}(\{\mathcal{M}\};\{\mu\}) \equiv \frac{\prod_{a=1}^{k}(\mu_a^2-m_i^2)}{\prod_{j\neq i}^{n}(m_j^2-m_i^2)}. \quad (3.83)$$

Substituting Eq. (3.82) into Eq. (3.80), we get

$$\int d^4p\ D^V_{XY} = \sum_{i=1}^{4} R_i^{[4,2]}(\{\mathcal{M}\};\{\mu\}) \int d^4p \frac{1}{q^2+m_i^2}, \tag{3.84}$$

where the mass sets are $\{\mathcal{M}\} = \left\{m_{X_V}, m_{Y_V}, m_{\eta_V}, m_{\eta'_V}\right\}$ and $\{\mu\} = \{m_{U_V}, m_{S_V}\}$. The integral in Eq. (3.84) is divergent. After regularization and renormalization, the infinite part is absorbed by the bare LECs. The finite part is

$$\int \frac{d^4p}{(2\pi)^4}\frac{1}{q^2+m^2} \to \frac{1}{16\pi^2} m^2 \ln\frac{m^2}{\Lambda^2} \equiv \frac{1}{16\pi^2} l(m^2), \tag{3.85}$$

where Λ is the scale used in the renormalization, and $l(m^2)$ is defined as

$$l(m^2) \equiv m^2 \ln\frac{m^2}{\Lambda^2}. \tag{3.86}$$

Assembling all these equations together, Eq. (3.80) finally takes the form

$$\int d^4p\ D^V_{XY} \to \sum_{i=1}^{n} R_i^{[4,2]}(\{\mathcal{M}\};\{\mu\}) l(m_i^2). \tag{3.87}$$

If there are degeneracies in the denominator mass set $\{\mathcal{M}\}$, like in the integral $\int d^4p D^V_{XX}$, one can proceed by taking derivatives on the mass set without degeneracies

$$\begin{aligned}
\int d^4p D^V_{XX} &= (-a^2\delta'_V)(-\frac{d}{dm^2_{X_V}}) \int d^4p \frac{(q^2+m^2_{U_V})(q^2+m^2_{S_V})}{(q^2+m^2_{X_V})(q^2+m^2_{\eta_V})(q^2+m^2_{\eta'_V})} \\
&= (-a^2\delta'_V)(-\frac{d}{dm^2_{X_V}}) \int d^4p \frac{1}{q^2+m_i^2} \\
&\to (-a^2\delta'_V)(-\frac{d}{dm^2_{X_V}}) \sum_{i=1}^{n} R_i^{[4,2]}(\{\mathcal{M}\};\{\mu\}) l(m_i^2) \\
&= (-a^2\delta'_V) \sum_{i=1}^{n} D^{[4,2]}_{i,X_V}(\{\mathcal{M}\};\{\mu\}) l(m_i^2),
\end{aligned} \tag{3.88}$$

where we defined the residue function D as

$$D^{[n,k]}_{j,i}(\{\mathcal{M}\};\{\mu\}) \equiv -\frac{d}{dm_i^2} R_j^{[n,k]}(\{\mathcal{M}\};\{\mu\}). \tag{3.89}$$

From the above discussion, one can have a general idea about the structure of Eqs. (3.78) and (3.79). The residue functions $R_i^{[n,k]}$ and $D_{i,j}^{[n,k]}$ are defined in Eq. (3.83) and Eq. (3.89) respectively. The function $l(m^2)$ is defined in Eq. (3.86), and $\tilde{l}(m^2)$ is

$$\tilde{l}(m^2) \equiv -\left(\ln\frac{m^2}{\Lambda^2}+1\right), \tag{3.90}$$

which comes from integrals in the form $\int d^4p\ \frac{1}{(p^2+m^2)^2}$. For completeness, we list all the "denominator" and "numerator" mass sets here:

$$\begin{aligned}
\{\mathcal{M}_{X_I}^{[2]}\} &\equiv \{m_{X_I}, m_{\eta_I}\},\\
\{\mathcal{M}_{Y_I}^{[2]}\} &\equiv \{m_{Y_I}, m_{\eta_I}\},\\
\{\mathcal{M}_{XY_I}^{[3]}\} &\equiv \{m_{X_I}, m_{Y_I}, m_{\eta_I}\},\\
\{\mathcal{M}_{X_V}^{[3]}\} &\equiv \{m_{X_V}, m_{\eta_V}, m_{\eta'_V}\},\\
\{\mathcal{M}_{Y_V}^{[3]}\} &\equiv \{m_{Y_V}, m_{\eta_V}, m_{\eta'_V}\},\\
\{\mathcal{M}_{XY_V}^{[4]}\} &\equiv \{m_{X_V}, m_{Y_V}, m_{\eta_V}, m_{\eta'_V}\},\\
\{\mathcal{M}_{X_A}^{[3]}\} &\equiv \{m_{X_A}, m_{\eta_A}, m_{\eta'_A}\},\\
\{\mathcal{M}_{Y_A}^{[3]}\} &\equiv \{m_{Y_A}, m_{\eta_A}, m_{\eta'_A}\},\\
\{\mathcal{M}_{XY_A}^{[4]}\} &\equiv \{m_{X_A}, m_{Y_A}, m_{\eta_A}, m_{\eta'_V}\},
\end{aligned} \tag{3.91}$$

$$\{\mu_{\Xi}^{[2]}\} \equiv \{m_{U_\Xi}, m_{S_\Xi}\}, \tag{3.92}$$

where the meson masses can be found in section (3.2.2).

Chapter 4

SU(2) Staggered Chiral Perturbation Theory

4.1 Motivation for SU(2) χPT

In three-flavor χPT, the expansion parameters are $m_\pi^2/\Lambda_\chi^2, m_K^2/\Lambda_\chi^2$, *etc.* Although the pion mass is much less than the chiral scale $\Lambda_\chi \sim 1$GeV, the kaon mass is not. The kaon part in the expansion is thus not converging as fast as the pion part. In order to make the χPT results more reliable, one needs to go higher orders in the expansion so that truncation errors are better under control.

The issues caused by kaons in χPT can be dealt with in another way. Instead of expanding around the three-flavor chiral limit $m_u = m_d = m_s = 0$, one performs expansions around the two-flavor chiral limit $m_u = m_d = 0, \quad m_s = m_s^{phy}$, where m_s^{phys} is the physical strange quark mass. In this way, the new expansion parameters are m_π^2/Λ_χ^2, *etc.* and the series converges faster than the original one. The two-flavor

chiral expansion can be systematically studied by using two-flavor χPT, where the chiral symmetry is restricted to the up and down quark sector.

4.2 SU(2) chiral perturbation theory in the continuum

At LO, the SU(2) chiral Lagrangian in Minkowski space is [26]

$$\mathcal{L}_2^{(4)} = \frac{F^2}{2}\nabla_\mu U^T \nabla^\mu U + 2BF^2(s^0 U^0 + p^i U^i), \tag{4.1}$$

where F is the pion decay constant of F_π in the lowest order, with normalization so that $F_\pi \cong 92$MeV. $U = (U^0, U^i)$ is a four-component real vector field of unit length, *i.e.*, $(U^0)^2 + \sum_i (U^i)^2 = 1$. The covariant derivative ∇_μ is defined by

$$\nabla_\mu U^0 = \partial_\mu U^0 + a_\mu^i(x) U^i, \tag{4.2}$$

$$\nabla_\mu U^i = \partial_\mu U^i + \epsilon^{ikl} v_\mu^k(x) U^l - a_\mu^i(x) U^0, \tag{4.3}$$

where $a_\mu^i(x)$ and $v_\mu^i(x)$ $(i = 1, 2, 3)$are components of external axial and vector currents $a_\mu(x)$ and $v_\mu(x)$

$$v_\mu = \frac{1}{2}\tau^i v_\mu^i, \tag{4.4}$$

$$a_\mu = \frac{1}{2}\tau^i a_\mu^i. \tag{4.5}$$

In Eq. (4.1) we also introduce external scalar and pseudoscalar currents s and p

$$s = s^0 I + s^i \tau^i, \tag{4.6}$$

$$p = p^0 I + p^i \tau^i, \tag{4.7}$$

where s^0, s^i, p^0, p^i are all real. Vectors $\chi^A = 2B(s^0, p^i)$ and $\tilde{\chi}^A = 2B(p^0, -s^i)$ transform like the vector U.

Alternatively, $\mathcal{L}_2^{(4)}$ can be written in "trace form" in terms of an SU(2) matrix Σ:

$$\mathcal{L}_2^{(4)} = \frac{F^2}{4}\mathrm{Tr}(D_\mu \Sigma^\dagger D_\mu \Sigma) + F^2 \chi^A U^A, \tag{4.8}$$

where the matrix field Σ can be related to the vector form of U by

$$\Sigma = U^0 I + i\tau^i U^i, \tag{4.9}$$

$$U^0 = \frac{1}{2}\mathrm{Tr}[\Sigma], \tag{4.10}$$

$$U^i = -\frac{i}{2}\mathrm{Tr}[\tau^i \Sigma], \tag{4.11}$$

where τ^i are three 2×2 Pauli matrices. The covariant derivative D_μ is defined as $D_\mu \Sigma \equiv \partial_\mu \Sigma - i r_\mu \Sigma + i \Sigma l_\mu$ with the left and right handed currents l_μ and r_μ

$$l_\mu = \frac{1}{2}(v_\mu + a_\mu), \tag{4.12}$$

$$r_\mu = \frac{1}{2}(v_\mu - a_\mu). \tag{4.13}$$

The external sources χ and $\chi^\dagger$ in the trace form are related to the fields s and p by

$$\chi \;\; = 2B(s + ip) \;\; = 2B[(s^0 + ip^0)I + \tau^i(s^i + ip^i)], \tag{4.14}$$

$$\chi^\dagger \; = 2B(s - ip) \;\; = 2B[(s^0 - ip^0)I + \tau^i(s^i - ip^i)]. \tag{4.15}$$

With these definitions and the following trace equations for Pauli matricies

$$\mathrm{Tr}(\tau^i) = 0, \tag{4.16}$$

$$\mathrm{Tr}(\tau^i \tau^j) = 2\delta^{ij}, \tag{4.17}$$

$$\mathrm{Tr}(\tau^i \tau^j \tau^k) = 2i\epsilon^{ijk}, \tag{4.18}$$

$$\mathrm{Tr}(\tau^i \tau^j \tau^k \tau^l) = 2(\delta^{ij}\delta^{kl} - \delta^{ik}\delta^{jl} + \delta^{il}\delta^{jk}), \tag{4.19}$$

one can relate terms in the trace form to terms in the vector form

$$\nabla^\mu U^T \nabla_\mu U = \frac{1}{2}\mathrm{Tr}(D^\mu \Sigma^\dagger D_\mu \Sigma), \tag{4.20}$$

$$\chi^T U = \frac{1}{4}\mathrm{Tr}(\Sigma^\dagger \chi + \Sigma \chi^\dagger), \tag{4.21}$$

$$\tilde{\chi}^T U = \frac{1}{4i}\mathrm{Tr}(\Sigma^\dagger \chi - \Sigma \chi^\dagger). \tag{4.22}$$

The equation of motion (EOM) for SU(2) χPT reads

$$\nabla^\mu \nabla_\mu U^A - U^A (U^T \nabla^\mu \nabla_\mu U) = \chi^A - U^A (U^T \chi), \tag{4.23}$$

in the vector form, or reads [24]

$$(D^2\Sigma)\Sigma^\dagger - \Sigma (D^2\Sigma)^\dagger - \chi\Sigma^\dagger + \Sigma\chi^\dagger + \frac{1}{2}\mathrm{Tr}(\chi\Sigma^\dagger - \Sigma\chi^\dagger) = 0, \tag{4.24}$$

in the trace form.

At NLO, the general form for the SU(2) chiral Lagrangian is [26]

$$\begin{aligned}\mathcal{L}_2^{(6)} =& l_1(\nabla^\mu U^T \nabla_\mu U)^2 + l_2(\nabla^\mu U^T \nabla^\nu U)(\nabla_\mu U^T \nabla_\nu U) \\ &+ l_2(\chi^T U)^2 + l_4(\nabla^\mu \chi^T \nabla_\mu U) + l_5(U^T F^{\mu\nu} F_{\mu\nu} U) \\ &+ l_6(\nabla^\mu U^T F_{\mu\nu} \nabla^\nu U) + l_7(\tilde{\chi}^T U)^2 + h_1 \chi^T \chi + h_2 \mathrm{Tr}(F_{\mu\nu} F^{\mu\nu}) \\ &+ h_3 \tilde{\chi}^T \tilde{\chi},\end{aligned} \tag{4.25}$$

where the tensor $F_{\mu\nu}$ is defined by

$$(\nabla_\mu \nabla_\nu - \nabla_\nu \nabla_\mu) U = F_{\mu\nu} U. \tag{4.26}$$

Note that the field strength $F_{\mu\nu}$ has two indices, of which one is to contract with the index of U. Writing the right hand side of Eq. (4.26) explicitly, it is $F_{\mu\nu}^{AB} U^A$ with indices $A, B = 1, 2, 3, 4$. In Eq. (4.25), terms with coefficients h_i are contact terms

that do not contain dynamical fields, and we will not show these terms explicitly in the following discussions.

Using Eqs. (4.20)-(4.19) and switching to Euclidean space, we can write the NLO SU(2) Lagrangian Eq. (4.25) in the trace form [24]

$$\begin{aligned}\mathcal{L}_2^{(6)} = &-\frac{l_1}{4}[\mathrm{Tr}(D_\mu\Sigma D_\mu\Sigma^\dagger)]^2 - \frac{l_2}{4}\mathrm{Tr}(D_\mu\Sigma^\dagger D_\nu\Sigma)\mathrm{Tr}(D_\mu\Sigma^\dagger D_\nu\Sigma),\\ &-\frac{l_3+l_4}{16}[\mathrm{Tr}(\chi\Sigma^\dagger+\Sigma\chi^\dagger)]^2 + \frac{l_4}{8}\mathrm{Tr}(D_\mu\Sigma^\dagger D_\mu\Sigma)\mathrm{Tr}(\chi\Sigma^\dagger+\Sigma\chi^\dagger),\\ &+\frac{l_7}{16}[\mathrm{Tr}(\chi\Sigma^\dagger-\Sigma\chi^\dagger)]^2,\\ &+l_5\mathrm{Tr}(\Sigma^\dagger F_{\mu\nu}^R\Sigma F_{\mu\nu}^L) - \frac{il_6}{2}\mathrm{Tr}(F_{\mu\nu}^L D_\mu\Sigma^\dagger D_\nu\Sigma + F_{\mu\nu}^R D_\mu\Sigma D_\nu\Sigma^\dagger),\\ &+[\text{contact terms}],\end{aligned} \tag{4.27}$$

where $D_\mu\Sigma \equiv \partial_\mu\Sigma - ir_\mu\Sigma + i\Sigma l_\mu$, and the field strength tensors $F_{\mu\nu}^R$ and $F_{\mu\nu}^L$ are

$$F_{\mu\nu}^R \equiv \partial_\mu r_\nu - \partial_\nu r_\mu - i[r_\mu, r_\nu], \tag{4.28}$$

$$F_{\mu\nu}^L \equiv \partial_\mu l_\nu - \partial_\nu l_\mu - i[l_\mu, l_\nu]. \tag{4.29}$$

They are related to the field strength $F_{\mu\nu}$ by

$$F_{\mu\nu}^R + F_{\mu\nu}^L = F_{\mu\nu} = F_{\mu\nu}^{AB}\tau^A\tau^B. \tag{4.30}$$

For partially-quenched SU(2) χPT, the NLO chiral Lagrangian takes the same form as the NLO Lagrangian in general SU(N) ($N > 3$) case. There are eleven terms at this order, among which four terms vanish in the full SU(2) limit due to Cayley-Hamilton relations for two-dimensional matrices. These terms are the so-called unphysical operators in the partially-quenched SU(2) χPT.

4.3 Cayley-Hamilton relations

The Cayley-Hamilton theorem states that every square matrix satisfies its own characteristic equation. For a $n \times n$ matrix A, its characteristic polynomial p is defined by

$$p(\lambda) = \det(\lambda I_n - A), \tag{4.31}$$

where I_n is the $n \times n$ identity matrix. The Cayley-Hamilton theorem says that we have the equality

$$p(A) = 0. \tag{4.32}$$

For example, if A is a 2×2 matrix

$$A = \begin{pmatrix} a & b \\ c & d \end{pmatrix}, \tag{4.33}$$

then we have

$$\begin{aligned} A^2 - (a+d)A + (ad-bc)I_2 \qquad &= 0, \\ \Rightarrow \quad A^2 - \mathrm{Tr}(A)A + \tfrac{1}{2}([\mathrm{Tr}(A)]^2 - \mathrm{Tr}(A^2)) \quad &= 0 \end{aligned} \tag{4.34}$$

The 2×2 matrices A and B satisfy

$$AB + BA - \mathrm{Tr}(A)B - \mathrm{Tr}(B)A + \mathrm{Tr}(A)\mathrm{Tr}(B) - \mathrm{Tr}(AB) = 0. \tag{4.35}$$

Multiplying both sides by a 2×2 matrix C and taking traces on both sides of the equation, we get

$$\begin{aligned} &\mathrm{Tr}(ABC) + \mathrm{Tr}(BAC) - \mathrm{Tr}(A)\mathrm{Tr}(BC) - \mathrm{Tr}(B)\mathrm{Tr}(AC) \\ &\qquad - \mathrm{Tr}(AB)\mathrm{Tr}(C) + \mathrm{Tr}(A)\mathrm{Tr}(B)\mathrm{Tr}(C) = 0. \end{aligned} \tag{4.36}$$

The chiral field Σ satisfies

$$\Sigma\Sigma^\dagger = 1, \tag{4.37}$$

$$\mathrm{Tr}(\Sigma^\dagger D_\mu \Sigma) = 0. \tag{4.38}$$

We can get various relations between terms in NLO SU(N) chiral Lagrangian by making appropriate choices for matrices A, B and C in Eq. (4.36). For example, if we let $A = D_\mu\Sigma\Sigma^\dagger$, $B = \Sigma D_\mu \Sigma^\dagger$, we have $\mathrm{Tr}(A) = \mathrm{Tr}(B) = 0$. Choosing C to be $D_\nu\Sigma D_\nu\Sigma^\dagger$ and $(\chi\Sigma^\dagger + \Sigma\chi^\dagger)$, we get respectively

$$\mathcal{O}_1 \equiv \mathrm{Tr}(D_\mu\Sigma D_\mu\Sigma^\dagger D_\nu\Sigma D_\nu\Sigma^\dagger) - \frac{1}{2}[\mathrm{Tr}(D_\mu\Sigma D_\mu\Sigma^\dagger)]^2 = 0, \tag{4.39}$$

$$\mathcal{O}_2 \equiv \mathrm{Tr}(D_\mu\Sigma D_\mu\Sigma^\dagger(\chi\Sigma^\dagger + \Sigma\chi^\dagger)) - \frac{1}{2}\mathrm{Tr}(D_\mu\Sigma D_\mu\Sigma^\dagger)\mathrm{Tr}(\chi\Sigma^\dagger + \Sigma\chi^\dagger) = 0. \tag{4.40}$$

If we choose $A = D_\mu\Sigma\Sigma^\dagger$, $B = \Sigma D_\nu\Sigma^\dagger$ and $C = AB = D_\mu\Sigma D_\nu\Sigma^\dagger$, we get

$$\begin{aligned}\mathcal{O}_3' \equiv&\mathrm{Tr}(D_\mu\Sigma D_\nu\Sigma^\dagger D_\mu\Sigma D_\nu\Sigma^\dagger) + \mathrm{Tr}(D_\mu\Sigma D_\mu\Sigma^\dagger D_\nu\Sigma D_\nu\Sigma^\dagger)\\ &- \mathrm{Tr}(D_\mu\Sigma D_\nu\Sigma^\dagger)\mathrm{Tr}(D_\mu\Sigma D_\nu\Sigma^\dagger) = 0.\end{aligned} \tag{4.41}$$

In practice, we use another operator $\mathcal{O}_3$ instead of $\mathcal{O}_3'$

$$\begin{aligned}\mathcal{O}_3 \equiv&\mathrm{Tr}(D_\mu\Sigma D_\nu\Sigma^\dagger D_\mu\Sigma D_\nu\Sigma^\dagger) + 2\mathrm{Tr}(D_\mu\Sigma D_\mu\Sigma^\dagger D_\nu\Sigma D_\nu\Sigma^\dagger) - \frac{1}{2}[\mathrm{Tr}(D_\mu\Sigma D_\mu\Sigma^\dagger)]^2\\ &- \mathrm{Tr}(D_\mu\Sigma D_\nu\Sigma^\dagger)\mathrm{Tr}(D_\mu\Sigma D_\nu\Sigma^\dagger) = 0.\end{aligned} \tag{4.42}$$

This operator is the sum of $\mathcal{O}_3'$ and $\mathcal{O}_1$ and it is linearly independent of $\mathcal{O}_1$ and $\mathcal{O}_2$. Actually, Eq. (4.42) is also true for three-dimensional matrices and it plays a role in generalizing SU(3) χPT to the partially-quenched case.

Furthermore, we have the following equations for SU(2) χPT:

$$\begin{aligned}\mathcal{O}_4 &\equiv 2\mathrm{Tr}(\chi\Sigma^\dagger\chi\Sigma^\dagger + \Sigma\chi^\dagger\Sigma\chi^\dagger) - [\mathrm{Tr}(\chi\Sigma^\dagger + \Sigma\chi^\dagger)]^2 - [\mathrm{Tr}(\chi\Sigma^\dagger - \Sigma\chi^\dagger)]^2 \\ &= [\mathrm{Tr}(\tau_i\chi)]^2 + [\mathrm{Tr}(\tau_i\chi^\dagger)]^2 - [\mathrm{Tr}(\chi)]^2 - [\mathrm{Tr}(\chi^\dagger)]^2. \end{aligned} \tag{4.43}$$

The last line in Eq. (4.43) do not involve Σ, hence the operator $\mathcal{O}_4$ is a contact term, and it does not have any physical effects in SU(2) theory. However, $\mathcal{O}_4$ does contribute to calculations of physical quantities in the PQ-SU(2) theory and general SU(N) ($N > 2$) χPT. Therefore, we treat it as a new operator in the PQ-SU(2) theory and list it in the chiral Lagrangian with coefficient p_2.

In the full SU(2) theory, each of the four operators $\mathcal{O}_1, \mathcal{O}_2, \mathcal{O}_3$ and $\mathcal{O}_4$ either vanishes, or becomes equivalent to a contact term, and thus does not contribute to calculations of physical quantities. However, in the partially-quenched case, these operators do not vanish, and they contribute to the quantities that will become physical quantities in the full limit. For these reasons, we call these four operators unphysical operators in the partially-quenched theory. Correspondingly, the PQ-SU(2) Lagrangian be can written as terms in the full SU(2) theory augmented by these unphysical operators $\mathcal{O}_1, \mathcal{O}_2, \mathcal{O}_3$ and $\mathcal{O}_4$ with coefficients p_3, p_1, p_4 and p_2 respectively.

Now one can write down the most general NLO Lagrangian for PQ-SU(2) χPT

$$\begin{aligned}
\mathcal{L}^{(4)}_{cont} &= -\frac{l_1^0}{4}[\mathrm{Tr}(D_\mu\Sigma^\dagger D_\mu\Sigma)]^2 - \frac{l_2^0}{4}\mathrm{Tr}(D_\mu\Sigma^\dagger D_\nu\Sigma)\mathrm{Tr}(D_\mu\Sigma^\dagger D_\nu\Sigma) \\
&+ p_3^0\Big(\mathrm{Tr}(D_\mu\Sigma^\dagger D_\mu\Sigma D_\nu\Sigma^\dagger D_\nu\Sigma) - \frac{1}{2}[\mathrm{Tr}(D_\mu\Sigma^\dagger D_\mu\Sigma)]^2\Big) \\
&+ p_4^0\Big(\mathrm{Tr}(D_\mu\Sigma^\dagger D_\nu\Sigma D_\mu\Sigma^\dagger D_\nu\Sigma) + 2\mathrm{Tr}(D_\mu\Sigma^\dagger D_\mu\Sigma D_\nu\Sigma^\dagger D_\nu\Sigma) \\
&- \frac{1}{2}[\mathrm{Tr}(D_\mu\Sigma^\dagger D_\mu\Sigma)]^2 - \mathrm{Tr}(D_\mu\Sigma^\dagger D_\nu\Sigma)\mathrm{Tr}(D_\mu\Sigma^\dagger D_\nu\Sigma)\Big) \\
&- \frac{l_3^0 + l_4^0}{16}[\mathrm{Tr}(\chi\Sigma^\dagger + \Sigma\chi^\dagger)]^2 + \frac{l_4^0}{8}\mathrm{Tr}(D_\mu\Sigma^\dagger D_\mu\Sigma)\mathrm{Tr}(\chi\Sigma^\dagger + \Sigma\chi^\dagger) \\
&+ \frac{p_1^0}{16}\Big(\mathrm{Tr}(D_\mu\Sigma^\dagger D_\mu\Sigma(\chi\Sigma^\dagger + \Sigma\chi^\dagger)) - \frac{1}{2}\mathrm{Tr}(D_\mu\Sigma^\dagger D_\mu\Sigma)\mathrm{Tr}(\chi\Sigma^\dagger + \Sigma\chi^\dagger)\Big) \\
&+ \frac{p_2^0}{16}\Big(2\mathrm{Tr}(\Sigma^\dagger\chi\Sigma^\dagger\chi + \Sigma\chi^\dagger\Sigma\chi^\dagger) - \mathrm{Tr}(\chi\Sigma^\dagger + \Sigma\chi^\dagger)^2 - \mathrm{Tr}(\chi\Sigma^\dagger - \Sigma\chi^\dagger)^2\Big) \\
&+ \frac{l_7^0}{16}[\mathrm{Tr}(\chi\Sigma^\dagger - \Sigma\chi^\dagger)]^2 \\
&- l_5^0\mathrm{Tr}(\Sigma^\dagger F_{R\mu\nu}\Sigma F_{L\mu\nu}) - \frac{il_6^0}{2}\mathrm{Tr}(F_{L\mu\nu}D_\mu\Sigma^\dagger D_\nu\Sigma + F_{R\mu\nu}D_\mu\Sigma D_\nu\Sigma^\dagger), \qquad (4.44)
\end{aligned}$$

where all coefficients are bare parameters and need to be renormalized later.

The Lagrangian is written in this form so that the bare coefficients l_i^0 ($i = 1, 2, \cdots, 7$) have the same values as the corresponding l_i with the standard definitions [26] in the two-flavor full QCD limit. The parameters p_1^0, p_2^0, p_3^0 and p_4^0 are the four extra LECs at NLO in the partially-quenched case. The four operators associated with p_i^0 are unphysical operators at $\mathcal{O}(p^4)$, which only appear in the two-flavor partially-quenched theory. These unphysical operators vanish in the unquenched SU(2) sector of the PQ theory as a result of the Cayley-Hamilton relations for 2-dimensional matrices. Among these operators, the two with factors p_1^0 and p_2^0 will contribute to the pion masses and decay constants at NLO. The other two with factors p_3^0 and p_4^0 only contribute to the same quantities at NNLO, since they contain

four derivatives. Here, I am only interested in pion masses and decay constants at NLO, so p_1^0 and p_2^0 will enter the calculations below, and p_3^0 and p_4^0 are irrelevant.

4.4 Staggered computations

In order to perform the corresponding analysis in the SU(2) case, one needs to calculate the 1-loop formulae for pseudoscalar meson masses and decay constants in two-flavor PQ-rSχPT. In addition, it is important to check that the presence of taste violations and rooting do not interfere with the decoupling of the strange quark as its mass is increased, allowing the SU(2) chiral theory to emerge from the SU(3) theory. This is a check on a technical step in the argument of Ref. [16] that rSχPT is the correct effective chiral theory for rooted staggered quarks. Finally, it is useful to relate the LECs in the two-flavor and three-flavor cases, and to find the scale dependence of the LECs in both cases, thereby checking their consistency. These calculations are presented below.

4.4.1 Brief review of SχPT

The key point of SχPT is to incorporate systematically the taste-violating effects at finite lattice spacing in the chiral perturbation theory for staggered fermions. The idea of how to develop χPT including scaling violations is due to Sharpe and Singleton [43], and was first applied to staggered quarks by Lee and Sharpe [30].

Basically, SχPT is constructed through two steps. First, one writes down the continuum Symanzik Effection Theory (SET) for staggered fermions. The taste-violating

four-quark operators appear at $\mathcal{O}(a^2)$ in the SET. The coefficient of each of these operators also depends on the coupling constant α_s, and it varies with different staggered actions used in simulations. Specifically, for unimproved staggered action, these operators appear at $\mathcal{O}(\alpha_s a^2)$, while for asqtad improved action, these operators appear at $\mathcal{O}(\alpha_s^2 a^2)$ [1]. For Highly Improved Staggered Quarks (HISQ), these operators also appear at $\mathcal{O}(\alpha_s^2 a^2)$ but with smaller coefficients than for asqtad quarks [44, 45]. In the second step, one maps operators in the SET to terms in the chiral Lagrangian using spurion analysis. The taste-violating four quark operators are mapped into the taste-breaking potential in the chiral Lagrangian. In the two-flavor case, these two steps can be done in the same manner as those in the three-flavor case given by Refs. [31]. The final form of the two-flavor chiral Lagrangian looks exactly the same as the three-flavor Lagrangian except that the chiral field Φ takes its definition in the two-flavor case.

For the purposes of constructing the chiral theory, the SET is taken as "given". We do not need to consider the issues of additive and multiplicative renormalizations that one would need to face in defining finite higher dimensional operators in perturbation theory. All we need to know are the symmetry properties of staggered fermions, which determine what operators can appear. Note further that the lattice spacing a is not a cutoff for the chiral theory, which will in practice be cut off using dimensional regularization. Instead a serves to parameterize symmetry breaking in the chiral theory, and plays a role closely analogous to that of the light quark masses.

In the SET there are also operators at $\mathcal{O}(a^2)$ which satisfy all the continuum symmetries of staggered fermions. Such operators produce "generic" discretization

effects and in general come with different powers of α_s than taste-violations. (For example, with asqtad quarks, the lowest order of generic discretization corrections is $\mathcal{O}(\alpha_s a^2)$ while the lowest order of taste-violations is $\mathcal{O}(\alpha_s^2 a^2)$.) These operators in the SET are logically distinct from $\mathcal{O}(a^2)$ taste-violating operators, and their sizes are "dialed" more or less independently by adjustments of the actions. In the asqtad case, it is know from simulations [1] that taste violating effects are the dominant cause of discretization effects at $\mathcal{O}(a^2)$ even though generic effects can appear at lower order in α_s. That is because the coefficients of the taste-violating operators turn out to be large. After being mapped to chiral theory, the generic SET operators give the same terms as those in the continuum Lagrangian, but multiplied by a coefficient of $\mathcal{O}(a^2)$. For the same reason above, these terms in the chiral Lagrangian representing generic discretization effects are essentially different from the taste-violating terms even though both of them can appear at the same order of lattice spacing a. It is therefore consistent to consider the effects of taste-violating operators independently of generic effects, and that is what I do here.

In practical numerical work, both effects need to be considered. The fact that taste-violations and generic finite lattice spacing effect usually are significantly small, have different mass dependence, and come with different powers of α_s allows a relatively clean separations if sufficient numbers of different lattice spacings are included. Of course, some systematic error will be present and needs to be estimated.

For convenience in numerical work, the effects of generic operators are often absorbed into effective a^2 dependence of the LECs. This is possible since the generic

operators have the same symmetries as the continuum QCD operators.[1] So, for example, one can take the results given here for SU(2) SχPT and effectively take into account generic operators simply by letting the LECs have a^2 dependence. But I emphasize that, logically, the generic effects should be thought of in χPT as new operators, just like the taste-violating effects, not as corrections to old operators. That way, we satisfy the requirement that all LECs in SχPT are a^2 independent, just as they are independent of the light quark masses.

4.4.2 Two-flavor PQ-SχPT at LO

In SχPT the theory becomes a joint expansion about the chiral and continuum limits. The effective Lagrangian was worked out for the single flavor case in Ref. [30], and later generalized to multi-flavor case in Ref. [31]. In Refs. [16, 35], it was shown that the replica method introduced for this problem in Ref. [39] is a valid method for taking rooting into account. The partial quenching can be treated either by the graded symmetry method [42, 46], or by the replica method [47]. Here, for simplicity, I use the replica method for both the rooting and the partial quenching. I take n'_r copies of each valence quark (x,y), and n_r copies of each flavor of sea quark (u,d). The chiral symmetry group is $SU(8(n'_r+n_r))_L \times SU(8(n'_r+n_r))_R$. The pseudoscalar mesons can now be collected into a $8(n'_r+n_r)\times 8(n'_r+n_r)$ matrix Φ, where the factors

[1] There are also operators that have continuum taste symmetry but violate rotational invariance. Their effects appear only at $\mathcal{O}(a^4)$ in the χPT for pseudoscalar mesons.

of 8 arise from 2 flavors of 4 tastes each:

$$\Phi = \begin{pmatrix}
X^{11} & \dots & X^{1n'_r} & P_+^{11} & \dots & P_+^{1n'_r} & \dots & \dots & \dots & \dots & \dots & \dots \\
\vdots & \ddots & \vdots & \vdots & \ddots & \vdots & \dots & \dots & \dots & \dots & \dots & \dots \\
X^{n'_r 1} & \dots & X^{n'_r n'_r} & P_+^{n'_r 1} & \dots & P_+^{n'_r n'_r} & \dots & \dots & \dots & \dots & \dots & \dots \\
P_-^{11} & \dots & P_-^{1n'_r} & Y^{11} & \dots & Y^{1n'_r} & \dots & \dots & \dots & \dots & \dots & \dots \\
\vdots & \ddots & \vdots & \vdots & \ddots & \vdots & \dots & \dots & \dots & \dots & \dots & \dots \\
P_-^{n'_r 1} & \dots & P_-^{n'_r n'_r} & Y^{n'_r 1} & \dots & Y^{n'_r n'_r} & \dots & \dots & \dots & \dots & \dots & \dots \\
\vdots & \vdots & \vdots & \vdots & \vdots & \vdots & U^{11} & \dots & U^{1n_r} & \pi_+^{11} & \dots & \pi_+^{1n_r} \\
\vdots & \vdots & \vdots & \vdots & \vdots & \vdots & \vdots & \ddots & \vdots & \vdots & \ddots & \vdots \\
\vdots & \vdots & \vdots & \vdots & \vdots & \vdots & U^{n_r 1} & \dots & U^{n_r n_r} & \pi_+^{n_r 1} & \dots & \pi_+^{n_r n_r} \\
\vdots & \vdots & \vdots & \vdots & \vdots & \vdots & \pi_-^{11} & \dots & \pi_-^{1n_r} & D^{11} & \dots & D^{1n_r} \\
\vdots & \vdots & \vdots & \vdots & \vdots & \vdots & \vdots & \ddots & \vdots & \vdots & \ddots & \vdots \\
\vdots & \vdots & \vdots & \vdots & \vdots & \vdots & \pi_-^{n_r 1} & \dots & \pi_-^{n_r n_r} & D^{n_r 1} & \dots & D^{n_r n_r}
\end{pmatrix}, \tag{4.45}$$

where each entry is a 4×4 matrix in taste space with, for example, $U^{ij} = \sum_{a=1}^{16} U_a^{ij} T_a$. X, Y, U, and D are the mesons made from $x\bar{x}, y\bar{y}, u\bar{u}$, and $d\bar{d}$ quarks respectively. P_+ is a charged valence meson made from $x\bar{y}$ and π_+ is the charged sea meson made from $u\bar{d}$. The hermitian generators T_a are defined to be:

$$T_a = \{\xi_5, i\xi_{\mu 5}, i\xi_{\mu\nu}, \xi_\mu, \xi_I\}. \tag{4.46}$$

The lowest order ($\mathcal{O}(p^2, m_q, a^2)$) Euclidean Lagrangian is:

$$\begin{aligned}\mathcal{L}^{(4)} =& \frac{f_{(2)}^2}{8}\mathrm{Tr}(D_\mu \Sigma D_\mu \Sigma^\dagger) - \frac{f_{(2)}^2}{8}\mathrm{Tr}(\chi\Sigma^\dagger + \chi\Sigma) \\ &+ \frac{2m_0^2}{3}(U_I^{11} + \ldots + U_I^{n_r n_r} + D_I^{11} + \ldots + D_I^{n_r n_r})^2 + a^2\mathcal{V},\end{aligned} \tag{4.47}$$

where $\Sigma = \exp(i\Phi/f)$ and χ is a $8(n'_r + n_r) \times 8(n'_r + n_r)$ diagonal matrix:

$$\chi = 2\mu_{(2)} Diag(\underbrace{m_x I, \ldots, m_x I}_{n'_r}, \underbrace{m_y I, \ldots, m_y I}_{n'_r}, \underbrace{m_u I, \ldots, m_u I}_{n_r}, \underbrace{m_d I, \ldots, m_d I}_{n_r}) \quad (4.48)$$

with I the 4×4 identity matrix in taste space. The covariant derivative D_μ in Eq. (4.47) is defined by

$$D_\mu \Sigma = \partial_\mu \Sigma - i l_\mu \Sigma + i \Sigma r_\mu, \qquad D_\mu \Sigma^\dagger = \partial_\mu \Sigma^\dagger - i r_\mu \Sigma^\dagger + i \Sigma^\dagger l_\mu, \quad (4.49)$$

where l_μ and r_μ are the left and right-handed currents respectively. Throughout this paper, I alway use the superscript or subscript "(2)" to indicate parameters in the two-flavor theory.

The taste-breaking potential $\mathcal{V} = \mathcal{U} + \mathcal{U}'$ is defined by:

$$\begin{aligned} -\mathcal{U} \equiv \sum_k C_k \mathcal{O}_k =& C_1^{(2)} \mathrm{Tr}(\xi_5^{(R)} \Sigma \xi_5^{(R)} \Sigma^\dagger) \\ &+ C_3^{(2)} \frac{1}{2} \sum_\nu [\mathrm{Tr}(\xi_\nu^{(R)} \Sigma \xi_\nu^{(R)} \Sigma) + h.c.] \\ &+ C_4^{(2)} \frac{1}{4} \sum_\nu [\mathrm{Tr}(\xi_{\nu 5}^{(R)} \Sigma \xi_{5\nu}^{(R)} \Sigma) + h.c.] \\ &+ C_6^{(2)} \sum_{\mu<\nu} \mathrm{Tr}(\xi_{\mu\nu}^{(R)} \Sigma \xi_{\nu\mu}^{(R)} \Sigma^\dagger), \end{aligned} \quad (4.50)$$

$$\begin{aligned} -\mathcal{U}' \equiv \sum_{k'} C_{k'} \mathcal{O}_{k'} =& C_{2V}^{(2)} \frac{1}{4} \sum_\nu [\mathrm{Tr}(\xi_\nu^{(R)} \Sigma) \mathrm{Tr}(\xi_\nu^{(R)} \Sigma) + h.c.] \\ &+ C_{2A}^{(2)} \frac{1}{4} \sum_\nu [\mathrm{Tr}(\xi_{\nu 5}^{(R)} \Sigma) \mathrm{Tr}(\xi_{5\nu}^{(R)} \Sigma) + h.c.] \\ &+ C_{5V}^{(2)} \frac{1}{2} \sum_\nu [\mathrm{Tr}(\xi_\nu^{(R)} \Sigma) \mathrm{Tr}(\xi_\nu^{(R)} \Sigma^\dagger)] \\ &+ C_{5A}^{(2)} \frac{1}{2} \sum_\nu [\mathrm{Tr}(\xi_{\nu 5}^{(R)} \Sigma) \mathrm{Tr}(\xi_{5\nu}^{(R)} \Sigma^\dagger)], \end{aligned} \quad (4.51)$$

where $\xi_5^{(R)}$ is the product of ξ_5 in taste space with the identity matrix in flavor and replica space, and similarly for $\xi_\nu^{(R)}, \xi_{\nu 5}^{(R)}$ and $\xi_{\mu\nu}^{(R)}$.

Due to the anomaly, the SU($8(n'_r + n_r)$) singlet receives a large contribution to its mass ($\propto m_0$), and thus does not play a dynamical role. Integrating out this singlet is equivalent to keeping the singlet explicitly in the Lagrangian (the third term in $\mathcal{L}^{(4)}$), and taking $m_0 \to \infty$ at the end of the calculation [37]. Here, the m_0^2 term is normalized so that for the hairpin diagram between two flavor-neutral taste singlet mesons, each composed of a single species, the vertex is $\frac{4m_0^2}{3}$, independent of the number of flavors. For the two-flavor SχPT with n_r replicas for each sea quark, the mass matrix for flavor-neutral taste singlet mesons takes the form:

$$\begin{pmatrix} m_{U_I^{11}} + \delta' & \delta' & \delta' & \delta' & \dots & \delta' \\ \delta' & \ddots & \delta' & \vdots & \ddots & \vdots \\ \delta' & \dots & m_{U_I^{n_r n_r}} + \delta' & \delta' & \dots & \delta' \\ \delta' & \dots & \delta' & m_{D_I^{11}} + \delta' & \delta' & \delta' \\ \vdots & \ddots & \vdots & \delta' & \ddots & \delta' \\ \delta' & \dots & \delta' & \delta' & \delta' & m_{D_I^{n_r n_r}} + \delta' \end{pmatrix}, \tag{4.52}$$

where every non-diagonal element is $\delta' \equiv \frac{4m_0^2}{3}$, and I have anticipated taking $n'_r \to 0$ to eliminate virtual loops of valence quarks. Diagonalizing the matrix and taking the limit of $m_0 \to \infty$, we obtain the mass of the η'_I:

$$m^2_{\eta'_I} = \frac{8m_0^2}{3} n_r. \tag{4.53}$$

Generally, if there are N_f flavors of sea quarks, the result will be $\frac{4m_0^2}{3} N_f n_r$.

4.4.3 Two-flavor PQ-rSχPT at NLO

At NLO, the two-flavor PQ-rSχPT Lagrangian has two parts:

$$\mathcal{L}^{(6)} = \mathcal{L}^{(6)}_{cont} + \mathcal{L}^{(6)}_{\text{t-v}}. \tag{4.54}$$

$\mathcal{L}^{(6)}_{cont}$ contains operators of $\mathcal{O}(p^4, p^2 m_q, m_q^2)$, which are of the same form as operators in two-flavor continuum PQ-χPT. $\mathcal{L}^{(6)}_{\text{t-v}}$ is of $\mathcal{O}(a^2p^2, a^2m_q, a^4)$. It contains all NLO taste-violating terms for staggered fermions [36].

The most general continuum NLO Lagrangian $\mathcal{L}^{(6)}_{cont}$ in Euclidean space was given in Eq. (4.44). This set of LECs can be related to the LECs used by Bijnens and Lähde [48] through:

$$\begin{aligned}
p_3^0 &= -L_3^{(2pq)} + 2L_0^{(2pq)}, & p_4^0 &= -L_0^{(2pq)},\\
l_1^0 &= 4L_1^{(2pq)} + 2L_3^{(2pq)} - 2L_0^{(2pq)}, & l_2^0 &= 4L_2^{(2pq)} + 4L_0^{(2pq)},\\
p_1^0 &= 16L_5^{(2pq)}, & p_2^0 &= -8L_8^{(2pq)},\\
l_3^0 &= 16L_6^{(2pq)} + 8L_8^{(2pq)} - 8L_4^{(2pq)} - 4L_5^{(2pq)}, & l_4^0 &= 8L_4^{(2pq)} + 4L_5^{(2pq)},\\
l_5^0 &= L_{10}^{(2pq)}, & l_6^0 &= -2L_9^{(2pq)},\\
l_7^0 &= -16L_7^{(2pq)} - 8L_8^{(2pq)}.
\end{aligned} \tag{4.55}$$

The general form of $\mathcal{L}^{(6)}_{\text{t-v}}$ ($\mathcal{O}(a^2p^2, a^2m_q, a^4)$) is given in Ref. [36]. Examples of operators in $\mathcal{L}^{(6)}_{\text{t-v}}$ that contribute here are:

$$a^2\text{Tr}(\partial_\mu\Sigma^\dagger\xi_5\partial_\mu\Sigma\xi_5), \quad a^2\text{Tr}(\xi_\mu\Sigma^\dagger\xi_\mu\chi^\dagger) + p.c., \tag{4.56}$$

(with *p.c.* indicating parity conjugate) where the first operator contributes both to pseudo-Goldstone masses and decay constants at NLO, and the second one only contributes to the pseudo-Goldstone masses at NLO. From this, it is clear that the

taste-violating analytic contributions to decay constants and masses at NLO are independent. We do not need any further details from Ref. [36] here, since it is not currently useful to relate the NLO analytic taste-violating contributions to parameters in the Lagrangian.

4.4.4 Rooting and partial quenching

In the continuum limit, there are four degenerate taste species for each quark flavor. We obtain physical results in rSχPT by taking the fourth root of each fermion determinant, which is known as the fourth root procedure. Although it has been shown that this procedure produces, non-perturbatively, violations of locality at non-zero lattice spacing [15], work over the last few years indicates that locality and universality are restored in the continuum limit of the lattice theory [18, 19], and that rSχPT is the correct chiral effective theory [16, 35], thereby reproducing continuum χPT in the $a \to 0$ limit. For a recent review of the fourth-root procedure see Ref. [12] and references therein.

For calculations in rSχPT, the fourth-root is taken by letting $n_r \to \frac{1}{4}$ at the end of the calculation [16, 35]. Similarly, virtual loops associated with the valence quarks are eliminated by taking $n'_r \to 0$ [47].

4.4.5 PION MASS AND DECAY CONSTANT

Following the procedures in Ref. [31], I calculate the light pseudoscalar mass and decay constant through NLO ($\mathcal{O}(m_q^2, m_q a^2)$). For simplicity, I always assume the up and down quark masses are equal, $m_u = m_d = m_l$. The dimensional regularization

scheme is employed, and the results in $d = 4 - \epsilon$ dimensional space-time are:

$$\begin{aligned}\frac{m^2_{P_5^+}}{(m_x+m_y)} =&\mu_{(2)}\Big\{1+\frac{1}{\Lambda^{d-4}16\pi^2 f^2_{(2)}}\Big[\sum_j R_j^{[2,1]}(\{\mathcal{M}^{[2]}_{XY_I}\})\mathcal{R}_\epsilon m_j^2(m_j^2)^{-\frac{\epsilon}{2}}\\ &-2a^2{\delta'_V}^{(2)}\sum_j R_j^{[3,1]}(\{\mathcal{M}^{[3]}_{XY_V}\})\mathcal{R}_\epsilon m_j^2(m_j^2)^{-\frac{\epsilon}{2}}+(V\leftrightarrow A)+a^2(\tilde{L}''^0_{(2)}+\tilde{L}'^0_{(2)})\Big]\\ &+\frac{\mu_{(2)}}{\Lambda^{d-4}f^2_{(2)}}(4l_3^0+p_1^0+4p_2^0)(2m_l)+\frac{\mu_{(2)}}{\Lambda^{d-4}f^2_{(2)}}(-p_1^0-4p_2^0)(m_x+m_y)\Big\},\end{aligned} \tag{4.57}$$

$$\begin{aligned}f_{P_5^+} =&f_{(2)}\Big\{1+\frac{1}{\Lambda^{d-4}16\pi^2 f^2_{(2)}}\Big[-\frac{1}{32}\sum_{Q,B}\mathcal{R}_\epsilon m^2_{Q_B}(m^2_{Q_B})^{-\frac{\epsilon}{2}}\\ &+\frac{1}{4}\Big(\mathcal{R}_\epsilon m^2_{X_I}(m^2_{X_I})^{-\frac{\epsilon}{2}}+\mathcal{R}_\epsilon m^2_{Y_I}(m^2_{Y_I})^{-\frac{\epsilon}{2}}\\ &+(m^2_{U_I}-m^2_{X_I})(-\mathcal{R}_\epsilon-1)(m^2_{X_I})^{-\frac{\epsilon}{2}}+(m^2_{U_I}-m^2_{Y_I})(-\mathcal{R}_\epsilon-1)(m^2_{Y_I})^{-\frac{\epsilon}{2}}\Big)\\ &-\frac{1}{2}\Big(R^{[2,1]}_{X_I}(\{\mathcal{M}^{[2]}_{XY_I}\})\mathcal{R}_\epsilon m^2_{X_I}(m^2_{X_I})^{-\frac{\epsilon}{2}}+R^{[2,1]}_{Y_I}(\{\mathcal{M}^{[2]}_{XY_I}\})\mathcal{R}_\epsilon m^2_{Y_I}(m^2_{Y_I})^{-\frac{\epsilon}{2}}\Big)\\ &+\frac{a^2{\delta'_V}^{(2)}}{2}\Big(R^{[2,1]}_{X_V}(\{\mathcal{M}^{[2]}_{X_V}\})(-\mathcal{R}_\epsilon-1)(m^2_{X_V})^{-\frac{\epsilon}{2}}+\sum_j D^{[2,1]}_{j,X_V}(\{\mathcal{M}^{[2]}_{X_V}\})\mathcal{R}_\epsilon m_j^2(m_j^2)^{-\frac{\epsilon}{2}}\\ &+(X\leftrightarrow Y)+2\sum_j R_j^{[3,1]}(\{\mathcal{M}^{[3]}_{XY_V}\})\mathcal{R}_\epsilon m_j^2(m_j^2)^{-\frac{\epsilon}{2}}\Big)+(V\leftrightarrow A)\\ &+a^2(\tilde{L}''^0_{(2)}-\tilde{L}'^0_{(2)})\Big]+\frac{\mu_{(2)}}{2\Lambda^{d-4}f^2_{(2)}}(4l_4^0-p_1^0)(2m_l)+\frac{\mu_{(2)}}{2\Lambda^{d-4}f^2_{(2)}}(p_1^0)(m_x+m_y)\Big\},\end{aligned} \tag{4.58}$$

where Λ is the scale introduced in the dimensional regularization, and all the scale factors are written explicitly. Here, $\mathcal{R}_\epsilon$ is defined to be:

$$\mathcal{R}_\epsilon = -\frac{2}{\epsilon} - \log(4\pi) + \gamma - 1 + \mathcal{O}(\epsilon), \tag{4.59}$$

where $\gamma = -\Gamma'(1)$ is Euler's constant. In Eqs. (4.57) and (4.58), $\mathcal{R}_\epsilon$ comes from the integral over the tadpole diagram with a single pole, while $(-\mathcal{R}_\epsilon - 1)$ comes from the integral over the tadpole diagram with a double pole. The index Q runs over the 4

mesons made from one valence and one sea quark, and B runs over the 16 tastes, which form five multiplets (P, V, A, T, I). ${\delta'_V}^{(2)}$ and ${\delta'_A}^{(2)}$ are LO taste-violating hairpin parameters, and $L''_{(2)}$ and $L'_{(2)}$ are NLO taste-violating parameters. The latter are simply the linear combinations of LECs coming from $\mathcal{O}(a^2p^2)$ and $\mathcal{O}(a^2m_q)$ taste-violating terms, for example, the operators given in Eq. (4.56). There are no contributions from $\mathcal{O}(a^4)$ terms to pseudo-Goldstone masses and decay constants, either because of the exact non-singlet chiral symmetry (for the masses) or because the operators do not contain derivatives (for the decay constant).

The residue functions R and D are defined as in the SU(3) case in Eqs. (3.83) and (3.89). For convenience, we show them here:

$$R_j^{[n,k]}(\{M\};\{\mu\}) \equiv \frac{\Pi_{a=1}^{k}(\mu_a^2 - m_j^2)}{\Pi'^{n}_{l=1}(m_l^2 - m_j^2)}, \tag{4.60}$$

$$D_{j,i}^{[n,k]}(\{M\};\{\mu\}) \equiv -\frac{d}{dm_i^2} R_j^{[n,k]}(\{M\};\{\mu\}), \tag{4.61}$$

where the prime on the product means that $l = j$ is omitted. The denominator mass-set arguments in these residue functions are defined by:

$$\begin{aligned} \{\mathcal{M}_{X_V}^{[2]}\} &\equiv \{m_{X_V}, m_{\eta'_V}\}, & \{\mathcal{M}_{Y_V}^{[2]}\} &\equiv \{m_{Y_V}, m_{\eta'_V}\}, \\ \{\mathcal{M}_{XY_I}^{[2]}\} &\equiv \{m_{X_I}, m_{Y_I}\}, & \{\mathcal{M}_{XY_V}^{[3]}\} &\equiv \{m_{X_V}, m_{Y_V}, m_{\eta'_V}\}. \end{aligned} \tag{4.62}$$

The numerator mass-set arguments for taste Ξ are always $\{\mu_\Xi\} \equiv \{m_{U_\Xi}\}$. We show

the masses explicitly here:

$$m^2_{\pi_B} = m^2_{U_B} = m^2_{D_B} = 2\mu_{(2)} m_l + a^2 \Delta^{(2)}_B, \tag{4.63}$$

$$m^2_{X_B} = 2\mu_{(2)} m_x + a^2 \Delta^{(2)}_B, \tag{4.64}$$

$$m^2_{Y_B} = 2\mu_{(2)} m_y + a^2 \Delta^{(2)}_B, \tag{4.65}$$

$$m^2_{\eta'_V} = m^2_{U_V} + \frac{a^2 \delta'^{(2)}_V}{2}, \tag{4.66}$$

$$m^2_{\eta'_A} = m^2_{U_A} + \frac{a^2 \delta'^{(2)}_A}{2}, \tag{4.67}$$

$$m^2_{\eta'_I} \sim \frac{2}{3} m^2_0, \tag{4.68}$$

where $\Delta^{(2)}_B$ are the taste splittings in SU(2) rSχPT. The final relation holds for $m^2_0 \gg m^2_{\pi_I}$. Here, η'_V and η'_A are, respectively, the taste-vector and taste-axial vector, flavor and replica neutral mesons whose masses are shifted by the taste-violating hairpin contributions. Since η'_I has a mass proportional to m^2_0, it decouples in the limit when m^2_0 is taken to infinity.

Using the identities of residue functions listed in the second paper of Ref. [31]:

$$
\begin{aligned}
\sum_{j=1}^{n} R_j^{[n,k]} &= \begin{cases} 1\ , & n = k+1; \\ 0\ , & n \geq k+2. \end{cases} \\
\sum_{j=1}^{n} R_j^{[n,k]} m_j^2 &= \begin{cases} \sum_{j=1}^{n} m_j^2 - \sum_{a=1}^{k} \mu_a^2\ , & n = k+1; \\ -1\ , & n = k+2; \\ 0\ , & n \geq k+3. \end{cases} \\
\sum_{j=1}^{n} D_{j,\ell}^{[n,k]} &= \begin{cases} 1\ , & n = k; \\ 0\ , & n \geq k+1. \end{cases} \\
\sum_{j=1}^{n} \left(D_{j,\ell}^{[n,k]} m_j^2 \right) - R_\ell^{[n,k]} &= \begin{cases} m_\ell^2 + \sum_{j=1}^{n} m_j^2 - \sum_{a=1}^{k} \mu_a^2\ , & n = k; \\ -1\ , & n = k+1; \\ 0\ , & n \geq k+2. \end{cases}
\end{aligned}
\tag{4.69}
$$

and ignoring terms vanishing at order ϵ or higher as $\epsilon \to 0$, one can simplify Eqs. (4.57) and (4.58) to:

$$\frac{m^2_{P_5^+}}{(m_x+m_y)} =\mu_{(2)}\Big\{1+\frac{1}{16\pi^2 f^2_{(2)}}\Big[(\mu_{(2)}(2m_x+2m_y-2m_l)+a^2\Delta_I^{(2)}+2a^2{\delta'_V}^{(2)}+2a^2{\delta'_A}^{(2)})\mathcal{R}_\epsilon$$
$$+\sum_j R_j^{[2,1]}(\{\mathcal{M}^{[2]}_{XY_I}\})l(m_j^2)-2a^2{\delta'_V}^{(2)}\sum_j R_j^{[3,1]}(\{\mathcal{M}^{[3]}_{XY_V}\})l(m_j^2)+(V\leftrightarrow A)$$
$$+\Lambda^{d-4}a^2(\tilde{L}''^0_{(2)}+\tilde{L}'^0_{(2)})\Big]$$
$$+\frac{\mu_{(2)}}{\Lambda^{d-4}f^2_{(2)}}(4l_3^0+p_1^0+4p_2^0)(2m_l)+\frac{\mu_{(2)}}{\Lambda^{d-4}f^2_{(2)}}(-p_1^0-4p_2^0)(m_x+m_y)\Big\}, \tag{4.70}$$

$$f_{P_5^+} =f_{(2)}\Big\{1+\frac{1}{16\pi^2 f^2_{(2)}}\Big[-(\mu_{(2)}(m_x+m_y+2m_l)+2a^2\Delta^{(2)}_{av}+2a^2{\delta'_V}^{(2)}+2a^2{\delta'_A}^{(2)})\mathcal{R}_\epsilon$$
$$-\frac{1}{32}\sum_{Q,B}l(m^2_{Q_B})+\frac{1}{4}\Big(l(m^2_{X_I})+l(m^2_{Y_I})+(m^2_{U_I}-m^2_{X_I})\tilde{l}(m^2_{X_I})$$
$$+(m^2_{U_I}-m^2_{Y_I})\tilde{l}(m^2_{Y_I})\Big)-\frac{1}{2}\sum_j R^{[2,1]}_{m_j}(\{\mathcal{M}^{[2]}_{XY_I}\})l(m_j^2)$$
$$+\frac{a^2{\delta'_V}^{(2)}}{2}\Big(R^{[2,1]}_{X_V}(\{\mathcal{M}^{[2]}_{X_V}\})\tilde{l}(m^2_{X_V})+\sum_j D^{[2,1]}_{j,X_V}(\{\mathcal{M}^{[2]}_{X_V}\})l(m_j^2)$$
$$+(X\leftrightarrow Y)+2\sum_j R_j^{[3,1]}(\{\mathcal{M}^{[3]}_{XY_V}\})l(m_j^2)\Big)+(V\leftrightarrow A)$$
$$+\Lambda^{d-4}a^2(\tilde{L}''^0_{(2)}-\tilde{L}'^0_{(2)})\Big]+\frac{\mu_{(2)}}{2\Lambda^{d-4}f^2_{(2)}}(4l_4^0-p_1^0)(2m_l)+\frac{\mu_{(2)}}{2\Lambda^{d-4}f^2_{(2)}}(p_1^0)(m_x+m_y)\Big\}, \tag{4.71}$$

where

$$\Delta^{(2)}_{av}\equiv\frac{1}{16}(\Delta_5^{(2)}+4\Delta_V^{(2)}+6\Delta_T^{(2)}+4\Delta_A^{(2)}+\Delta_I^{(2)}) \tag{4.72}$$

is the average taste splitting in the two-flavor case. The chiral logarithm functions l and $\tilde{l}$ in Eqs. (4.70) and (4.71) are given by [31]:

$$l(m^2)\equiv m^2\ln\frac{m^2}{\Lambda^2}\qquad\text{[infinite volume]}, \tag{4.73}$$
$$\tilde{l}(m^2)\equiv-\left(\ln\frac{m^2}{\Lambda^2}+1\right)\qquad\text{[infinite volume]}. \tag{4.74}$$

Finite volume corrections at NLO may be incorporated by adjusting $l(m^2)$ and $\tilde{l}(m^2)$ as in Ref. [31, 49].

Recall that in continuum SU(2) χPT, because the NLO Lagrangian contains all the possible analytic terms consistent with the symmetries, the divergences generated from one-loop graphs built from LO vertices can be absorbed by an appropriate renormalization of the bare NLO LECs l_i^0 and contact term coefficients h_i^0 [26]:

$$l_i^0 = (\Lambda)^{d-4}(l_i + \gamma_i \frac{\mathcal{R}_\epsilon}{32\pi^2}),\ i = 1, \cdots, 7, \tag{4.75}$$

$$h_i^0 = (\Lambda)^{d-4}(h_i + \delta_i \frac{\mathcal{R}_\epsilon}{32\pi^2}),\ h = 1, 2, 3, \tag{4.76}$$

where $\mathcal{R}_\epsilon$ has the same definition as above, and l_i and h_i are renormalized coefficients (which often appear as l_i^r and h_i^r in literature). For SU(2) χPT, the values of γ_i and δ_i are listed in Ref. [26]. For the general case in SU(N) χPT, similar results can be found in Ref. [50]. In Eqs. (4.75) and (4.76), as one changes the scale Λ, l_i and h_i should also change in such a way that the bare quantities l_i^0 and h_i^0 are scale independent. Specifically, under a change in the chiral scale Λ to Λ', the SU(2) LECs change by:

$$l_i(\Lambda') = l_i(\Lambda) - \frac{\gamma_i}{32\pi^2} \log \frac{\Lambda'^2}{\Lambda^2}, \tag{4.77}$$

This renormalization procedure can be applied in SU(2) rSχPT in the same way. The only difference is that, at each order of chiral expansion, there are additional taste-violating terms. The presence of these terms in effective field theory reflects the fact that the continuum SU(4) taste symmetry is broken by finite lattice spacing effects. In the two-flavor case, the full chiral symmetry $SU_L(8) \times SU_R(8)$ is broken both by taste-violating terms and by the usual mass terms. Effectively, the taste-

violating terms are acting just like the mass terms, and they can be treated in the same way once the power counting scheme is specified. In practice, we use the power counting rule $p^2 \sim m_q \sim a^2$ in SU(2) rSχPT [31, 12]. As a result, the LO contribution for a physical quantity is at $\mathcal{O}(p^2), \mathcal{O}(m_q)$ and $\mathcal{O}(a^2)$, coming from the terms in Eq. (4.47). At NLO, the one-loop graphs built from LO vertices will generate divergences at $\mathcal{O}(p^4), \mathcal{O}(p^2 m_q), \mathcal{O}(m_q^2), \mathcal{O}(a^2 p^2), \mathcal{O}(a^2 m_q)$ and $\mathcal{O}(a^4)$. By construction, Eq. (4.54) is the most general Lagrangian in the same order which satisfies all the symmetries of staggered quarks. Indeed, all possible terms in this Lagrangian are found by treating mass terms and taste-violating terms in the same footing, using a spurion analysis [12]. Since the staggered symmetries (a subset of $SU_L(8) \times SU_R(8)$ in the two-flavor case) are not violated by dimensional regularization, it is possible to absorb all the one-loop divergences by renormalization of the NLO LECs in $\mathcal{L}^{(4)}_{cont}$ and NLO taste-violating parameters in $\mathcal{L}^{(4)}_{\text{t-v}}$. This is indeed the case in current calculations of the pseudo-Goldstone pion mass and decay constant. However, since I am only concentrating on these two physical quantities, I can only derive the renormalization conditions for certain linear combinations of LECs and taste-violating parameters. Since valence quark masses m_x, m_y, sea quark mass m_l and lattice spacing a^2 each can vary independently, one can collect the coefficients for each term separately and obtain the following renormalizations:

$$l_3^0 = \Lambda^{d-4}(l_3 - \frac{1}{64\pi^2}\mathcal{R}_\epsilon), \tag{4.78}$$

$$l_4^0 = \Lambda^{d-4}(l_4 + \frac{1}{16\pi^2}\mathcal{R}_\epsilon), \tag{4.79}$$

$$p_1^0 = \Lambda^{d-4}(p_1 + \frac{1}{8\pi^2}\mathcal{R}_\epsilon), \tag{4.80}$$

$$p_2^0 = \Lambda^{d-4}p_2, \tag{4.81}$$

$$(\tilde{L}''^0_{(2)} + \tilde{L}'^0_{(2)}) = \Lambda^{d-4}(\tilde{L}''_{(2)} + \tilde{L}'_{(2)} - (\Delta_I + 2\delta'_V + 2\delta'_A)\mathcal{R}_\epsilon), \tag{4.82}$$

$$(\tilde{L}''^0_{(2)} - \tilde{L}'^0_{(2)}) = \Lambda^{d-4}(\tilde{L}''_{(2)} - \tilde{L}'_{(2)} + 2(\Delta_{av} + \delta'_V + \delta'_A)\mathcal{R}_\epsilon), \tag{4.83}$$

Again, the renormalized coupling constants in SU(2) SχPT are scale dependent. They should change with the scale Λ in such a way that the bare coefficients are scale independent. It is easily seen from Eqs. (4.78)-(4.83) that, under a change in the chiral scale Λ to Λ', the LECs change by:

$$l_3(\Lambda') = l_3(\Lambda) + \frac{1}{64\pi^2}\log\frac{\Lambda'^2}{\Lambda^2}, \tag{4.84}$$

$$l_4(\Lambda') = l_4(\Lambda) - \frac{1}{16\pi^2}\log\frac{\Lambda'^2}{\Lambda^2}, \tag{4.85}$$

$$p_1(\Lambda') = p_1(\Lambda) - \frac{1}{8\pi^2}\log\frac{\Lambda'^2}{\Lambda^2}, \tag{4.86}$$

$$p_2(\Lambda') = p_2(\Lambda), \tag{4.87}$$

$$(\tilde{L}''_{(2)} + \tilde{L}'_{(2)})(\Lambda') = (\tilde{L}''_{(2)} + \tilde{L}'_{(2)})(\Lambda) + (\Delta_I + 2\delta'_V + 2\delta'_A)\log\frac{\Lambda'^2}{\Lambda^2}, \tag{4.88}$$

$$(\tilde{L}''_{(2)} - \tilde{L}'_{(2)})(\Lambda') = (\tilde{L}''_{(2)} - \tilde{L}'_{(2)})(\Lambda) - 2(\Delta_{av} + \delta'_V + \delta'_A)\log\frac{\Lambda'^2}{\Lambda^2}. \tag{4.89}$$

After the renormalizations in Eq. (4.78) through Eq. (4.83), the pion mass and decay constant can be written in terms of renormalized LECs and taste-violating parameters:

$$\frac{m^2_{P_5^+}}{(m_x+m_y)} =\mu_{(2)}\Big\{1+\frac{1}{16\pi^2 f^2_{(2)}}\Big[\sum_j R_j^{[2,1]}(\{\mathcal{M}^{[2]}_{XY_I}\})l(m_j^2) \\ - 2a^2{\delta'_V}^{(2)}\sum_j R_j^{[3,1]}(\{\mathcal{M}^{[3]}_{XY_V}\})l(m_j^2) + (V\leftrightarrow A) + a^2(\tilde{L}''_{(2)}+\tilde{L}'_{(2)})\Big] \\ + \frac{\mu_{(2)}}{f^2_{(2)}}(4l_3+p_1+4p_2)(m_u+m_d) + \frac{\mu_{(2)}}{f^2_{(2)}}(-p_1-4p_2)(m_x+m_y)\Big\}, \tag{4.90}$$

$$f_{P_5^+} =f_{(2)}\Big\{1+\frac{1}{16\pi^2 f^2_{(2)}}\Big[-\frac{1}{32}\sum_{Q,B} l(m^2_{Q_B}) \\ + \frac{1}{4}\Big(l(m^2_{X_I})+l(m^2_{Y_I})+(m^2_{U_I}-m^2_{X_I})\tilde{l}(m^2_{X_I})+(m^2_{U_I}-m^2_{Y_I})\tilde{l}(m^2_{Y_I})\Big) \\ - \frac{1}{2}\Big(R^{[2,1]}_{X_I}(\{\mathcal{M}^{[2]}_{XY_I}\})l(m^2_{X_I}) + R^{[2,1]}_{Y_I}(\{\mathcal{M}^{[2]}_{XY_I}\})l(m^2_{Y_I})\Big) \\ + \frac{a^2{\delta'_V}^{(2)}}{2}\Big(R^{[2,1]}_{X_V}(\{\mathcal{M}^{[2]}_{X_V}\})\tilde{l}(m^2_{X_V}) + \sum_j D^{[2,1]}_{j,X_V}(\{\mathcal{M}^{[2]}_{X_V}\})l(m_j^2) \\ + (X\leftrightarrow Y) + 2\sum_j R_j^{[3,1]}(\{\mathcal{M}^{[3]}_{XY_V}\})l(m_j^2)\Big) + (V\leftrightarrow A) \\ + a^2(\tilde{L}''_{(2)}-\tilde{L}'_{(2)})\Big] + \frac{\mu_{(2)}}{2f^2_{(2)}}(4l_4-p_1)(m_u+m_d) + \frac{\mu_{(2)}}{2f^2_{(2)}}(p_1)(m_x+m_y)\Big\}. \tag{4.91}$$

4.5 Relation of SU(2) and SU(3) staggered chiral perturbation theories

Now that we have the results for the pion mass and decay constant to NLO in SU(2) PQ-rSχPT, we can study the relations of the LECs and taste-violating parameters between the two-flavor and the three-flavor cases. This can be done by comparing formulae for physical quantities in SU(2) theory and the corresponding formulae in SU(3) theory, in the case where the light quark masses and taste splittings are much

smaller than the strange quark mass, *i.e.*,

$$\frac{m_x}{m_s}, \frac{m_y}{m_s}, \frac{m_l}{m_s}, \frac{a^2\Delta_B}{\mu m_s}, \frac{a^2\delta'_{V(A)}}{\mu m_s} \sim \epsilon \ll 1. \tag{4.92}$$

For small ϵ, we expect the SU(2) theory to be generated from the SU(3) one as in Ref. [27]. Since, at NLO in SU(3) χPT, there are terms which go like $\frac{\mu m_s}{(4\pi f)^2}$ times logarithms, we will in general need to expand to $\mathcal{O}(\epsilon)$ to pick up all terms that appear at NLO in SU(2) χPT, such as $\frac{\mu m_l}{(4\pi f)^2}$ or $\frac{a^2\Delta_B}{(4\pi f)^2}$. Of course, all dependence on m_x, m_y, m_l and a^2 must be explicit, because the LECs do not depend on the light quark masses and have no power-law dependence on lattice spacings.

I will first focus on the taste-splittings $\Delta_B^{(2)}$ and the taste-violating hairpin parameters $\delta_{V(A)}^{\prime(2)}$. In Eqs. (4.90) and (4.91), $\Delta_B^{(2)}$ and $\delta_{V(A)}^{\prime(2)}$ only appear in the NLO part, and the same statement is true for Δ_B and $\delta'_{V(A)}$ in the corresponding SU(3) formulae, so it suffices to use the relations between $\Delta_B^{(2)}$ and Δ_B, and $\delta_{V(A)}^{\prime(2)}$ and $\delta'_{V(A)}$, at LO in rSχPT.

At LO in SU(3) rSχPT, we have the mass of a flavor-nonsinglet meson:

$$m_{U_B}^2 = 2\mu m_l + a^2\Delta_B. \tag{4.93}$$

By comparing with Eq. (4.63), we conclude that at LO, for each taste index B, we have

$$a^2\Delta_B^{(2)} = a^2\Delta_B. \tag{4.94}$$

On the other hand, the mass of η_V, the lighter of the two flavor-neutral, taste-

vector mesons that mix in the SU(3) rSχPT is:

$$m_{\eta_V}^2 = \frac{1}{2}\left(m_{U_V}^2 + m_{S_V}^2 + \frac{3}{4}a^2\delta_V' - Z\right), \tag{4.95}$$

$$Z = \sqrt{(m_{S_V}^2 - m_{U_V}^2)^2 - \frac{a^2\delta_V'}{2}(m_{S_V}^2 - m_{U_V}^2) + \frac{9(a^2\delta_V')^2}{16}}. \tag{4.96}$$

In the limit $m_l = m_u \ll m_s$ and $a^2\delta'_{V(A)} \ll \mu m_s$, it should become the mass of what we call η_V' here, as given in Eq. (4.66). Indeed, we have:

$$m_{\eta_V}^2 \underset{m_l \ll m_s}{\longrightarrow} m_{U_V}^2 + \frac{1}{2}a^2\delta_V' + \mathcal{O}(\frac{(a^2\delta_V')^2}{\mu m_s}). \tag{4.97}$$

Comparing Eq. (4.66) and Eq. (4.97), we find that, at LO in rSχPT,

$$a^2{\delta_V'}^{(2)} = a^2\delta_V', \tag{4.98}$$

where corrections of $\mathcal{O}(\frac{(a^2\delta_V')^2}{\mu m_s})$ generate NLO effects in SU(2) rSχPT, since they are of $\mathcal{O}(a^4)$. A similar relation holds for ${\delta_A'}^{(2)}$ and δ_A' at LO:

$$a^2{\delta_A'}^{(2)} = a^2\delta_A'. \tag{4.99}$$

If we expand the NLO SU(3) formulae for m_π^2 and f_π in Ref. [31] in powers of ϵ, we find that the three-flavor formulae reproduce the form of the two-flavor formulae, as expected. Both are expansions in orders of $m_x, m_y, m_l, a^2\Delta_B$ and $a^2\delta'_{V(A)}$. Since the light valence quark masses, sea quark masses and lattice spacings can vary independently, we can match the coefficient of each term.

By comparing formulae in SU(2) SχPT and SU(3) SχPT, and utilizing Eqs. (4.94), (4.98) and (4.99), one obtains the relations between SU(2) LECs and SU(3) LECs up

to NLO. I find:

$$f_{(2)} = f(1 - \frac{1}{16\pi^2 f^2}\mu m_s \log\frac{\mu m_s}{\Lambda^2} + \frac{16L_4}{f^2}\mu m_s), \tag{4.100}$$

$$\mu_{(2)} = \mu(1 - \frac{1}{48\pi^2 f^2}\frac{4\mu m_s}{3}\log\frac{\frac{4\mu m_s}{3}}{\Lambda^2} + \frac{32(2L_6 - L_4)}{f^2}\mu m_s), \tag{4.101}$$

$$p_1 = 16L_5 - \frac{1}{16\pi^2}(1 + \log\frac{\mu m_s}{\Lambda^2}), \tag{4.102}$$

$$p_2 = -8L_8 + \frac{1}{16\pi^2}\frac{1}{6}(\log\frac{\frac{4}{3}\mu m_s}{\Lambda^2}) + \frac{1}{16\pi^2}\frac{1}{4}(1 + \log\frac{\mu m_s}{\Lambda^2}), \tag{4.103}$$

$$l_3 = 8(2L_6 - L_4) + 4(2L_8 - L_5) - \frac{1}{16\pi^2}\frac{1}{36}(1 + \log\frac{\frac{4}{3}\mu m_s}{\Lambda^2}), \tag{4.104}$$

$$l_4 = 8L_4 + 4L_5 - \frac{1}{16\pi^2}\frac{1}{4}(1 + \log\frac{\mu m_s}{\Lambda^2}), \tag{4.105}$$

$$\tilde{L}''_{(2)} = \tilde{L}'' - \frac{1}{6}\Delta_I(1 + \log\frac{\frac{4}{3}\mu m_s}{\Lambda^2}) - \frac{1}{2}\Delta_{av}(1 + \log\frac{\mu m_s}{\Lambda^2}), \tag{4.106}$$

$$\tilde{L}'_{(2)} = \tilde{L}' - \frac{1}{6}\Delta_I(1 + \log\frac{\frac{4}{3}\mu m_s}{\Lambda^2}) + \frac{1}{2}\Delta_{av}(1 + \log\frac{\mu m_s}{\Lambda^2}), \tag{4.107}$$

where L_4, L_5, L_6 and L_8 are renormalized SU(3) LECs, $\tilde{L}''$ and $\tilde{L}'$ are the NLO taste-violating parameters in SU(3) rSχPT. Here I use the tilde to distinguish them from L'' and L' after redefinitions in Ref. [1]. Namely, in SU(3) rSχPT, L'' and L' are related to $\tilde{L}''$ and $\tilde{L}'$ through

$$\frac{1}{16\pi^2}(L'' - L') = \frac{1}{16\pi^2}(\tilde{L}'' - \tilde{L}') - (8L_5 + 24L_4)\Delta^{(2)}_{av}, \tag{4.108}$$

$$\frac{1}{16\pi^2}(L'' + L') = \frac{1}{16\pi^2}(\tilde{L}'' + \tilde{L}') - (32L_8 - 16L_5 + 96L_6 - 48L_4)\Delta^{(2)}_{I}. \tag{4.109}$$

Eqs. (4.104) and (4.105) are the same as the equations in the full QCD continuum case [27]. Eqs. (4.102) and (4.103) relate the unphysical LECs in the partially-quenched two-flavor theory to the physical LECs in the three-flavor theory. Eqs. (4.106) and (4.107) give us relations between taste-violating parameters in the two-flavor and three-flavor theories. If we require the SU(2) SχPT to describe

the same physics in the two-flavor sector of the underlying SU(3) SχPT, all the parameters in the SU(2) theory should vary with the strange quark mass m_s according to Eqs. (4.102)-(4.107).

The renormalizations of $\tilde{L}''_{(2)}$ and $\tilde{L}'_{(2)}$ are complicated and involve the taste-splitting terms Δ_I and Δ_{av}. It is more convenient to redefine $\tilde{L}''_{(2)}$ and $\tilde{L}'_{(2)}$ by associating particular $O(a^2)$ terms with the l_i [1]. The following replacements:

$$\begin{aligned}
\frac{\mu_{(2)}}{2f_{(2)}^2}(p_1)(m_u+m_d) &\to \frac{p_1}{2f_{(2)}^2}(\mu_{(2)}(m_u+m_d)+a^2\Delta_{av}^{(2)}),\\
\frac{\mu_{(2)}}{2f_{(2)}^2}(4l_4-p_1)(m_x+m_y) &\to \frac{4l_4-p_1}{2f_{(2)}^2}(\mu_{(2)}(m_x+m_y)+a^2\Delta_{av}^{(2)}),\\
\frac{\mu_{(2)}}{f_{(2)}^2}(4l_3+p_1+4p_2)(m_u+m_d) &\to \frac{4l_3+p_1+4p_2}{f_{(2)}^2}(\mu_{(2)}(m_u+m_d)+a^2\Delta_I^{(2)}),\\
\frac{\mu_{(2)}}{f_{(2)}^2}(-(p_1+4p_2))(m_x+m_y) &\to \frac{-(p_1+4p_2)}{f_{(2)}^2}(\mu_{(2)}(m_x+m_y)+a^2\Delta_I^{(2)})
\end{aligned} \tag{4.110}$$

absorb splittings into the mass-dependent counterterms to make them correspond to the meson masses (or average values thereof) that appear in the loops. Eq. (4.110) is equivalent to defining new parameters $L''_{(2)}$ and $L'_{(2)}$:

$$\frac{1}{16\pi^2}(L''_{(2)}-L'_{(2)}) = \frac{1}{16\pi^2}(\tilde{L}''_{(2)}-\tilde{L}'_{(2)})+2l_4\Delta_{av}^{(2)}, \tag{4.111}$$

$$\frac{1}{16\pi^2}(L''_{(2)}+L'_{(2)}) = \frac{1}{16\pi^2}(\tilde{L}''_{(2)}+\tilde{L}'_{(2)})-4l_3\Delta_I^{(2)}. \tag{4.112}$$

After these redefinitions, $L''_{(2)}$ will become independent of chiral scale, and $L'_{(2)}$ is renormalized according to:

$$L'_{(2)}(\Lambda') = L'_{(2)}(\Lambda)+2(\delta_V'^{(2)}+\delta_A'^{(2)})\log\frac{\Lambda'^2}{\Lambda^2}. \tag{4.113}$$

The renormalizations of other LECs remain unchanged.

After these redefinitions, the new $L''_{(2)}$ and $L'_{(2)}$ are related to the corresponding SU(3) quantities L'' and L' by:

$$\begin{aligned} L''_{(2)} - L'_{(2)} &= (L'' - L') - \Delta_{av}(1 + \log\frac{\mu m_s}{\Lambda^2}) + 16\pi^2\Delta_{av}(8L_5 + 24L_4 - 2l_4) \\ &= (L'' - L') + \Delta_{av}\left[128\pi^2 L_4 - \frac{1}{2}(1 + \log\frac{\mu m_s}{\Lambda^2})\right] \qquad (4.114) \\ L''_{(2)} + L'_{(2)} &= (L'' + L') - \frac{1}{3}\Delta_I(1 + \log\frac{\frac{4}{3}\mu m_s}{\Lambda^2}) + 16\pi^2\Delta_I(32L_8 - 16L_5 + 96L_6 - 48L_4 - 4l_3) \\ &= (L'' + L') + \Delta_I\left[16\pi^2(32L_6 - 16L_4) - \frac{2}{9}(1 + \log\frac{\frac{4}{3}\mu m_s}{\Lambda^2})\right] \qquad (4.115) \end{aligned}$$

Using the standard scale renormalization of the L_i [27],

$$L_i(\Lambda') = L_i(\Lambda) + \frac{C_i}{256\pi^2}\log\frac{\Lambda'^2}{\Lambda^2} \qquad (4.116)$$

with

$$C_4 = -1\ ; \qquad C_5 = -3\ ; \qquad (4.117)$$

$$2C_6 - C_4 = -2/9\ ; \qquad 2C_8 - C_5 = 4/3, \qquad (4.118)$$

it is easy to check that the factors in square parenthesis in Eqs. (4.114) and (4.115) are scale independent. This is a consistency check, since $L''_{(2)}$ and $L'_{(2)}$ transform in the same way as L'' and L', respectively, under scale change.

4.6 Remarks and conclusion

I calculated the pseudo-Goldstone pion mass and decay constant to NLO in two-flavor PQ-rSχPT using the replica method. I also checked that SU(2) rSχPT emerges from SU(3) rSχPT in the limit $\frac{m_x}{m_s}, \frac{m_y}{m_s}, \frac{m_l}{m_s}, \frac{a^2\Delta_B}{\mu m_s}, \frac{a^2\delta'_{V(A)}}{\mu m_s} \ll 1$, as assumed in Ref. [16]. Finally, I derived the relations for the LECs and taste-violating parameters between

the two-flavor and three-flavor cases. Some of the formulae here (Eqs. (4.90) and (4.91)) are used for the SU(2) chiral fits to MILC data [51].

At the present stage, we have MILC data for the light pseudoscalar mass and decay constant at five lattice spacings from 0.15 fm to 0.045 fm, generated with 2+1 flavors of asqtad improved staggered quarks. For each lattice spacing, we have many different sea quark masses as well as many different combinations of valence quark masses. For most ensembles, the strange quark mass is near its physical value, and the light sea quark masses are much smaller. If light valence quark masses and taste splittings are also taken significantly smaller than the strange quark mass, we expect that SU(2) rSχPT would apply. Preliminary results indicate that it is indeed the case. Since the strange quark mass is close to the physical value in the ensembles used for the fits, the SU(2) LECs only suffer small changes due to variations in the strange quark mass. We can fit to lattice data using Eqs. (4.90) and (4.91) to get values of SU(2) LECs, the pion decay constant f_π, and the physical light quark mass $\hat{m}$, as well as the chiral condensate in the two-flavor chiral limit. Furthermore, we can do a systematic NNLO SU(2) chiral fit if continuum NNLO chiral logarithms [48] and possible analytic terms are included, and if taste-violations are relatively small. The results appear to be consistent with the results of the SU(3) analysis [51].

However, to make the formulae complete and results more accurate, it may be important to incorporate the effects of the variations in the strange quark mass by doing appropriate adjustments on certain parameters in the two-flavor theory. In practice, for each strange quark mass, the four LECs l_3, l_4, p_1 and p_2 may be adjusted according to Eqs. (4.102)-(4.105), and the two taste-violating parameters, $L''_{(2)}$ and

$L'_{(2)}$, may be adjusted according to Eq. (4.114) and Eq. (4.115). One then performs chiral fits to all the lattice data simultaneously. At the final step, physical values of LECs can be obtained by extrapolating to the physical strange quark mass.

An extension of the present work to the case of quantities involving the strange quark such as f_K or m_K^2 using the method of heavy kaon χPT [52, 53] may be very useful. Work on that is in progress.

Chapter 5

SU(2) Chiral Fitting to MILC Data

The MILC Collaboration has been running QCD simulations with "2+1" asqtad improved staggered fermions. At the present stage, dynamical gauge ensembles are available with many combinations of light sea quark masses and strange quark masses. Lattice spacings range from 0.15 fm to 0.045 fm. On each ensemble, physical quantities, including light pseudoscalar meson masses and pion decay constants, are measured with several choices of light valence quark masses. By fitting lattice data to the formulae for light pseudoscalar masses and decay constants in the partially-quenched case, we can extract the values of SU(3) LECs (L_i), decay constant, quark masses and the chiral condensate in the chiral limit [2, 51].

5.1 Light pseudoscalar meson mass and decay constant

Mesons are created (or annihilated) by bilinear quark operators. With the staggered fermion formalism, there are four taste species for each flavor of quarks. Therefore, each meson comes with sixteen varieties, labeled by the index t. For a pion composed of x and y valence quarks with taste index t, the interpolating operator is given by $O_\pi = \bar{\psi}_x(\gamma_5 \otimes \xi_t)\psi_y$, where the Dirac matrix is γ_5 since the pion is a pseudoscalar.

One can find the lightest pseudoscalar meson mass m_{PS} through the asymptotic behavior of the zero-momentum correlation function

$$C_{PP} = \frac{1}{V_s}\sum_{\vec{y}}\langle O_P(\vec{y},t)O_P^\dagger(\vec{x},0)\rangle = c_{PP}e^{-m_{PS}t} + \cdots , \tag{5.1}$$

where V_s is the spatial volume. With m_{PS} available, the pion decay constant can be obtained from c_{PP} by [1]

$$f_{PS} = (m_x + m_y)\sqrt{\frac{V_s c_{PP}}{4m_{PS}^3}}, \tag{5.2}$$

where m_x and m_y are the masses of the valence quarks of pion.

In practice, a Coulomb wall source or a random wall source is used instead of the point source to reduce the contaminations from excited states in Eq. (5.1). After these measurements, we have the light pseudoscalar meson masses and decay constants for each gauge ensemble and each combination of valence quark masses.

Lattice	$r_1^2\Delta_P$	$r_1^2\Delta_A$	$r_1^2\Delta_T$	$r_1^2\Delta_V$	$r_1^2\Delta_I$	slope
$a \approx 0.18$fm	0.0	0.573682	0.913424	1.22711	1.50066	6.38638
$a \approx 0.15$fm	0.0	3.914643e-01	6.177688e-01	7.961597e-01	9.851499e-01	6.761193e+00
$a \approx 0.12$fm	0.0	2.270460e-01	3.661620e-01	4.802591e-01	6.008212e-01	6.831904e+00
$a \approx 0.09$fm	0.0	0.0746922	0.123776	0.159322	0.220652	6.638563e+00
$a \approx 0.06$fm	0.0	0.026348	0.0429778	0.0574378	0.0703879	6.486649e+00
$a \approx 0.045$fm	0.0	0.0104093	0.0169792	0.0226919	0.0278081	6.417427e+00
continuum	0.0	0.0	0.0	0.0	0.0	6.735978e+00

5.2 Measuring taste splittings

Due to taste-violating effects, there are mass splittings between different taste copies of a meson with given flavor structure. At LO in ChPT, the taste splittings of a pion P composed of two valence quarks x and y are $a^2\Delta_B$ in Eqs. (3.56). These splittings are functions of the lattice spacing a, so for each lattice spacing, one collects all the pion masses with different taste structures and fits them to Eqs. (3.56), to find the splittings in each taste channel. On the m_π^2 vs m_q plots, the splittings can be read from the intercepts of the fit lines. For example, the fit results for "coarse" ($a \approx 0.12$fm) lattices are shown in figure (5.1).

Doing this for each lattice spacing, we find all the splittings and list them in table (5.2). Note that the taste splittings are correct to LO, that is, the errors appear at NLO $\mathcal{O}(a^2, m_q, p^2)$. These values can be used in the NLO part of the formulae for pion masses or decay constants.

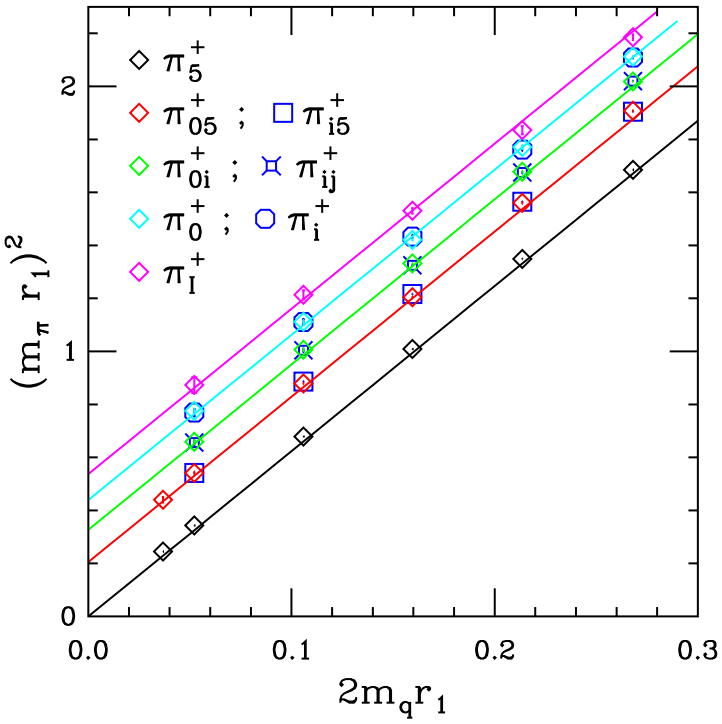

Figure 5.1: Squared masses of pions for various tastes on the lattices with $a \approx 0.12$fm are shown as functions of quark masses. The splittings appear to be independent of quark masses. All quantities are in units of r_1. (The scale r_1 is defined below in section (5.3).) Plot is from Ref. [1].

5.3 Determining lattice spacings

Quantities measured on the lattice are dimensionless numbers, *i.e.*, $m_\pi a$. Only in the continuum limit and with physical quark masses can one compare these numbers to the values of physical quantities. In order to obtain dimensionful results from simulations with unphysical quark masses and finite lattice spacings, one needs to set up a scheme to determine the lattice spacing a. A commonly used method is to use a Sommer scale r [54]. By definition, the distance r satisfies $r^2F(r) = C$, where C is a constant and $F(r)$ is the force between a static quark and anti-quark. The MILC collaboration uses r_1 defined by $C = 1$, which has smaller statistical errors than r_0 defined by $C = 1.65$ [55].

For each ensemble, one measures the quark anti-quark potential $V(R)$ and finds the corresponding r_1 by solving $r^2F(r) = 1$ [12]. Here r_1 still takes the dimensionless form r_1/a. One then fits all the r_1/a values from each ensemble to a smooth function of the gauge coupling and quark masses. There are two different choices of the fit function: one is to fit $\log(r_1/a)$ to a polynomial in β and $2am_l + am_s$ [12], another is to use the function form by Allton [56]:

$$\frac{a}{r_1} = \frac{C_0 f + C_2 g^2 f^3 + C_4 g^4 f^3}{1 + D_2 g^2 f^2}, \tag{5.3}$$

where

$$\begin{aligned} f = (b_0 g^2)^{(-b_1/(2b_0^2))} \exp(-1/(2b_0 g^2)) \ , \qquad & b_0 = (11 - 2n_f/3)/(4\pi)^2 \ , \\ b_1 = (102 - 38n_f/3)/(4\pi)^4 \ , \qquad & am_{tot} = 2am_l/f + am_s/f \ , \\ C_0 = C_{00} + C_{01l} am_l/f + C_{01s} am_s/f + C_{02}(am_{tot})^2 \ , \qquad & C_2 = C_{20} + C_{21} am_{tot}, \end{aligned} \tag{5.4}$$

where n_f is the number of flavors, which is set to be 3 since the simulation is done with 2+1 dynamical quarks. Here, am_l, am_s are sea quark masses in lattice units. C_{00}, C_{01l}, C_{01s}, C_{02}, C_{20}, C_{21}, C_4 and D_2 are parameters that can be determined by fitting the function in Eq. (5.3) to values of $r1/a$ measured on different lattices.

To find r_1 in physical units, one needs to determine some physical quantities on the lattice and compare to the experimental value. Often, the 2S-1S energy splittings of the $b\bar{b}$ meson $\Delta_{2S-1S}r_1$ is used. For each ensemble, one fits the splittings to the form $\Delta^{phys}_{2S-1S}r_1(a, am_l, am_s) = \Delta^{phys}_{2S-1S}(r_1^{phys} + c_1a^2 + c_2am_l/(am_s))$. After extrapolating in m_l and a, and using the experimental value of Δ^{phys}_{2S-1S}, one finds $r_1^{phys} = 0.318$fm with an error of 0.007fm [1]. This has recently been updated by HPQCD collaboration to $r_1^{phys} = 0.3133(23)(3)$fm [57], where the first error is the combined statistical and systematic error, and the second is from uncertainties in finite volume corrections to the chiral analysis.

Another method to determine r_1^{phys} is to match the value of the pion decay constant f_π obtained from SU(3) chiral analysis to its experimental value, $f_\pi = 130.4 \pm 0.2$MeV [58]. That gives $r_1^{phys} = 0.3117(6)(^{+12}_{-31})$fm where the first error is statistical and the second is systematic.

Finally, the lattice spacing can be determined by $a = (a/r_1) \times r_1^{phys}$, where $(a/r_1)$is the smoothed value from Eq. 5.3. The smoothed function depends on the sea quark masses used in the simulations, *e.g.*, am_l, am_s. For ensembles with the same β but different sea quark masses, the values of r_1/a are different, hence the lattice spacings vary with sea quark masses. Therefore, we call this scale setting scheme a mass-dependent scheme. Since in chiral perturbation theory, all dependence on the quark

masses should be explicit, a mass-independent scale setting scheme is necessary. This can be done by using Eq. 5.3 with the quark masses am_l, am_s set to be physical values determined for each lattice spacing. In the mass independent scheme, the value of r_1/a only depends on β and the tadpole improvement factor u_0.

Through our analysis, all of the quantities take their dimensionless forms by multiplying appropriate powers of r_1. They can be converted to physical units using r_1^{phys} when necessary.

5.4 NNLO SU(2) chiral analysis

5.4.1 Motivation for SU(2) chiral analysis

At present, most lattice QCD simulations are performed at unphysical light dynamical quark masses. Fitting of lattice data to forms calculated in chiral perturbation theory (χPT) [27, 26] makes possible a controlled extrapolation of lattice results to the physical light quark masses and to the chiral limit. This approach also allows one to determine the values of LECs in the theory, which are of phenomenological significance. Although three-flavor χPT has been used successfully for simulations with 2+1 dynamical quarks, we are still interested in the applications of two-flavor χPT for the following reasons:

1. The up and down dynamical quark masses in simulations are usually much smaller than the strange quark mass, which is near its physical value; hence SU(2) χPT may serve as a better approximation and probably converges faster

than SU(3) χPT.

2. Fits to SU(2) χPT can give us direct information about the LECs in the two-flavor theory, especially l_3 and l_4.

3. By comparing results from these two different fits, we can study the systematic errors resulting from the truncations of each version of χPT.

Recently, some groups have used SU(2) χPT for chiral fits to data from three-flavor simulations [52, 59]. Here, we will perform such an SU(2) chiral analysis for MILC data from simulations with 2+1 flavors of staggered fermions.

5.5 Fitting in detail

5.5.1 Fit formulae for pion mass and decay constant

From Chapter 4, we already have the formulae for the pseudoscalar pion mass and decay constant up to NLO in partially-quenched SU(2) rSχPT. In order to perform a systematic chiral analysis at NNLO, we need to include the effects of operators of order $\mathcal{O}(m_q^3, a^2m_q^2, a^4m_q, a^6)$ and corresponding loop effects. These loop effects will contribute to the decay constant and the ratio $m_\pi^2/(m_x+m_y)$ at $\mathcal{O}(m_q^2, a^2m_q, a^4)$.

Analytic terms at $\mathcal{O}(m_q^2)$ can be included in the formula of pion mass by adding four additional terms:

$$\frac{(m_{P_5^+}^{NNLO})^2}{(m_x+m_y)} = \mu(1+\text{NLO}+\beta_1^{(m)}(\chi_x+\chi_y)^2+\beta_2^{(m)}\chi_{ud}^2+\beta_3^{(m)}(\chi_x+\chi_y)\chi_{ud}+\beta_4^{(m)}(\chi_x-\chi_y)^2), \tag{5.5}$$

where we assume the up and down sea quark masses are degenerate, $\chi_u = \chi_d = \chi_{ud}$. The form of these terms is constrained by the interchanging symmetries $x \leftrightarrow y$ and $u \leftrightarrow d$. Similarly there are an additional four terms for the pion decay constant:

$$f_{P_5^+}^{NNLO} = f(1+\text{NLO}+\beta_1^{(f)}(\chi_x+\chi_y)^2+\beta_2^{(f)}\chi_{ud}^2+\beta_3^{(f)}(\chi_x+\chi_y)\chi_{ud}+\beta_4^{(f)}(\chi_x-\chi_y)^2) \quad (5.6)$$

These new parameters $\beta_1^{(m)}--\beta_4^{(m)}$ and $\beta_1^{(f)}--\beta_4^{(f)}$ are linear combinations of NNLO LECs at $\mathcal{O}(m_q^3)$. For our purposes of chiral fitting, it is enough to know that Eq. (5.5) and Eq. (5.6) contain the most general terms at $\mathcal{O}(m_q^3)$.

At NNLO, there are also $\mathcal{O}(m_q a^2)$ terms contributing to the ratio in Eq. (5.5) and decay constant. Since we allow the l_i to vary with lattice spacing in the fit, some effects from these terms are actually included in our fitting.

The $\mathcal{O}(a^4)$ terms are neglected because we expect the effects from these terms are small. One can measure the size of $\mathcal{O}(a^2)$ taste-violations by the quantity [1]

$$\chi_{a^2} \equiv \frac{a^2\overline{\Delta}}{8\pi^2 f_\pi^2}, \quad (5.7)$$

where $a^2\overline{\Delta}$ is the average taste-violating term (see below). For fine lattices ($a \approx$ 0.09fm), $a^2\overline{\Delta} \approx (200\text{MeV})^2$ and χ_{a^2} is about 0.03. Hence we expect the contributions of $\mathcal{O}(a^4)$ terms are at the order of $\chi_{a^2}^2 \sim 0.1\%$ and thus negligible, and terms of $\mathcal{O}(m_q a^2)$ are subleading (see below).

Since $m_{P_5^+}^2/(m_x + m_y)$ divides by quark masses, one might worry that terms of $\mathcal{O}(a^6)$ in the chiral Lagrangian might contribute at $\mathcal{O}(a^6/m_q)$. This can not happen because P_5^+ is a Goldstone pion, so $m_{P_5^+}^2$ is always proportional to $(m_x + m_y)$ and $\mathcal{O}(a^6)$ terms are excluded. For $f_{P_5^+}$, only those terms in chiral Lagrangian which have at least two derivatives can make contributions to the pion decay constant, so terms

of $\mathcal{O}(a^6)$ in the chiral Lagrangian do not contribute to the decay constant. Terms of $\mathcal{O}(p^2a^4)$ in the Lagrangian do contribute and give the terms of $\mathcal{O}(a^4)$ in $f_{P_5^+}$.

Since NNLO chiral logarithms for SχPT are not available at the moment, we use instead the continuum NNLO chiral logarithms by Bijnens and Lahde [48]. When applied at finite lattice spacing a, there is an ambiguity in defining the pion mass in the continuum formulae. In practice, we use the root mean square (RMS) average pion mass in calculations of NNLO chiral logarithms:

$$m_{RMS}^2 = m_{xy}^2 + a^2\overline{\Delta}, \tag{5.8}$$

where $\overline{\Delta}$ is the average taste splittings $\overline{\Delta} = \frac{1}{16}\sum_B \Delta_B$. This is systematic at NNLO as long as the taste splittings between different pions are significantly smaller than the pion masses themselves. This condition is best satisfied on the superfine ($a \approx 0.06$fm) and ultrafine ($a \approx 0.045$fm) lattices, and corresponds to the dropping of $\mathcal{O}(a^4)$ and $\mathcal{O}(m_q a^2)$ terms above from the systematic analysis.

Note that in the continuum NNLO chiral logarithms, the convention of NLO LECs used by Bijnens and Lahde, $L_i^{(2pq)}$, is different from what we are using. One thus needs to express their NLO LECs in terms of our NLO LECs defined in Eq. (4.44). Let l_i and p_i denote the renormalized ones of l_i^0 and p_i^0, and $L_i^{r(2pq)}$ denote the renormalized

ones of $L_i^{(2pq)}$. These two sets of parameters are related by

$$
\begin{aligned}
L_0^{r(2pq)} &= -p_4, & L_1^{r(2pq)} &= \frac{l_1}{4} + \frac{p_3+p_4}{2}, \\
L_2^{r(2pq)} &= \frac{l_2}{4} + p_4, & L_3^{r(2pq)} &= -p_3 - 2p_4, \\
L_4^{r(2pq)} &= \frac{l_4}{8} - \frac{p_1}{32}, & L_5^{r(2pq)} &= \frac{p_1}{16}, \\
L_6^{r(2pq)} &= \frac{l_3+l_4}{16} + \frac{p_2}{16}, & L_7^{r(2pq)} &= -\frac{l_7}{16} + \frac{p_2}{16}, \\
L_8^{r(2pq)} &= -\frac{p_2}{8}, & L_9^{r(2pq)} &= -\frac{l_6}{2}, \\
L_{10}^{r(2pq)} &= l_5. & & \qquad (5.9)
\end{aligned}
$$

The NNLO analytic terms involve linear combinations of NNLO LECs. In order to make these LECs chiral scale invariant on the lattice ($a \neq 0$), one needs to make some modifications of the quark masses which appear in NNLO analytic terms to match the RMS pion mass (Eq. (5.8)) used in NNLO chiral logarithms [60].

$$m_x \to \tilde{m}_x = m_x + \frac{a^2\overline{\Delta}}{2\mu}, \qquad (5.10)$$

and similarly for m_y and m_l. This will be done in future analysis, and it has not been included in current work yet. We note that the results are already independent of the chiral scale in the continuum limit.

In addition, sometimes we add NNNLO analytic terms to the pion mass and decay constant. Specifically, we add in terms at $\mathcal{O}(m_q^3)$ in the formulae for $m^2_{P_5^+}/(m_x+m_y)$ and $f_{P_5^+}$. When $\chi_u = \chi_d \equiv \chi_{ud}$, there are five possible forms of these terms which

satisfy the interchanging symmetries.

$$\frac{m^2_{P_5^+}}{m_x+m_y} = \mu(1+NLO+NNLO+\rho_1^{(m)}(\chi_x+\chi_y)^3+\rho_2^{(m)}(\chi_x+\chi_y)^2\chi_{ud} + \rho_3^{(m)}(\chi_x-\chi_y)^2\chi_{ud}+\rho_4^{(m)}(\chi_x+\chi_y)\chi_{ud}^2+\rho_5^{(m)}\chi_{ud}^3), \quad (5.11)$$

$$f_{P_5^+} = f(1+NLO+NNLO+\rho_1^{(f)}(\chi_x+\chi_y)^3+\rho_2^{(f)}(\chi_x+\chi_y)^2\chi_{ud} + \rho_3^{(f)}(\chi_x-\chi_y)^2\chi_{ud}+\rho_4^{(f)}(\chi_x+\chi_y)\chi_{ud}^2+\rho_5^{(f)}\chi_{ud}^3). \quad (5.12)$$

Fits including these NNNLO terms are only used to estimate the errors from truncations of χPT.

To summarize, at NNLO, we add four analytic terms for $m^2_{P_5^+}$ and $f_{P_5^+}$ each. Continuum NNLO chiral logarithms are used with pion mass set to be the RMS average pion mass. This completes our NNLO formulae used for central value fits. NNNLO analytic terms are only included in fits to estimate systematic errors.

5.5.2 Datasets used for SU(2) analysis

At the present stage, we have MILC data for the light pseudoscalar mass and decay constant at five lattice spacings from 0.15 fm to 0.045 fm, generated with 2+1 flavors of asqtad improved staggered quarks. For each lattice spacing, we have several different sea quark masses as well as many different combinations of valence quark masses. In order for the SU(2) formulae to apply, we require both sea and valence quark masses to be significantly smaller than the strange quark mass, *i.e.*, $m_\pi^{sea} \ll m_K$, and $m_\pi^{valence} \ll m_K$. In the fits described below, we use the following cutoff on our data sets:

$$m_l \le 0.2 m_s^{phys}, \qquad m_x+m_y \le 0.5 m_s^{phys}, \qquad \max(m_x,m_y) \le 0.32 m_s^{phys}, \quad (5.13)$$

where m_l is the light sea quark mass, and m_x and m_y are the valence masses in the pion.

To be able to consider the strange quark as "heavy" and eliminate it from the chiral theory, it is also necessary that taste splittings between different pion states be much smaller than the kaon mass. Furthermore, taste splittings should be significantly smaller than the pion mass itself for the continuum formulae for the NNLO chiral logarithms to be approximately applicable.

The lattices that are at least close to satisfying all these conditions include four fine ($a \approx 0.09\,\text{fm}$) ensembles, three superfine ($a \approx 0.06\,\text{fm}$) ensembles and one ultrafine ensemble ($a \approx 0.045\,\text{fm}$). Relevant parameters for these ensembles are listed in Table 5.1.

In Table 5.2, we list the Goldstone, RMS and singlet pion masses on representative ensembles. It can be seen that for the fine ($a \approx 0.09\,\text{fm}$) ensembles, either some pion masses are close to the kaon mass, as on ensemble $(am_l, am_s) = (0.0062, 0.031)$, or the taste splittings between pions are comparable to the pion mass, as on ensemble $(am_l, am_s) = (0.00155, 0.031)$. As a result, the data from fine lattices may not be well described by SU(2) formulae with continuum NNLO chiral logarithms. Our central fit uses superfine and ultrafine data only, while we include fits to all three kinds of lattices to estimate systematic errors.

5.5.3 Fitting strategies

All of the following fitting strategies are the same as those used in the three-flavor chiral analysis. Here I just give a brief review.

Ensemble	am_l	am_s	β	size	$m_\pi L$
$\approx 0.09\,\mathrm{fm}$ (F)	0.0062	0.031	7.09	$28^3 \times 96$	4.14
$\approx 0.09\,\mathrm{fm}$ (F)	0.00465	0.031	7.085	$32^3 \times 96$	4.10
$\approx 0.09\,\mathrm{fm}$ (F)	0.0031	0.031	7.08	$40^3 \times 96$	4.22
$\approx 0.09\,\mathrm{fm}$ (F)	0.00155	0.031	7.075	$64^3 \times 96$	4.80
$\approx 0.06\,\mathrm{fm}$ (SF)	0.0036	0.018	7.47	$48^3 \times 144$	4.50
$\approx 0.06\,\mathrm{fm}$ (SF)	0.0025	0.018	7.465	$56^3 \times 144$	4.38
$\approx 0.06\,\mathrm{fm}$ (SF)	0.0018	0.018	7.46	$64^3 \times 144$	4.27
$\approx 0.045\,\mathrm{fm}$ (UF)	0.0028	0.014	7.81	$64^3 \times 192$	4.56

Table 5.1: Ensembles used in this analysis. Here, (F), (SF) and (UF) stand for fine, superfine and ultrafine lattices respectively. The quantities am_l and am_s are the light and strange sea quark masses in lattice units; $m_\pi L$ is the (sea) Goldstone pion mass times the linear spatial size. The fine ensembles are not used in our central value fit, but only in estimating systematic errors.

a	$\approx 0.09\,\text{fm}$ (F)		$\approx 0.06\,\text{fm}$ (SF)		$\approx 0.045\,\text{fm}$ (UF)
am_S	0.031		0.018		0.014
am_l	0.00155	0.0062	0.0018	0.0036	0.0028
m_K(MeV)	559	607	515	543	551
$m_\pi^{\text{Goldstone}}$(MeV)	177	355	224	317	324
m_π^{RMS}(MeV)	281	416	258	341	334
m_π^{I}(MeV)	346	463	280	359	341

Table 5.2: Kaon masses and lightest (sea) pion masses on some sample ensembles. Here three different pion masses are shown: Goldstone, RMS and singlet. $r_1 = 0.3117\,\text{fm}$ is used.

Correlated least chi square fit

Our goal is to fit the lattice data, *i.e.*, pion masses or decay constants, to the desired formulae and find the optimal choices for the values of parameters in the theory. Suppose the fitting function takes the form $f(x_i, \{\lambda\})$ with x_i as the "coordinates" and $\{\lambda\}$ as the free parameters in the theory. The usual least chi square fit method is to find the set of $\{\lambda\}$ which minimizes χ^2. If the data are not correlated, χ^2 is defined as

$$\chi^2 = \sum_i (f(x_i, \{\lambda\}) - f_i)^2/\sigma_i^2, \tag{5.14}$$

where f_i is the measured lattice data at point x_i, and σ_i is the corresponding standard deviation of the mean. This is equivalent to maximizing the probability distribution

of finding the data set f_i

$$P(f_i) \propto \exp\left[-\frac{1}{2}\sum_i (f_i - f(x_i, \{\lambda\}))^2\right]. \tag{5.15}$$

If the data are correlated, the correlations can be taken into account by using the covariance matrix C. Let n be the number of data points, C is a $n \times n$ matrix with each element C_{ij} representing the correlations between i-th and j-th data. In this case, the chi square function is

$$\chi^2 = \sum_{i,j} (f(x_i, \{\lambda\}) - f_i) C_{ij}^{-1} (f(x_j, \{\lambda\}) - f_j). \tag{5.16}$$

For lattice calculations, measurements are performed on gauge configurations generated by Markov chain processes. There are still remnant auto correlations after we pick configurations with large separations in the chain. One ought to consider the effects from autocorrelations in the analysis, otherwise the errors will be underestimated. There are two ways to deal with this. One is to block successive configurations and estimate errors from the variance of blocks, then increase the size of blocks until the errors become stable. Another way, which is used in this work, is to use the measured autocorrelations in the data to rescale the covariance matrix and then use the rescaled covariance matrix in the analysis. This can be understood in the sense that there is an effective non-correlating length l, and the variance obtained by effective correlation configurations is roughly $\sqrt{l}$ times the variance obtained from the original configurations. Usually, this factor $\sqrt{l}$ is not very large, $\approx 10 - 15\%$ in our case, corresponding to an approximately 10% change in the value of χ^2 from the fits. This, however, could produce large changes (orders of magnitude) to the confidence

level if the degrees of freedom (DOF) is large. The effects are milder in small DOF cases, but can still be important.

Even if successive configurations are not correlated, physical quantities are still correlated with each other [12]. As a result, one should always include the effects from correlations by using the full covariance matrix in the fits.

Bayesian methods

Constrained curve fits are used in our analysis since they provide an elegant procedure for incorporating systematic uncertainties due to under-constrained parts of a theory [61]. The Bayesian method turns out to be a very useful tool for fits with constraints. The discussion in this part will follow the relevant part in Ref. [4] closely.

The essential point of Bayesian methods is the application of Bayes' theorem. For two events A and B, the Bayes' theorem relates two conditional probabilities $P(A|B)$ and $P(B|A)$ in the following way

$$P(A|B) = \frac{P(B|A)P(A)}{P(B)}. \tag{5.17}$$

Here, $P(A)$ is the probability of event A independent of event B, $P(B)$ is the probability of event B independent of event A. $P(A|B)$ is the conditional probability of event A given B, $P(B|A)$ is the conditional probability of B given A.

Bayes' theorem can be applied to our fitting in the following way: event A is that the parameters in our model take certain values $\{\lambda\}$, event B is that the measured values are $\{f_i\}$. What we need is that given the measured data $\{f_i\}$, which set of parameters $\{\lambda\}$ has the largest likelihood, *i.e.*, the largest $P(A|B) = P(\{\lambda\}|\{f_i\})$. In

this case, Bayes' theorem takes the form

$$P(\{\lambda\}|\{f_i\}) = \frac{P(\{f_i\}|\{\lambda\})P(\{\lambda\})}{P(\{f_i\})}. \tag{5.18}$$

In the numerator, the first factor is just the probability function in Eq. (5.15). The second factor $P(\{\lambda\})$ is the probability that the parameters take the value $\{\lambda\}$ independent of our measurements. In another words, this is a prior probability. The denominator $P(\{f_i\})$ is just a normalization factor and it can be ignored here. Therefore, We have

$$P(\{\lambda\}|\{f_i\}) \propto P(\{f_i\}|\{\lambda\})P_{prior}(\{\lambda\}). \tag{5.19}$$

In practice, we assume that the prior distribution can be approximated by the Gaussian

$$P_{prior}(\{\lambda\}) = e^{-\chi^2_{prior}(\{\lambda\})/2}, \tag{5.20}$$

where $\chi^2(\{\lambda\})$ is defined as

$$\chi^2_{prior}(\{\lambda\}) \equiv \sum_n \frac{(\lambda_n - \tilde{\lambda}_n)^2}{\tilde{\sigma}_n^2}. \tag{5.21}$$

Here, $\tilde{\lambda}_n$ and $\tilde{\sigma}_n$ are "priors" input to the fitting. Their values should be chosen on the basis of prior knowledge like experimental values or previous fit results.

In summary, one can use the augmented χ^2_{aug} [61]

$$\begin{aligned} \chi^2_{aug} &\equiv \chi^2 + \chi^2_{prior}, \\ &= \chi^2 + \sum_n \frac{(\lambda_n - \tilde{\lambda}_n)^2}{\tilde{\sigma}_n^2}, \end{aligned} \tag{5.22}$$

and minimize this new chi square instead of the original one. The fit will favor the parameter λ_n in the interval $\tilde{\lambda}_n \pm \tilde{\sigma}_n$.

Suppose $\{\lambda\} = \{\lambda^*\}$ minimizes χ^2_{aug}, the error of a function $g(\{\lambda\})$ can be approximated by

$$\sigma_g^2 \approx \sum_{ij} C_{ij} \partial_i g(\{\lambda^*\}) \partial_j g(\{\lambda^*\}). \tag{5.23}$$

5.5.4 Finite volume corrections

If the system is in a finite spatial volume L^3, one can incorporate the finite volume effects by modifying the one-loop integrals $l(m^2)$ and $\tilde{l}(m^2)$ [62, 49] which appear in NLO formulae of $m^2_{P_5^+}$ and $f_{P_5^+}$

$$l(m^2) \Rightarrow l(m^2) \equiv m^2 \left(\ln \frac{m^2}{\Lambda^2} + \delta_1(mL) \right), \tag{5.24}$$

$$\tilde{l}(m^2) \Rightarrow \tilde{l}(m^2) \equiv - \left(\ln \frac{m^2}{\Lambda^2 + 1} \right) + \delta_3(mL), \tag{5.25}$$

where L is the spatial dimension. The finite volume correction terms $\delta_1(mL)$ and $\delta_3(mL)$ are [49]

$$\delta_1(mL) = 4 \sum_{\vec{r} \neq 0} \frac{K_1(mL|\vec{r}|)}{mL|\vec{r}|}, \tag{5.26}$$

$$\delta_3(mL) = 2 \sum_{\vec{r} \neq 0} K_0(mL|\vec{r}|), \tag{5.27}$$

where K_0 and K_1 are Bessel functions of imaginary argument. The corrections due to finite time extent are negligible because the time dimension is between 2.4 to 3 times larger than the spatial dimension.[1]

There could be residual finite volume corrections from terms beyond one-loop in $S\chi PT$. Such effects were investigated by Colangelo and Haefeli [63] in full continuum

[1] The only one exception is the fine lattice ensemble with $am_l/am_s = 0.00155/0.031$, of which the dimension is $64^3 \times 96$.

QCD and it was shown that higher order corrections could be $30\% - 50\%$ of the one-loop results [1]. For the volume and meson masses relevant to our computations, the residual finite volume corrections are roughly 0.002797 for f_π and 0.00065147 for m_π. This was determined by direct calculation on a lattice with 40% bigger volume. We make the corresponding modifications in the last step before we give the quoted value of f_π.

5.6 Central value fit

For the central value fit, we use three superfine ensembles $(am_l, am_s) = \{(0.0018, 0.018)$, $(0.0025, 0.018)$, $(0.0036, 0.018)\}$ and one ultrafine ensemble $(am_l, am_s) = (0.0028, 0.014)$. Fine ensembles $(am_l, am_s) = \{(0.00155, 0.031)$, $(0.0031, 0.031)$,$(0.00465, 0.031)$, $(0.0062, 0.031)\}$ are only used to estimate systematic errors.

5.6.1 List of parameters

There are a total of 29 parameters in our fits. The following list shows how these parameters are treated in the central fit.

(a) LO: 2 unconstrained parameters, $\mu_{(2)}$ and $f_{(2)}$.

(b) NLO (physical): 4 parameters, l_3, l_4 and two extra LECs p_1, p_2 that only appear in partially-quenched χPT. All of these parameters are unconstrained.

(c) NLO (taste-violating): 4 parameters. δ'_V, δ'_A are constrained within errors at the values determined from SU(3) SχPT fits [1, 2]; $L''_{(2)}$ and $L'_{(2)}$ are constrained

around 0, with width of 0.3 as estimated in Ref. [1].

(d) NNLO (physical, $\mathcal{O}(p^4)$): 5 parameters (l_1, l_2, l_7, p_3, p_4) that first appear in meson masses and decay constants in the NNLO chiral logarithms. l_1 and l_2 are constrained by the range determined from continuum phenomenology [64]; l_7 is not constrained since it is not directly known from phenomenology [64]. The partially-quenched parameters p_3 and p_4 are not constrained.

(e) NNLO (physical, $\mathcal{O}(p^6)$): 8 parameters c_i, constrained around 0 with width 1 in "natural units" (see Ref. [1]).

(f) The physical LO and NLO parameters are allowed to vary with lattice spacing by an amount proportional to $\alpha_s(a\Lambda)^2$, which is the size of the "generic" discretization errors with asqtad quarks, where Λ is some typical hadronic scale. This introduces 6 additional parameters that are constrained around 0 with width corresponding to a scale $\Lambda = 0.7\,\mathrm{GeV}$.

Alternative versions of the fits, in which the width of the constraints are changed, or some constrained parameters are left unconstrained (or *vice versa*), have also been tried, and the results from those fits are included in the systematic error estimates.

Our central value fit has a χ^2 of 36 with 33 degrees of freedom, giving a confidence level CL=0.33. In Fig. 5.2, we show the fit results for f_π and $m_\pi^2/(m_x + m_y)$ as functions of the sum of the quark masses $(m_x + m_y)$. The red solid curves show the complete results through NNLO for full QCD in the continuum, where we have set taste splitting and taste-violating parameters to zero, extrapolated physical parameters as $a \to 0$ linearly in $\alpha_s a^2$, and set valence quark masses and light sea quark

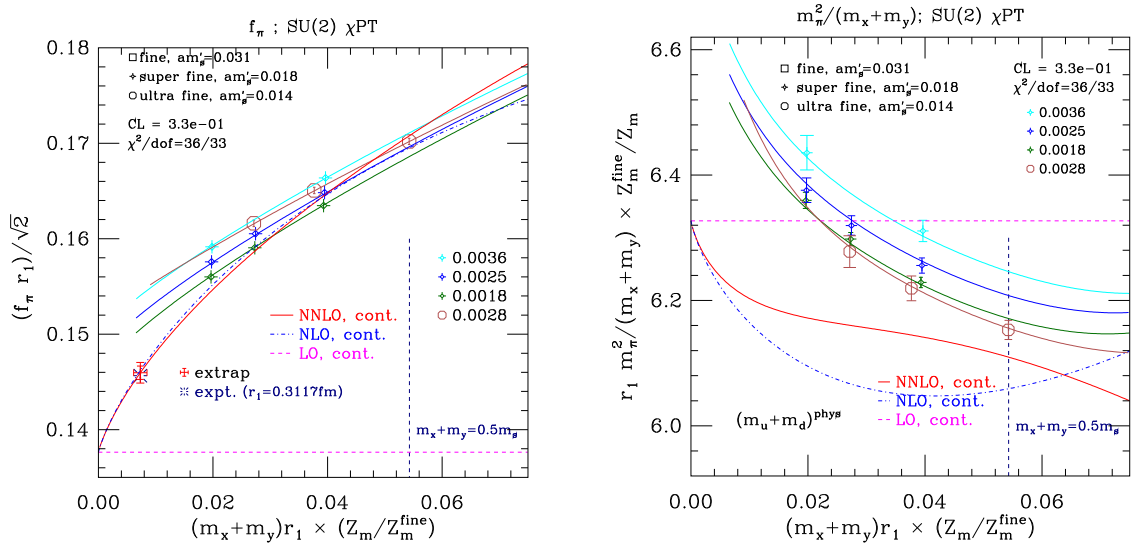

(a) (b)

Figure 5.2: SU(2) chiral fits to f_π(left) and $m_\pi^2/(m_x + m_y)$(right). Only points with the valence quark masses equal ($m_x = m_y$) are shown on the plots

masses equal. Continuum results through NLO and at tree level are shown by blue dotted and magenta dashed curves, respectively. It can be seen that the convergence of SU(2) χPT is much better for the decay constant than for the mass. Nevertheless, the chiral corrections in both cases appear to be under control.

At the last step, we find the physical values of the average u, d quark mass $\hat{m}$ by requiring that the π has its physical mass, and then find the decay constant corresponding to this point in Fig. 5.2 (left). With the scale parameter $r_1 = 0.3117(6)\left(^{+12}_{-31}\right)$ fm determined from NNLO SU(3) χPT f_π analysis, we obtain the result for f_π:

$$f_\pi = 130.7 \pm 1.0\left(^{+1.4}_{-0.4}\right)\ \text{MeV} \tag{5.28}$$

where the first error is statistical and the second is systematic. This agrees with the SU(3) analysis, which is tuned to reproduce the PDG 2008 value, $f_\pi = 130.4 \pm 0.2\,\text{MeV}$ [58]. We have also tried the fits with $r_1^{phys} = 0.3135$fm and 0.3080fm and

include them in estimating systematic errors.

5.6.2 Quark masses and condensates

In this study, calculations are done in partially-quenched rSχPT. To obtain the "full QCD" results, one first sets the valence quarks masses equal to the sea quark masses, *i.e.*, $m_x = m_y = m_l$ for a pion, or $m_x = m_l, m_y = m_s$ for a kaon. This can be done for each ensemble with different choices of m_l and m_s. The pion and kaon masses still do not take their physical values at this step. One can reach the physical point by tuning the bare quark masses am_l and am_s to give pion and kaon their physical QCD masses in the isospin limit, $m_{\hat{\pi}}$ and $m_{\hat{K}}$ [1]

$$m^2_{\hat{\pi}} \equiv m^2_{\pi^0}, \tag{5.29}$$

$$m^2_{\hat{K}} \equiv \frac{1}{2}(m^2_{K^0} + m^2_{K^+} - (1+\Delta_E)(m^2_{\pi^+} - m^2_{\pi^0})), \tag{5.30}$$

where $\Delta_E \approx 1$ is the violation parameter of Dashen's theorem.

The renormalized quark masses depend on the regularization scheme we are using. Usually, the quark masses in the $\overline{\text{MS}}$ scheme are quoted for continuum QCD at energy scale Λ. For lattice calculations, one uses the scheme with regularization point $1/a$, and the renormalized quark masses at this point takes different values from those in the $\overline{\text{MS}}$ scheme. One can relate these two renormalized quark masses and obtain the $\overline{\text{MS}}$ quark masses from bare quark masses on the lattice

$$m^{\overline{\text{MS}}}(\Lambda) = Z_m(a\Lambda)\frac{(am)_0}{au_{0P}}, \tag{5.31}$$

where Z_m is the renormalization factor and u_{0P} is the tadpole improvement factor,

which appears here because the MILC improved staggered action defines the lattice quark mass in an unconventional manner [1].

The renormalization factor Z_m can be calculated perturbatively [65]. In our analysis, we use two loop perturbative results [66] to obtain physical light and strange quark masses in the $\overline{\rm MS}$ scheme at 2GeV.

The quark condensates in the chiral limit are related to LO LECs by $\langle \bar{u}u \rangle = -f^2\mu/2$.

5.6.3 Summary of results

In summary, we obtain the following results from SU(2) chiral analysis:

$$\begin{aligned} f_2 &= 123.3 \pm 0.9 \pm 1.4\,\text{MeV} & B_2 &= 2.87(3)(5)(14)\,\text{MeV} \\ \bar{l}_3 &= 2.5 \pm 0.6\,\left(^{+1.0}_{-0.1}\right) & \bar{l}_4 &= 3.9(2)(2) \\ \hat{m} &= 3.23(3)(7)(16)\,\text{MeV} & \langle \bar{u}u \rangle_2 &= -[280(2)\,\left(^{+3}_{-8}\right)\,(4)\,\text{MeV}]^3 \end{aligned} \tag{5.32}$$

where the quark masses and chiral condensate are evaluated in the $\overline{\rm MS}$ scheme at 2 GeV. We use the two-loop renormalization factor in the conversion [66]. Errors from perturbative calculations are listed as the third error in these quantities. All the quantities agree with results from SU(3) SχPT fits [2] within errors.

5.7 Discussion and Outlook

We have performed NNLO SU(2) chiral fits to recent asqtad data in the light pseudoscalar sector. Results for SU(2) LECs, the pion decay constant, and the chiral

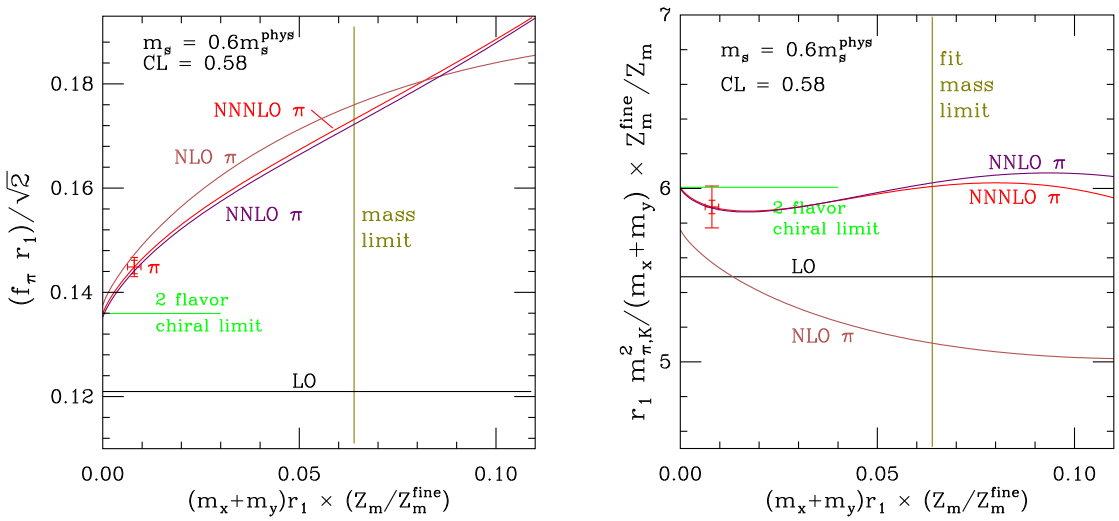

(a) (b)

Figure 5.3: Test of convergence of SU(3) χPT fits in the continuum, with the strange quark mass fixed at $0.6m_s^{phys}$. Plots are from Ref. [2].

condensate in the two-flavor chiral limit are in good agreement with those obtained from NNLO SU(3) fits (supplemented by higher-order analytic terms for quantities involving strange valence quarks)[2]. For comparison, the plots from SU(3) chiral analysis are shown in figure (5.3).

By comparing figure (5.2) with figure (5.3), it can be seen that SU(2) χPT within its applicable region converges much faster than SU(3) χPT. For the point 0.05 on the x-axis in Fig. 5.2, the ratio of the NNLO correction to the result through NLO is 0.3% for f_π and 2.6% for $m_\pi/(m_x + m_y)$. In contrast, the corresponding numbers in the SU(3) fits are 2.9% and 15.6% respectively, although the large correction in the mass case is partly the result of an anomalously small NLO term. Note that the SU(3) plots use a non-physical strange quark mass, $m_s = 0.6m_s^{phys}$, while for the SU(2) plots, the strange quark mass is near the physical value, $m_s \approx m_s^{phys}$. This

explains why the two-flavor chiral limits on the SU(3) and SU(2) plots are not the same.

Since the simulated strange quark masses vary slightly between different ensembles, the parameters in SU(2) SχPT should also change with ensemble [67]. We plan to incorporate this effect in our fit to see if we can improve the confidence levels. Another step would be to include the kaon as a heavy particle in SU(2) SχPT [53] in order to study the physics involving the strange quark, *e.g.*, the kaon mass and decay constant. This approach has recently been used in Refs. [52, 59].

Appendix I γ Matrices and Euclidean Field Theory

γ matrices

The γ matrices are hermitian and satisfy anti-commutation relation $\{\gamma_\mu, \gamma_\nu\} = 2\delta_{\mu\nu}$. In Euclidean space, they take the form

$$\gamma = \begin{pmatrix} 0 & i\sigma \\ -i\sigma & 0 \end{pmatrix}, \quad \gamma_4 = \begin{pmatrix} I & 0 \\ 0 & -I \end{pmatrix}, \quad \gamma_5 = \begin{pmatrix} 0 & I \\ I & 0 \end{pmatrix}, \tag{5.33}$$

where σ is the Pauli matrices and I is the 2×2 unit matrix. In this representaion, γ_1 and γ_3 are pure imaginary, while γ_2, γ_4 and γ_5 are real. (Gupta P32)

The left and right handed fermion fields $q^{R,L}$ are defined by:

$$q^R = \frac{1+\gamma_5}{2}q, \qquad q^L = \frac{1-\gamma_5}{2}q, \tag{5.34}$$

$$\bar{q}^R = \bar{q}\frac{1-\gamma_5}{2}, \qquad \bar{q}^L = \bar{q}\frac{1+\gamma_5}{2}. \tag{5.35}$$

Minkowski and Euclidean field theory

A d-dimensional field theory in Minkowski spacetime can be related to a d-dimensional Euclidean field theory through analytical continuation. Under Wick rotation

$$x_0 \equiv t \rightarrow -i\tau \equiv -ix_4, \tag{5.36}$$

$$p_0 \equiv E \rightarrow ip_4, \tag{5.37}$$

we have

$$x_E^2 = -x_M^2, \tag{5.38}$$

$$p_E^2 = -p_M^2, \tag{5.39}$$

$$S_M = iS_E, \tag{5.40}$$

$$\mathcal{L}_M = -\mathcal{L}_E, \tag{5.41}$$

where $\mathcal{L}_E$ is defined to be $-\mathcal{L}_M(t \rightarrow -i\tau)$. In Minkowski space, an operator in Heisenberg picture, $A(t)$, is related to the operator in Schrodinger picture through ($\hbar = 1$)

$$A(t) = e^{iHt} A e^{-iHt}. \tag{5.42}$$

In Euclidean space, the same equation becomes

$$A_E(t) = e^{H\tau} A_E e^{-H\tau}. \tag{5.43}$$

Appendix II Detailed Descriptions of Computer Codes

INTRODUCTION TO THE FITTING CODE

The whole set of fitting codes is divided to four parts located in the following directories:

DAT data files and scripts to thin out data

Function: Make suitable data file for SU(2) analysis from the raw data file

MESCHACH *.h head files for matrix operations

EXEC executable files, input and output files

*.c C code, *.for Fortran code (from Bijnens) and makefile

Function: Make sunsettable

Make output file by fitting to the data using input file.

Sample input file: *in_r103133* input file with r1=0.3133fm, for NNLO fit

in_r103133_NNNLO input file with r1=0.3133fm, for NNLO fit with NNNLO analytic terms.

Sample data file: *PQ_meson.0124.0072.0056.dat*

Sample output file: *o_fsu_massind_allton_0124_0072_0056_r103133*

fsu : fit to fine, superfine and ultrafine lattices

massind_allton: mass-independent scheme, allton-style r1 fitting

r103133: use r1=0.3133fm

PLOT scripts to analyze data and make plots

Function: From the output file, make the sbq file, which gives physical quark masses, extrapolates parameters to the continuum and infinite volume cases, and calculates central values and errors of parameters.

For example, if the output file is *o_fsu_massind_allton_0124_0072_0056_r103133*, the sbq file is *FIT_o_fsu_massind_allton_0124_0072_0056_r103133_YES*

SUMMARY scripts to make summary tables.

From the output file and sbq file, extract final results and put them in table files in .tex format.

For ChPT LECs, calculate the scale independent parameters $\bar{l_i}$ and put them in table files.

STEPS TO PERFORM A COMPLETE SU(2) CHIRAL ANALYSIS FROM A CERTAIN DATA FILE

(Note: In the following, I always assume that r1phys equals 0.3133fm and the massind_allton option (mass independent scheme and allton-style fitting function) is used.)

STEP 1:

Put data files and the covariance matrix file under the directory /DAT.

Data files: *f*031 (fine lattice ms*r1 = 0.031)

sf018 (superfine lattice ms*r1 = 0.018)

uf014 (ultrafine lattice ms*r1 = 0.014)

Covariance matrix file: *cov_r1*

Use the script file *dat_files_thin_F0310124_SF0072_UF0056.csh* to make the PQ data file and pts files (used to make plots).

Here, the cutoff on (mx + my)*r1 is 0.0124 for fine lattice, 0.0072 for superfine lattice and 0.0056 for ultrafine lattice.

The PQ data file generated is named *PQ_meson.0124.0072.0056.dat*. It contains the data points from these three lattices and the corresponding covariance matrix.

The script also produces pts files which contain only the so-called "pion" points (mx = my). These pts files are used by the plot scripts in Step 3:

fine_.031.pts

super_fine_.018.pts

ultra_fine_.014.pts

STEP 2:

Files needed in this step:

Executable files:

schpt2_makesunsettable

schpt2_massind_allton

Input file:

in_r103133

Data file:

PQ_meson.124.0072.0056.dat

Copy the PQ data file *PQ_meson.0124.0072.0056.dat* to directory /EXEC, make sure the executable files and input files are ready under /EXEC. Here we use sample input file *in_r103133*, where the r1phys is set to be 0.3133fm.

(1) Make sunset table for the PQ data file

./schpt2_makesunsettable PQ_meson.0124.0072.0056.dat in_r103133

Enter mu_min, mu_max, mu_step under the prompt. Typical values are "1.0 10.0 0.1", which means that the parameter mu ranges from 1.0 to 10.0 with the step 0.1. For each data set in the PQ data file, the contributions from 2-loop sunset diagrams are calculated and stored in the output sunset table file *PQ_meson.0124.0072.0056.dat_sunsettabl*

(2) Fit to pion mass and decay constant simultaneously.

./schpt2_massind_allton PQ_meson.0124.0072.0056.dat in_r103133 ¿ o_su_massind_allton_r103

The output file is *o_su_massind_allton_r103133*. Here 'su' means 'superfine' and 'ultrafine'. This file gives the correlation matrix, its eigenvalues, covariance matrix, information for each iteration and final fit results.

STEP 3:

Files needed in this step:

Executable files:

schpt2_massind_allton_plot

schpt2_massind_allton_nofinitev_plot

schpt2_massind-allton_extrap

schpt2_massind_allton_extrap_TRIVIAL

schpt2_massind_allton_extrap_NLO

schpt2_massind_allton_nofinitev_extrap

schpt2_massind_allton_nofinitev_extrap_TRIVIAL

schpt2_massind_allton_nofinitev_extrap_NLO

schpt2_massind_allton_nofinitev_extraperr

r1_allton-extrap_massind

Fit file:

o_su_massind_allton_r103133

pts files:

fine_.031.pts

super_fine_.018.pts

ultra_fine_.014.pts

Copy the fit file *o_su_massind_allton_r103133* to /PLOT. Copy the pts files, e.g. *fine_.031.pts*, from /DAT to /PLOT. Use the script *makeplot_2loop.csh* to generate plot files. Make sure the template plot files *fpi_template_massind.ax*

and mpisq-over-m_template_massind.ax

are present under /PLOT.

For example, here is the command used to generate plot files for fit file *o_su_massind_allton_r10*

./makeplot_2loop.csh o_su_massind_allton_r103133 esfuf YES

The omit option "esfuf" means that only superfine and ultrafine points are used

in the plots. Yes means that the taste-violating terms are set to zero.

The output files are sbq file *FIT_o_su_massind_allton_r103133*, and plot files *fpi_o_su_massind_* and *mpisq-over-m_o_su_massind_allton_r103133.ax*. One can use axis to show the plots:

axis < fpi_o_su_massind_allton_r103133.ax |plot -T X

axis < mpisq-over-m_o_su_massind_allton_r103133.ax |plot -T X

One can also use axis to export the plots to .eps files:

axis < fpi_o_su_massind_allton_r103133.ax |plot -T PS ¿ fpi.eps

axis < mpisq-over-m_o_su_massind_allton_r103133.ax |plot -T PS ¿ mpisq-over-m.eps

STEP 4:

Copy the fit file *o_su_massind_allton_r103133* and the sbq file *FIT_o_su_massind_allton_r103133* to /SUMMARY. Use the script files under /SUMMARY to generate files which list the final results in tables. Each script file generates a table for one parameter. These scripts do not take any parameters. They will look for all the output files with filename o_* and corresponding sbq files FIT_o_*, then extract the values of certain parameter, sort them and make a table file in .tex format.

For a list of the script files and their functions, see the /SUMMARY section below.

Here is one example:

./dof.csh

This script will generate a table file ftable_sorted.tex containing the values of fpi in the two-flavor chiral limit extracted from all sbq files under /SUMMARY.

DETAILED DESCRIPTIONS OF ALL FILES

/DAT

Dat files: *f031 sf018 uf014* for fine, superfine, ultrafine respectively

Covariance matrix: *cov_r1*

dat_files_thin_F031009_SF0072_UF0056_ml0101502ms.csh

Script to thin out data. Here 009, 0072 and 0056 are cutoff values of am_x + am_y for fine (ams = 0.031), superfine, ultrafine lattices respectively. "ml0101502ms" means that we only use the data with light sea quark masses ml equal to 0.1, 0.15 and 0.2ms.

Output of the script is the data file *PQ_meson.009.0072.0056.dat*. It includes the data and covariance matrix.

The script also generates points files used for plots:

fine_.031.pts

super_fine_.018.pts

ultra_fine_.014.pts

If the name of data file is *PQ_meson.009.0075.dat*

, it means that the file contains superfine and ultrafine data only with cutoffs 009 and 0075.

# of blocks for each lattice

set xc0492_082 = 400

set xc0328_082 = 500

set xc0164_082 = 646

set xc0082_082 = 600

set mc484_0484 = 598

set mc29_0484 = 600

set mc194_0484 = 621

set mc097_0484 = 621

set mc0484_0484 = 600

set c03_05 = 362

set c02_05 = 485

set c01_05 = 894

set c007_05 = 836

set c005_05 = 527

set c03_03 = 360

set c01_03 = 349

set c005_005 = 701

set f0124_031 = 531

set f0093_031 = 1124

set f0062_031 = 591

set f00465_031 = 480

set f0031_031 = 945

set f00155_031 = 491

set f0062_0186 = 985

set f0031_0186 = 580

set f0031_0031 = 380

set sf0072_018 = 625

set sf0054_018 = 465

set sf0036_018 = 751

set sf0025_018 = 768

set sf0018_018 = 826

set sf0036_0108 = 601

set uf0028_014 = 801

One sum up the number of blocks for lattices used in the fit, and then write this number in front of the covariance matrix.

For example, for fits using sf0018_018, sf0025_018, sf0036_018 and uf0028_014, the total number of blocks is

826 + 768 + 751 + 801 = 3146

/EXEC

Since the ALLTON style fitting function to r1 and mass-independent scheme are always used in our chiral fits, I will only show options with "allton" and "massind" defined in the following introductions to the code.

linalg.c

Some routines to solve linear equations

matinv() inverse (dim) x (dim) matrix x, put result in y

lineq() solve mat*ans = vec

factor() Gaussian elimination

subst()

whichspacing.c

Translate between different naming conventions of lattice spacings.

schpt2.c

Main function to calculate the pion mass and decay constant

STANDALONE MODE:

1. read in r1/a, par[], flag, mA, mB, mL, mS (in units of a)

2. set mA, mB, mL, mS to be r1*mA, r1*mB, r1*mL, r1*mS, set mAlat and mBlat to be a*mA

and a*mB

3. set b[0]–b[90] to be par[0]–par[90]

c[0] = flag, c[1]–c[4] = mA, mB, mL, mS

4. IN PLOT MODE

if flag=0

mpisqo2mq = f(dindex, c, b) where dindex is the index o f the point in the array of 2-loop sunset graph values stored in the table. If dindex is -1, the sunset table is NOT used.

if MASSIND and EXTRAP

adjust = 1/rntoutput

else adjust = 1.0

look for sunset table

print mA+mB, mpisqo2mp*adjust,

adjust*sqrt((mA+mB)*mpisqo2mq)*hc/r1phys (pion mass in MeV), mAlat, mBlat

if flag=1

fpi = f(dindex, c, b)

print mA+mB, fpi*adjust, adjust*fpi*sqrt(2)*hc/r1phys (fpi131 in

MeV), mAlat, mBlat

if flag=2

print l21p3

if flag=3

print l4

if flag=4

print lp

if flag=5

print l3

IN EXTRAPERR MODE, get derivative w.r.t. parameters

if flag=0 print df(dindex, c, b, i) *(mA + mB) // get

derivative of mass 2

if flag=1 print df(dindex, c, b, i) //df/db[i]

if flag=2,3,4,5 print df(dindex, c, b, i)

5. IF NOT IN PLOT MODE

if flag=0

print ”mV, 2mS, M 2/(mq1+mq2)”, mA+mB, 2*mS, f(dindex, c, b)

if flag=1

print ”mV,2mS, fpi”, mA+mB, 2*mS, f(dindex, c, b)

STANDALONE MODE ENDS

Functions:

f_init(FILE *filep)

IF NOT IN PLOT MODE, PRINT OUT PROMPT MESSAGES

fscanf num_spacing, input_spacing, splittings, slope, a2rat, Zm,

\etc.

fscanf r1phys

set Lamsq = (meta*r1phys/hc) 2 = fpichinf2_.xmu2 (used in

Bijnens’ code)

set li and kki to be 0 in Bijnens’ code

IN EXTRAP MODE

read input_spacing to be extrapolated to

read in finite volume corrections from table

initial set up for Bijnens’ code

IF NOT MAKESUNSETTABLE and NOT STANDALONE

read in sunset table

f(dindex, c, b)

set flag, mA, mB, mL, mS to be c[0]–c[4]

set parameters to be b[0]–b[90]

for ALLTON, set A00d – B20d

call r1_variation() to get spacing, beta, latL, r1/a, \etc.

(Here we are using the actual data, and the REALDATA part in r1_variation() is executed)

get L/r1 = Lor1 = latL/r1av

get int_5, ... slope, a2rat, Zmrat for this lattice spacing

get gen_ratio according to whether FINE_PRIMARY is defined or

not. gen_ratio is used to calculate generic a 2 variations.

if NOT MAKESUNSETTABLE and NOT TESTSUNSETTABLE, adjust the parameter mu

mu = mu*Zmrat*(1 + mud*gen_ratio)

adjust all the parameters with variations and gen_ratio

If we let the fit parameters C00, C01u, C01s, C02, C20, C21, C40, D20 in r1 formula to change, r1true will be different from r1nom, and we need to do some additional adjustments to the parameters resulted from the different r1 being used.

rnt = r1nom/r1true

rat2 = (r1av/r1true) 2

rt2an = r1true 2/r1nom/r1av

rntoutput = rnt

if NOT MAKESUNSETTABLE and NOT TESTSUNSETTABLE

mu = mu*rnt

fp93 = fp93*rnt

fp131 = fp131*rnt

slope = slope/rnt

deltap_mu5 *= rat2 ;

deltap_mu *= rat2 ;

Ln *= rat2 ;

Lnp *= rat2 ;

int_5 *= rat2 ;

int_mu5 *= rat2 ;

int_munu *= rat2 ;

int_mu *= rat2 ;

int_I *= rat2 ;

fpichinf2_.fpi0 = fp93/sqrt(logcoeff)

(use fp93/logcoeff for 2-loops)

convert my NLO LECs to Bijnens' set

if STANDALONE

if NOT PLOT

print r1*mA, r1*mB, r1*mL r1*mS choice

Denom = 16 pi 2/fp131 2

AnalyticDenom = fp93 2

use mu everywhere in the fit!

slopep=mu

calculate pion masses with various taste and flavor structure,

mu is used instead of slope

initiate masses used in Bijnens' NNLO logs

m11 = av_split + mu*2mA

m22 = av_split + mu*2mB

m44 = av_split + mu*2mL

if flag=0 return eval_mpisq()

if flag=1 return eval_fpi()

if flag¿1 return eval_li()

df(dindex, c, b, i)

calculate the derivative w.r.t. parameter par[i]

ddf(dindex, c, b, i)

calculate the second derivative w.r.t. par[i]

whichcase()

decide if masses are degenerate, and if so, use the corresponding degenerate formulas

for pion mass or pion decay constant.

for SU(2) PQChPT, only four possibilities: ABL, ABNL, ALNB NNN

ABL: m_x = m_y = m_l

ABNL: m_x = m_y != m_l

ALNB: m_x = m_l != m_y or (m_y = m_l != m_x)

NNN: m_x != m_y != m_l

eval_mpisq()

Function to evaluate m_pi 2 for different degenerate cases

dm_tree is NLO analytic contribution

dm_loop_mu, dm_loop_mu5 dm_loop_i are one loop contributions

their calculations differ for different degenerate cases.

dm_sunset and dm_nosunset are NNLO chiral logs

if dindex ¿=0, obtain dm_sunset from sunsettable

dm_2loop = dm_nosunset + logcoeff*logcoeff*dm_sunset/fp93 4

dm_square is the mock NNLO chiral logs, obselete

dm_quad is quadratic, NNLO analytic terms

dm_cube is cubic, NNNLO analytic terms

eval_fpi()

Function to evaluate fpi, similar to eval_mpisq()

eval_li()

evaluate pp1, ell4, pp2, ell3 (Names of these LECs need to be changed)

chiral(mass2)

chiral log function mass2*log(mass2/Lamsq)/Denom

chiral_pole2(mass2)

chiral log function (-1-log(mass2/Lamsq))/Denom

msq_etap(m2, m2S, dp)

obtain the mass of \eta', used in SU(3) fit, obselete in SU(2) fit since the expression of msq_etap is an inline function now.

Residue functions R and D

R42()

R31()

...

D21()

...

Finite volume corrections using cubic interpolation

d1()

if m*L is within the range of finite volume table d1array, calculate FV correction by using cubic interpolation.

If not, use delta1() to calculate directly.

d3()

if m*L is within the range of finite volume table d1array, calculate FV correction by using cubic interpolation.

If not, use delta3() to calculate directly.

(obsoleted) Finite volume corrections using linear interpolation

d1lin()

d3lin()

Modified Bessel functions

K1() and I1()

K0() and I0()

mNNLO(Mass1, Mass2, Mass4, interp, epsinterp, epsbij)

return contributions from NNLO chiral logs to mpi 2/(mx+my)

convention: return mp6x21nf2_(&mass11,&mass22,&mass44) / ((mass11 + mass22)/2.0

fNNLO(Mass1, Mass2, Mass4, interp, epsinterp, epsbij)

return fp6x21nf2_(&mass11,&mass22,&mass44)

fNNLOsunset()

return the contributions from 2-loop sunset diagrams to fpi

mNNLOsunset()

return the contribtuions from 2-loop sunset diagrams to mpi 2/(mx+my)

fNNLOnosunset()

return the contributions from 2-loop non-sunset diagrams to fpi

mNNLOnosunset()

return the contributions from 2-loop non-sunset diagrams to mpi 2/(mx+my)

cofit_np.c

Main file to do correlated least square fit

fit data is stored in datum *data,

fit function is f() with first and second-derivative as df() and ddf().

#ifdef MAKESUNSETTABLE

make sunset table for data file with mu from mumin to mumax with certain stepsize

usually it is 1.0 to 10.0 with stepsize 0.1

main file to do the fitting

usage: schpt2_massind_allton datafile input_file ¿ output_file

Function:

main()

1. Data structure:

*par parameter array

*priorval prior central values

*priorerr prior errors

2. read in eps, max itermations, range of x to be fitted, \etc

3. read in parameters, priors, prior errors from input file

read in data from data file

4. IF MAKESUNSETTABLE

from mu_min to mu_max with step size mu_step,

print the value of sunset diagram with current mu to

sunset_file

ELSE

read in covariance from data file

make sure nblocks ¿ ndata

5. Get eigenvalues of the correlation matrix and print them out

If eigcut = 0, skip this part

else

if EIGAV

average small eigenvalues which are less than eigcut

else

ignore small eigenvalues which are less than eigcut and corresponding eigenvectors.

endif

Reconstruct covariance matrix using the eigenvectors and the averaged eigenvalues.

6. use matinv() to invert covariance matrix, and store it in covarinv

7. minimize chi_square and obtain values of parameters.

8. Error analysis:

second derivative of chi_square W.R.T. each parameter (Hessian

Matrix) is stored in wparmat1[][]. Inverse Hessian Matrix is stored in

delpar[][], its scaled version is stored in wparmat2[][]

wparmat1[][] = df/dpar * covarinv * df/par

wparmat2[][] = wparmat1 * delpar

wparmat1[][] = 4 * delpar * wparmat2

= 4 * delpar * wparmat1 * delpar

wparmat1 is the final parameter variance matrix

final error for parameter i par[i] is

sqrt(nblocks/(nblocks-ndata)) * 2 * delpar[i][i] *

sqrt(nblocks/(nblocks-ndata)) * wparmat1[i][i]

dumpmat()

function to print out a matrix

phi()

function to obtain phi = sum_i (f(b)_i - data_i) * covarinv[i][j] * (f(b)_j - data_j)

+ sum_j (b_j - prior_j)*(b_j - prior_j)/priorerr[j] 2

where b_j is the parameters in fitting function f()

dphi()

function to calculate dphi/d par[i]

ddphi()

function to calculate d 2 phi / d 2 par[i]

Functions to calculate CL

gammaq(0.5*dof, 0.5*chisq) get pre-adjusted confidence level

conf_int(chisq, nblocks, ndof) get confidence level

minp.c

Function to minimize a given function phi(x) using Newtons or gradient descent methods.

Results are put in vector x[].

r1_ALLTON-variation.c

r1nom: nominal values of r1/a

r1av: typical r1/a for this lattice spacing. assume this is what goes into the splittings and slope determination.

r1true: r1/a changed from nominal values by shifts in smoothed-r1 fit parameters. it is set to be r1nom in actual fits.

physical quark masses in units of a

amudphys[EXTRA_COARSE] = 0.00192137 ;

amudphys[MEDIUM_COARSE] = 0.00158039 ;

amudphys[COARSE] = 0.00126372 ;

amudphys[FINE] = 0.000953432 ;

amudphys[SUPER_FINE] = 0.000688411 ;

amudphys[ULTRA_FINE] = 0.000497461 ; /* GUESS!!!!!! */

amudphys[CONTINUUM] = 0.00102384 ;

amsphys[EXTRA_COARSE] = 0.0535114 ;

amsphys[MEDIUM_COARSE] = 0.0438377 ;

amsphys[COARSE] = 0.0349209 ;

amsphys[FINE] = 0.0260627 ;

amsphys[SUPER_FINE] = 0.018747 ;

amsphys[ULTRA_FINE] = 0.013547 ; /* GUESS!!!!!! */

amsphys[CONTINUUM] = 0.0277394 ;

if EXTRAP: given lattice spacing, find the lowest mass am_l, am_s

calculate r1nom by using the smoothed formulas

if REALDATA: given r*m_l, r*_m_s, figure out am_l, am_s and r1/a

calculate r1nom by using r1*m_s/(a * m_s)

find beta, latL, r1av, etc

if FINDSCALE: given am_l, am_s, figure out beta, lattice spacing, latL, r1av, r1nom

= r1*m_s / am_s, etc.

calculate r1nom by using the smoothed formulas

Functions:

r1_variation()

find sea quark masses am_l and beta, r1/a

set amudphys_c, amudphys_f, amsphys_c, amsphys_f

if ALLTON

set A00n – B20n

if MASSIND

set amudphys[lattice spacing] and amsphys[lattice

spacing]

if ALLTON

set nf=3, b0, b1

if MASSIND

set r1avs[lattice spacing]. //r1avs[CONTINUUM]

= r1avs[FINE]

if EXTRAP

set mLa mSa to be lightest mass sets for input_spacing

if REALDATA

find mLa mSa r1/a from r1*mS r1*mL

From mLa, mSa, get beta, latL, spacing, g2, r1av=r1avs[spacing]

if spacing==CONTINUUM

r1nom = r1av

mSa = mSap

mLa = mLap

else

r1nom = r1*mS/mSa

if MASSIND (use physical quark masses)

set amtot and m_ud m_s by using amudphys[spacing] and amsphys[spacing]

if EXTRAP

calculate r1nom in mass independent scheme

else (NOT MASSIND, use actual quark masses)

amtot = 2mLa + mSa

m_ud = mLa

m_s = mSa

if FINDSCALE

calculate r1nom

calculate r1true by using the smoothing function

if EXTRAP

if NOT MASSIND

r1nom = r1av

r1true = r1av

r1_ALLTON_main.c

Main routine to generate r1 executable files

Usage:

EXTRAP: r1_extrap C00d C10d C01d C20d spacing

FINDSCALE: r1_findscale C00d C10d C01d C20d am_l am_s

REALDATA: r1_realdata C00d C10d C01d C20d r1*m_l r1*m_s

OUTPUT:

printf("mLa= %e\tmSa= %e\tbeta= %e\nr1av= %e\tr1nom= %e\tr1true= %e\n",

mLa,mSa,beta,r1av,r1nom,r1true);

namespacing(spacing);

Lor1 = latL/r1true ;

printf("L= %d\tL/r1true= %e\t spacing= %d\tspacing_name = %s\n",latL,Lor1,spacing,outpu

makefile

schpt2_massind_allton

Main executable file to do fitting

schpt2_massind_allton.o: ${SOURCE} ${EXTRA_HEADERS}

cc -c -o $@ -O3 ${SOURCE} \

-DMASSIND -DALLTON -DEPS=1.0e-9 -DTABLE \

-DTABLENAME=\"/usr/local/share/public/finite_vol_table_0.00001.txt\"

schpt2_massind_allton: schpt2_massind_allton.o \

r1_massind.o whichspacing.o ${FORTRANBINS} ${LIBRARY} ${EXTRA_BINS}

gfortran -o $@ ${EXTRA_BINS} schpt2_massind_allton.o r1_massind.o whichspacing.o ${FORTRANBINS} ${LIBRARY} -lm

Other versions:

schpt2_massind_allton_ms (strange quark mass effects included)

schpt2_massind_allton_goldstone (use the goldstone pion masses in NNLO calculations)

schpt2_massind_allton_plot

Executable file in standalone mode . Output is given for the purpose of plotting

schpt2_massind_allton_plot.o: ${SOURCE} ${EXTRA_HEADERS}

cc -c -o $@ -O3 ${SOURCE} \

-DMASSIND -DALLTON -DSTANDALONE -DPLOT -DEPS=1.0e-9

schpt2_massind_allton_plot: schpt2_massind_allton_plot.o \

r1_massind.o whichspacing.o ${FORTRANBINS} ${LIBRARY}

gfortran -o $@ schpt2_massind_allton_plot.o r1_massind.o whichspacing.o ${FORTRANBINS} ${LIBRARY} -lm

Other versions:

schpt2_massind_allton_plot_ms

schpt2_massind_allton_nofinitev_plot (print the results of fpi and mpisq in the infinite volume case)

schpt2_massind_allton_nofinitev_plot_ms

schpt2_massind_allton_extrap

Executable file in standalone mode. Output is

schpt2_massind_allton_extrap.o: ${SOURCE} ${EXTRA_HEADERS}

cc -c -o $@ -O3 ${SOURCE} \

-DMASSIND -DALLTON -DSTANDALONE -DPLOT -DEXTRAP -DEPS=1.0e-9 -DCAREFUL

schpt2_massind_allton_extrap: schpt2_massind_allton_extrap.o \

r1_massind_extrap.o whichspacing.o ${FORTRANBINS} ${LIBRARY}

gfortran -o $@ schpt2_massind_allton_extrap.o r1_massind_extrap.o whichspacing.o ${FORTRANBINS} ${LIBRARY} -lm

Other versions:

schpt2_massind_allton_extrap_TRIVIAL (print the contributions to fpi and mpisq at the lowest order)

schpt2_massind_allton_extrap_NLO (print the contributions to fpi and mpisq up to NLO)

schpt2_massind_allton_extrap_ms

schpt2_massind_allton_nofinitev_extrap

schpt2_massind_allton_nofinitev_extrap_TRIVIAL

schpt2_massind_allton_nofinitev_extrap_NLO

schpt2_massind_allton_nofinitev_extrap_ms

schpt2_massind_allton_nofinitev_extraperr

Executable file to extrapolate the errors

schpt2_massind_allton_nofinitev_extraperr.o: ${SOURCE} ${EXTRA_HEADERS}

cc -c -o $@ -O3 ${SOURCE} \

-DMASSIND -DALLTON -DSTANDALONE -DPLOT -DNOFINITEV -DEXTRAP

-DEXTRAPERR -DCAREFUL

schpt2_massind_allton_nofinitev_extraperr: schpt2_massind_allton_nofinitev_extraperr.o

\

r1_massind_extrap.o whichspacing.o ${FORTRANBINS} ${LIBRARY}

gfortran -o $@ schpt2_massind_allton_nofinitev_extraperr.o r1_massind_extrap.o whichspac-

ing.o ${FORTRANBINS} ${LIBRARY} -lm

Other verions:

schpt2_massind_allton_nofinitev_extraperr_ms

schpt2_massind_allton_standalone

Executable file in standalone mode

schpt2_massind_allton_standalone.o: ${SOURCE} ${EXTRA_HEADERS}

cc -c -o $@ -O3 ${SOURCE} \

-DMASSIND -DALLTON -DSTANDALONE -DEPS=1.0e-9

schpt2_massind_allton_standalone: schpt2_massind_allton_standalone.o \

r1_massind.o whichspacing.o ${FORTRANBINS} ${LIBRARY}

gfortran -o $@ schpt2_massind_allton_standalone.o r1_massind.o whichspacing.o ${FORTRANBI

${LIBRARY} -lm

Other versions;

schpt2_massind_allton_standalone_ms

schpt2_makesunsettable

Executable file to make the 2-loop sunset table

Other versions:

schpt2_makesunsettable_goldstone

Helper functions to find smoothed r1/a

r1_allton-findscale_massind: ${R1_MAIN} ${R1_SOURCES} ${EXTRA_HEADER}

cc -o $@ -O3 ${R1_MAIN} ${R1_SOURCES} -DFINDSCALE -DALLTON -DMASSIND

-lm

r1_allton-extrap_massind: ${R1_MAIN} ${R1_SOURCES} ${EXTRA_HEADER}

cc -o $@ -O3 ${R1_MAIN} ${R1_SOURCES} -DEXTRAP -DALLTON -DMASSIND

-lm

r1_allton-realdata_massind: ${R1_MAIN} ${R1_SOURCES} ${EXTRA_HEADER}

cc -o $@ -O3 ${R1_MAIN} ${R1_SOURCES} -DALLTON -DMASSIND -lm

/PLOT

makeplot_2loop.csh

Main script to make plots

Usage: makeplot_2loop.csh fitfile omit YES/NO

Omit options: none keep all points

c omits all coarse, medium_coarse, extra_coarse

ef031sf omits all except f031, sf

esfuf omits all except sf, uf

YES/NO

YES: set taste-violating parameters to zero, likecontinuum

NO: keep taste-violating parameters.

1. set r1find = r1_allton_extrap_massind

2. Make sbqfile from the fitfile

$sbq_all_2loop.csh $fitfile YES/NO 1.2 $r1type ¿ $sbqfile

3. find quantities from sbqfile

amL

fpi, fpierr in physical units

(continuum) r1 , r1phys

fpi, fpierr in units of r1, r1*fpi, r1*fpierr

oldconfidence, oldchisq, olddof,

confidence, chisq, dof,

4. For each spacing except omitted ones, make points file $spacing_shiftZ_NOFV_$fitroots.pts

finite_vol_correct_all_pts_2loop.csh $spacing.pts $fitfile

Now all points are adjusted to infinite volume.

5. Extract points used in the plots.

extract_pts_all_2loop_mloverms0101502.csh $fitfile

6. Draw fit lines

make_fit_lines_some_2loop.csh $fitfile $omit YES/NO

7. Make .ax plot files

(1). make .ax plot file for fpi

pts file fpi_pion_points

lines file fpi_lines

plotfile fpi_$fitroot.ax

start from the template plot file

make substitutions for all quantities, fpi,

fpierr, oldconfidence, oldchisq, \etc.

add points file fpi_pion_points, and lines file

fpi_lines to the plotfile

finite_vol_correct_all_pts_2loop.csh

Make finite volume corrections to all points

Usage: finite_vol_correct_all_pts_2loop.csh $pointfile $fitfile

Output:

outfile = $ptsfile_NOFV_$fit.pts

NOT corrected for new smoothed r1

outfileZ = $ptsfile_shiftZ_NOFV_$fit.pts

r1(mx+my) and r1*msq/(mx+my) adjusted for Zm/Zm_fine

corrected for new smoothed r1

1. Get information for available lattice spacings from $fitfile and write to

tempconstants1

mass intercepts, slope, a2rat_taste, a2rat_generic, Z_m, \etc

2. Write $numspacings, tempconstants1, r1phys to temphead

3. RANGETYPE = “”

4. If allton and massind is in the name

r1name = _massind_allton

r1find = r1_allton-findscale_massind

5. If noal is in the name

noaltype = _noal

6. If fv is in the name, use LFACTOR execs. (obsoleted)

fvtype = _fv

lfactor = ...

7. Set two executable files

executable_FV = schpt2$fvtype$noaltype$r1name$rangetype_plot

executable_NOFV = schpt2$fvtype$noaltype$r1name$rangetype_nofinitev_plot

8. Get final fit parameters from fitfile, put in $parline

9. For each line in the ptsfile, read the information

r1pts, x, oldpt, err, type1, mA, mB, mL, mS, \etc.

get r1 and SPACING by using r1find = r1_allton-findscale_massind

r1find 0 0 0 0 $mL $mS ¿! tempr1 (mass is in units of r1)

find SPACING, Zr

10. For each line containg data, do the following

write temphead, r1pts, parline, mA, mB, mL, mS to tempinput

exec_FV < tempinput >! tempoutput1

exec_NOFV < tempinput >> tempoutput1

put good lines to tempoutput

grep '\!' tempoutput1 ¿! tempoutput

get afv from output of exec_FV (finite volume)

get anofv from output of exec_NOFV (infinite volume)

newpt = oldpt + anofv - afv

echo $x $newpt $err \etc. to $outfile

adjust by Zr

adjust by r1/r1pts

newpt = newpt/Zr, err = err/Zr, x = x*Zr

newpt = newpt* r1/r1pts, err = err*r1/r1pts, x =

x*r1/r1pts.

write x newpt err to $outfileZ

extract_pts_all_2loop_mloverms0101502.csh

Usage: extract_pts_all_2loop_mloverms0101502.csh $fitfile

Output: fpi_pion_points

msq_pion_points

extract data points for fpi or msq, do the following:

1. for fine031 sf uf lattices, do the following (use fine031 as example)

(1) pointsfile = fine_.031_shiftZ_NOFV_$fitfile.pts

(2) select the real pion points, i.e. points with mx=my=ml

(2) set ms, ml set, colors set, symbol for each lattice spacing

(3) find the pointsfile, then for each ml, write the color,

symbol, data in pointsfile corresponding to this (ms, ml) to $output

make_fit_lines_some_2loop_from0.csh

Function: make selected fit lines starting from the chiral limit (m_x + m_y = 0)

Usage: make_fit_lines_some_2loop_from0.csh $fitfile omit YES/NO

Output: fpi_lines

msq_lines

1. If allton is in the fitfile name

r1type = "ALLTON"

if massind is in the fitfile name

r1type = "massind"

2. FVflag = "NOFV"

rangeDflag = "rangeD"

sbqfile = FIT_$fitfile_YES(NO)

make sbqfile if it does not exist

mscont = continuum a*ms

3. Set ml according to the omit option,

For example, if omit = esfuf

masses = (0036 0025 0018 0028 fullphys fullphysTRIVIAL fullphysNLO)

fullphysTRIVIAL is the LO contribution,

fullphysNLO is the contributions up to NLO

fullphys is the full NNLO results

4. for each m in the set, do the following

set spacing, color, step, mB, mL = m, mS (all in lattice units)

fullphys: mB = mL mS = $mscont

fit_line_all_2loop.csh $fitfile $spacing $flag $step $mB $mL $mS

$FVflag $rangeDflag $r1type $continuumorder ¿! tempfitlinebig

5. write comment, color, output line in tempfitlinebig to $output

fit_line_all_2loop.csh

Function: generic script code to make fit line with various parameters.

Usage: fit_line_all_2loop.csh fitfile spacing flag mAmin mAmax step mB mL mS FVflag rangeDflag ALLr1/SOMEr1/massind continuumorder

Options: flag = 1 fpi

= 0 mpi 2/mq

mAmin mAmax step

the start point, end point and stepsize of the fit line.

mB mL mS

mB=mA pion

mB=mS kaon

mB=mL mA=mB=mL full pion

mL=mA

for full kaon, use mB=mS, mL=mA

FVflag

FV: finite volume

NOFV: infinite volume

rangeDflag

not used anymore. It is set to be “”.

1. if spacing information not included in fitfile, exit

flag =0: type = PQ_msq

=1: type = PQ_f

2. if ALLTON and massind

r1type = _massind_allton

r1extrap = r1_allton_extrap_massind

r1find = r1_allton_findscale_massind

3. if FV, exectable = schpt2_..._plot

if continuumorder = TRIVIAL exectable =

schpt2_...extrap_TRIVIAL

if continuumorder = NLO exectable = schpt2_...extrap_NLO

if continuumorder = full exectable = schpt2_...extrap

similary for NOFV, use the nofinitev_plot or nofinitev_extrap

4. Draw certain type of lines according to the value of mB.

if mB = mA

PQ pion

type = PQ_msq_pion, or PQ_f_pion

if mB = mS

if mL = mA

full kaon

type = full_msq_K, or full_f_K

else PQ K

type = PQ_msq_K, or PQ_f_K

if mB = mL

full pion

type = full_msq_pion, or full_f_pion

else NNN pion

5. for this lattice spacing, find Zr in fitfile

get nominal r1/a

if spacing = continuum

r1extrap 0 0 0 0 $spacing ¿! tempr1

else

r1find 0 0 0 0 mL mS

6. zx = zy = Zr, for fpi, zy =1

get r1phys from fitfile

output ${no}${rtype}_${type}_${spacing}_${mBtype}${mL}_${mS}

7. get npar, parline. To avoid csh errors, split parline to two parts

write numspacings, information (slope,a2rat_taste, Zm, \etc) of

lattice spacings, r1phys to tempplot

if spacing=continuum, write spacing to tempplot and use the extrap

code later

write parline flag mA mB mL mS to tempplot

here mA takes value from mAmin to mAmax with stepsize

8. executable < tempplot ¿! tempout1

write good lines to tempout

grep '\!' tempout1 ¿! tempout

9. for each line in tempout, adjust the points by

(mx+my)-¿ Zr*(mx+my) mpi 2/(mx+my)-¿mpi 2/(mx+my)*Zr fpi-¿fpi

sbq_all_2loop.csh

Function: From a fitfile, generate the corresponding sbq file containing information about physical quark masses, fit results for each lattice, etc.

Usage: sbq_all_2loop.csh fitfile YES/NO Delta_E ALLr1/SOMEr1/massind [fpifv fKfv mpifv mKfv]

Delta_E: parameterizes violations of Dashen's theorem

Delta_E=0 is Dashen's theorem, Delta_E=1.2 is typical expected value

[fpifv fKfv mpifv mKfv] are residual finite volume corrections

As of 7/10/07, they are [0.002797 0.00048303 .00065147 .000714505]

1. calculate pi0 = mpihat, mk = mKhat and mkp = mK+

2. for each spacing in the fitfile, do the following

solve_all_2loop.csh $fitfile $spacing .0013 .035 $pi0 $mk $mkp

YES/NO $range $r1type ¿! solvetemp

here, $range is set to be rangeD

get ainv from solvetemp

get a2rat from fitfile, a2rat_phys = a2rat_fine

write final solve information to output file

write the line containing m_u to tempit and output file (use

|tee)

write the line containing fpi131phys in solvetemp to output file

write the line containing ml= in solvetemp to output file

get ml ms mu md msoml from solvetemp

write fchiral3 fchiral2 fpi.fchiral2 B03 psi-bar psi \etc in

solvetemp to output file

write the line containing LEC in solvetemp to output file

if spacing != continuum

write a2rat ml*($2 in tempit) to tempml.dat

write a2rat mu*($2 in tempit) to tempmu.dat

write a2rat md*($2 in tempit) to tempmu.dat

write a2rat fpi131phys*(1+fpifv), $5 to tempfpi.dat

set noxc nomc nosf ainvc ainvf noc \etc by setting the value of

a2rat

3. make input files for stline fits

for various fits: tempin_xmcfs, tempin_cf tempin_fsu

4. extrapolate MSbar masses and ratios

fitstline tempml.dat tempin_fsu ¿! tempfit

print "extrapolated from fine superfine ultrafine, ml =

%f"

fitstline tempmu.dat tempin_fsu ¿! tempfit

print mu = %f

fitstline tempmd.dat tempin_fsu ¿! tempfit

print md = %f

fitstline tempfpi.dat tempin_fsu ¿! tempfit

print fpi = %f

5. set zmf = 1.39391

get parline from fitfile and store it in partemp

get Bc eBc, fc, efc, dB, edB, df, edf, \etc from partemp

edB = $2/(1-a2rat+d)

calculate f frac_ef B frac_eB cond fchiral3 \etc.

write the results to output file

solve_all_2loop.csh

Function: Solve physical light quark mass m_l, and obtain strange quark mass m_s by using the input from SU(3) chiral analysis.

Usage: solve_all_2loop.csh fitfile spacing mLstart mSstart mpihat mKhat mKplus YES/NO RANGE ALLr1/SOMEr1/massind

1. if allton and massind

r1type = _massind_allton

r1exec = r1_allton-extrap_massind

if rangeD

executable = schpt2_..._nofinitev_extrap

executable_err = schpt2_..._nofinitev_extraperr

2. zmf = 1.39391

zmc = 1.34394 (Why use zmc here???)

get Zr from fitfile (Zmrat)

zm = zmf * Zr

3. r1exec C00d C10d C01d C20d $spacing ¿! tempr1

get r1nom on fiducial lattice from tempr1

get r1phys from fitfile

get ainv on fiducial lattice from tempr1

4. echo parline = $parline

5. write numspacing, information about lattice spacing in fitfile,

r1phys, $spacing to temphead

6. set mSomL and muod for different lattice spacings and likecontinuum

= YES/NO

7. iterate to find mL which makes pion mass physical, using

extrapolate.awk

print final mL mS values (amL amS mSomL)

8. print physical quark masses hpqcd:hep-lat/0510053 , to tempoutput

mL*ainv*zm

mS*ainv*zm

mU*ainv*zm

md = mu/muod

9. find derivatives of mass and fpi with respect to mL

piL and fpiL

since we are not considering mS variances of LECs, mS is irrelevant

here, and f2S, B02S are not used in the two-flavor case.

10. calculate the errors of fpi131phys and light quark mass ml by doing the following:

get parameter variance matrix for msq and fpi, for pion and K

respectively (K is only relevant in SU(3) case).

dfpip[i], dfKp[i], dpi[i], dK[i]

delta[][] is the nfree*nfree dimensional variance matrix read from

fitfile

get the full derivative, dfpi[k] (k=1...nfree) only takes value for

free parameters.

dL[] = - dpi[i]/piL

dfpi[] = dfpip[i] + dL[]*fpiL (chain rule)

errfpi += dfpi[] * delta[][] * dfpi[]

errmL += dL[] * delta[][] * dL[]

errfpi = sqrt(errfpi) / (fpir1/physfpi)

mLerr = sqrt(errmL) / mL

print out fpi131phys, mLerr

11. calculate fchiral3, fchiral2, B03, B02 and their errors.

dL = -dpi[i] / piL

dfpi = dfpip[] + dL * fpiL

df3 = df3p[]

df2 = df2p + dS * f2S

dfpiof2[] = (f2r1*dfpi - fpir1*df2)/f2r1/f2r1

dfpiof3[] = (f3r1*dfpi - fpir1*df3)/f3r1/f3r1

dB03 = dB03p[]

dB02 = dB02p[] + dS*B02S

dB02oB03[] = (B03r1*dB02 - B02r1*dB03)/B03r1/B03r1

dC3 = f3r1* (2*B03r1*df4 + f3r1*dB03)

dC2 = f2r1* (2*B02r1*df2 + f2r1*dB02)

r1 = sqrt(2)*fpir1/physfpi

errf3 = df3 * delta[][] * df3

errf2 = df2 * delta[][] * df2

errfpiof2 = dfpiof2 * delta[][] * dfpiof2

.

.

.

errC2oC3 = dC2oC3[] * delta[][] * dC2oC3[]

errf3 = sqrt(errf3)/r1

.

.

.

errC2oC3 = sqrt(errC2oC3)

print out fchiral3, ... ¡psi-bar psi¿_2/¡psi-bar psi¿_3 and errors.

12. print LECs and errors

obtain dLip[] from temperr generated by using exec_err

dLi[] = dLip[]

errLi = dLi[] * delta[][] * dLi

print out LECs and errors

13. Hessian errors.

read inverse Hessian matrix from the fitfile

use inverse Hessian matrix to calculate errors of fpi131phys,

mL-frac-err, \etc.

/SUMMARY

Enumerate all the output files o_*** in current directory and find the corresponding sbq files FIT_***. Extract the results from these files, put them into table files in .tex format.

This directory contains the following script files. These scripts do not have arguments.

dof.csh

Output: *ftable_sorted.tex*

obtain fpi in the two-flavor chiral limit from sbq file, and put them in a table file ftable_sorted in plain text format, then use the maketable.csh to convert to a table file in .tex format.

dofphys.csh

Output: *fphystable_sorted.tex*

obtain the pion decay constant fpi131phys in physical units and make the table file.

doubaru.csh

Output: *ubarutable_sorted.tex*

obtain the chiral condensate \bar{u}u in the two-flavor chiral limit and make the table file.

dompi.csh

Output: *mpitable_sorted.tex*

obtain the B_0 in the two-flavor chiral limit and make the table file.

dol3.csh

Output: *l3table_sorted.tex*

obtain the values of LEC l_3 from sbq file, then convert to \bar{l_3} using the formula:

\bar{l_3} = -64*pi 2*l_3 - ln (mpiphys 2/mu 2)

where mpiphys is the physical pi + mass, set to be 0.139 GeV here, and mu is the regularization scale set to be m_\eta = 0.5473 GeV.

dol4.csh

Output: *l4table_sorted.tex*

obtain the values of LEC l_4 from sbq file, then convert to \bar{l_4} using the formula:

\bar{l_4} = 16*pi 2*l_4 - ln (mpiphys 2/mu 2)

where mpiphys is the physical pi + mass, set to be 0.139 GeV here. mu is the regularization scale set to be m_\eta = 0.5473 GeV.

Bibliography

[1] C. Aubin et al. Light pseudoscalar decay constants, quark masses, and low energy constants from three-flavor lattice QCD. *Phys. Rev.*, D70:114501, 2004.

[2] A. Bazavov et al. Results from the MILC collaboration's SU(3) chiral perturbation theory analysis. *PoS*, LAT2009:079, 2009.

[3] Kenneth G. Wilson. Confinement of quarks. *Phys. Rev. D*, 10(8):2445–2459, Oct 1974.

[4] Thomas DeGrand and Carleton Detar. *Lattice Methods for Quantum Chromodynamics*. World Scientific Publishing, Singapore, 2006.

[5] H. J. Rothe. *Lattice gauge theories: An Introduction*. World Scientific Publishing, Singapore, 2005.

[6] J. Smit. *Introduction to quantum fields on a lattice: A robust mate*. Cambridge University Press, Cambridge, 2002.

[7] Istvan Montvay and Gernot Münster. *Quantum Field on a Lattice*. Cambridge University Press, Cambridge, 1994.

[8] Rajan Gupta. Introduction to lattice QCD. 1997.

[9] K. G. Wilson. Quarks: From Paradox to Myth. *Subnucl. Ser.*, 13:13–32, 1977.

[10] John Kogut and Leonard Susskind. Hamiltonian formulation of wilson's lattice gauge theories. *Phys. Rev. D*, 11(2):395–408, Jan 1975.

[11] A. Duncan, R. Roskies, and H. Vaidya. Monte carlo study of long-range chiral structure in qcd. *Physics Letters B*, 114(6):439 – 444, 1982.

[12] A. Bazavov et al. to appear in Rev. Mod. Phys.

[13] H. Kluberg-Stern, A. Morel, O. Napoly, and B. Petersson. Flavours of lagrangian susskind fermions. *Nuclear Physics B*, 220(4):447 – 470, 1983.

[14] Maarten F. L. Golterman and Jan Smit. Self-energy and flavor interpretation of staggered fermions. *Nuclear Physics B*, 245:61 – 88, 1984.

[15] Claude Bernard, Maarten Golterman, and Yigal Shamir. Observations on staggered fermions at non-zero lattice spacing. *Phys. Rev.*, D73:114511, 2006.

[16] C. Bernard. Staggered chiral perturbation theory and the fourth-root trick. *Phys. Rev.*, D73:114503, 2006.

[17] Claude Bernard, Maarten Golterman, and Yigal Shamir. Effective field theories for rooted staggered fermions. *PoS*, LAT2007:263, 2007.

[18] Yigal Shamir. Locality of the fourth root of the staggered-fermion determinant: Renormalization-group approach. *Phys. Rev.*, D71:034509, 2005.

[19] Yigal Shamir. Renormalization-group analysis of the validity of staggered-fermion QCD with the fourth-root recipe. *Phys. Rev.*, D75:054503, 2007.

[20] G. Peter Lepage and Paul B. Mackenzie. On the viability of lattice perturbation theory. *Phys. Rev.*, D48:2250–2264, 1993.

[21] Kostas Orginos, Doug Toussaint, and R. L. Sugar. Variants of fattening and flavor symmetry restoration. *Phys. Rev.*, D60:054503, 1999.

[22] G. Peter Lepage. Flavor-symmetry restoration and Symanzik improvement for staggered quarks. *Phys. Rev.*, D59:074502, 1999.

[23] Satchidananda Naik. On-shell improved action for qcd with susskind fermions and the asymptotic freedom scale. *Nuclear Physics B*, 316(1):238 – 268, 1989.

[24] Stefan Scherer. Introduction to chiral perturbation theory. *Adv. Nucl. Phys.*, 27:277, 2003.

[25] Steven Weinberg. Phenomenological lagrangians. *Physica A: Statistical and Theoretical Physics*, 96(1-2):327 – 340, 1979.

[26] J.Gasser and H. Leutwyler. *Annals of Physics*, 158:142, 1984.

[27] J. Gasser and H. Leutwyler. Chiral perturbation theory: Expansions in the mass of the strange quark. *Nuclear Physics B*, 250(1-4):465 – 516, 1985.

[28] H. Leutwyler. On the foundations of chiral perturbation theory. *Ann. Phys.*, 235:165–203, 1994.

[29] Maarten Golterman. Applications of chiral perturbation theory to lattice QCD. 2009.

[30] Weonjong Lee and Stephen R. Sharpe. Partial flavor symmetry restoration for chiral staggered fermions. *Phys. Rev. D*, 60(11):114503, Nov 1999.

[31] C. Aubin and C. Bernard. Pion and Kaon masses in Staggered Chiral Perturbation Theory. *Phys. Rev.*, D68:034014, 2003.

[32] C. Aubin and C. Bernard. Pseudoscalar decay constants in staggered chiral perturbation theory. *Phys. Rev.*, D68:074011, 2003.

[33] K. Symanzik. Continuum limit and improved action in lattice theories : (i). principles and [phi]4 theory. *Nuclear Physics B*, 226(1):187 – 204, 1983.

[34] Stephen R. Sharpe. B(K) Using staggered fermions: An update. *Nucl. Phys. Proc. Suppl.*, 34:403–406, 1994.

[35] Claude Bernard, Maarten Golterman, and Yigal Shamir. Effective field theories for QCD with rooted staggered fermions. *Phys. Rev.*, D77:074505, 2008.

[36] Stephen R. Sharpe and Ruth S. Van de Water. Staggered chiral perturbation theory at next-to-leading order. *Phys. Rev.*, D71:114505, 2005.

[37] Stephen R. Sharpe and Noam Shoresh. Partially quenched chiral perturbation theory without Φ_0. *Phys. Rev.*, D64:114510, 2001.

[38] Stephen R. Sharpe and Noam Shoresh. Physical results from unphysical simulations. *Phys. Rev.*, D62:094503, 2000.

[39] C. Aubin and C. Bernard. Staggered chiral perturbation theory. *Nucl. Phys. Proc. Suppl.*, 129:182–184, 2004.

[40] A. Morel. Chiral logarithms in quenched qcd. *J. Phys. France*, 48(7):1111–1119, 1987.

[41] Stephen R. Sharpe and Ruth S. Van de Water. Unphysical operators in partially quenched QCD. *Phys. Rev.*, D69:054027, 2004.

[42] Claude W. Bernard and Maarten F. L. Golterman. Chiral perturbation theory for the quenched approximation of QCD. *Phys. Rev.*, D46:853–857, 1992.

[43] Stephen R. Sharpe and Robert L. Singleton, Jr. Predicting the Aoki phase using the chiral Lagrangian. *Nucl. Phys. Proc. Suppl.*, 73:234–236, 1999.

[44] E. Follana et al. Highly Improved Staggered Quarks on the Lattice, with Applications to Charm Physics. *Phys. Rev.*, D75:054502, 2007.

[45] A. Bazavov et al. HISQ action in dynamical simulations. *PoS*, LATTICE2008:033, 2008.

[46] Claude W. Bernard and Maarten F. L. Golterman. Partially quenched gauge theories and an application to staggered fermions. *Phys. Rev.*, D49:486–494, 1994.

[47] P. H. Damgaard and K. Splittorff. Partially quenched chiral perturbation theory and the replica method. *Phys. Rev.*, D62:054509, 2000.

[48] Johan Bijnens and Timo A. Lahde. Masses and decay constants of pseudoscalar mesons to two loops in two-flavor partially quenched chiral perturbation theory. *Phys. Rev.*, D72:074502, 2005.

[49] C. Bernard. Chiral Logs in the Presence of Staggered Flavor Symmetry Breaking. *Phys. Rev.*, D65:054031, 2002.

[50] J. Bijnens, G. Colangelo, and G. Ecker. Renormalization of chiral perturbation theory to order p**6. *Annals Phys.*, 280:100–139, 2000.

[51] A. Bazavov et al. SU(2) chiral fits to light pseudoscalar masses and decay constants. *PoS*, LAT2009:077, 2009.

[52] C. Allton et al. Physical Results from 2+1 Flavor Domain Wall QCD and SU(2) Chiral Perturbation Theory. *Phys. Rev.*, D78:114509, 2008.

[53] A. Roessl. Pion kaon scattering near the threshold in chiral SU(2) perturbation theory. *Nucl. Phys.*, B555:507–539, 1999.

[54] R. Sommer. A New way to set the energy scale in lattice gauge theories and its applications to the static force and alpha-s in SU(2) Yang-Mills theory. *Nucl. Phys.*, B411:839–854, 1994.

[55] Claude W. Bernard et al. The static quark potential in three flavor QCD. *Phys. Rev.*, D62:034503, 2000.

[56] C. R. Allton. Lattice Monte Carlo data versus perturbation theory. 1996.

[57] C. T. H. Davies, E. Follana, I. D. Kendall, G. Peter Lepage, and C. McNeile. Precise determination of the lattice spacing in full lattice QCD. *Phys. Rev.*, D81:034506, 2010.

[58] C. Amsler et al. Review of particle physics. *Physics Letters B*, 667(1-5):1 – 6, 2008. Review of Particle Physics.

[59] D. Kadoh et al. SU(2) and SU(3) chiral perturbation theory analyses on meson and baryon masses in 2+1 flavor lattice QCD. *PoS*, LATTICE2008:092, 2008.

[60] Claude Bernard. Light-light & heavy-light chiral fits. *MILC meeting*, Jan 2010.

[61] G. P. Lepage et al. Constrained curve fitting. *Nucl. Phys. Proc. Suppl.*, 106:12–20, 2002.

[62] J. Gasser and H. Leutwyler. Light quarks at low temperatures. *Physics Letters B*, 184(1):83 – 88, 1987.

[63] Gilberto Colangelo and Christoph Haefeli. An asymptotic formula for the pion decay constant in a large volume. *Phys. Lett.*, B590:258–264, 2004.

[64] Johan Bijnens. Chiral Perturbation Theory Beyond One Loop. *Prog. Part. Nucl. Phys.*, 58:521–586, 2007.

[65] C. Aubin et al. First determination of the strange and light quark masses from full lattice QCD. *Phys. Rev.*, D70:031504, 2004.

[66] Quentin Mason, Howard D. Trottier, Ron Horgan, Christine T. H. Davies, and G. Peter Lepage. High-precision determination of the light-quark masses from realistic lattice qcd. *Phys. Rev. D*, 73(11):114501, Jun 2006.

[67] Xining Du. Staggered chiral perturbation theory in the two-flavor case. 2009.